Primary and Auxiliary Subunits of Sodium Channel Na_v1 in *Lymnaea Stagnalis*

by

Julia E. Fux

A thesis
presented to the University of Waterloo
in fulfillment of the
thesis requirement for the degree of
Master of Science
in
Biology

Waterloo, Ontario, Canada, 2014

AUTHOR'S DECLARATION

I hereby declare that I am the sole author of this thesis. This is a true copy of the thesis, including any required final revisions, as accepted by my examiners.

I understand that my thesis may be made electronically available to the public.

Abstract

Voltage gated sodium channels (Na_v) are major contributors in the neuronal signal transduction, responsible for the action potential upstroke. They are members of the large 4x6 ion channel family, which also include the voltage gated calcium channels, and NALCN channels. The evolution of sodium selectivity in ion channels predates the development of the nervous system and sodium channels can be found in almost all animal lineages, including the most ancestral ones, like Placozoa and Apusozoa phylums.

Two types of sodium channels, Na_v1 and Na_v2, are differentiated mainly based upon the structure of the inner pore, which dictates the ion selectivity of the channel. Na_v1, which is represented in humans by 9 subtypes, $Na_v1.1$-9, carries a selectivity filter motif DEKA which makes it highly selective for sodium ions. Na_v2 which is ancestral to Na_v1 has been lost in the vertebrate lineage but is found in the majority of invertebrates. Despite the structural homology with Na_v1, the selectivity filter DEEA makes the Na_v2 channel calcium selective. We have sequenced, cloned and identified splice variants in sodium channel Na_v1 from a pulmonate fresh water snail, *Lymnaea stagnalis.* We also identified the sequence of the *Lymnaea* Na_v2 channel, which is possibly expressed in the snail external sensory organs.

Unlike the highly conserved α- subunits, the multifunctional auxiliary subunits of human sodium channel, β1-4, have no structural analogs among invertebrates, although insectal Tip-E and TEH have a similar function. We have identified putative molluscan sodium channel auxiliary subunits, LNa_vB1-4, which are secreted proteins with a conserved CUB domain, analogous to the CAM like immunoglobulin V-folds in mammalian β-subunits. CUB domains are found in auxiliary subunits of nematode and mammalian ligand gated channels, such as kainite receptors and acetylcholine receptors. Our hypothesis is that the $Na_vβ$ subunits are an example of convergence, which evolved independently in different invertebrates and vertebrate groups to serve similar functions.

Acknowledgements

First and foremost I would like to express my sincere gratitude to my mentor Prof. J. David Spafford. David has not only guided me through the challenging, at times frustrating, but on the whole exciting process of research for three years, but also encouraged and inspired me when things didn't go smoothly.

My warmest thanks go to the colleagues, who have been working alongside me during these years. Emily Irving 'showed me the ropes', Adrienne Boone generously shared with me her vast experience and knowledge of molecular biology. I also want to thank Adriano Senatore, whose thorough approach to scientific research set the standards to follow and Wendy Guan, who spent hours patiently guiding me through the confusing world of electrophysiology.

A separate 'thank you' to Neil Hsueh who did an amazing job making antigens for the snail sodium channel and thus greatly helped in advancing my project. And to Amrit Mehta and Rob Stevens who, although not directly involved in my research were always there to hear me rant about it.

I would like to thank Dr Ke Dong of Michigan State University and Dr Lory Isom from University of Michigan who not only generously shared with me the plasmids needed for my experiments, but also provided an unique outside perspective on my field of research.

I would also like to thank my committee members, Dr Bernard Dunker and Dr Bruce McKay for taking the time to thoroughly read and understand my project and for providing a valuable input to shape and perfect my thesis.

Finally, I would like to thank my husband, Vadim Fux, who pushed me, believed in me and stood by me every step of the way. I cannot see myself completing this project without his continuous and unwavering support.

Dedication

To my mom who never stops being curious

To my dad who never stops being kind

Table of Contents

List of Figures

List of Tables

Chapter 1. Introduction

1.1 Sodium channels properties and role in neuronal signaling

Voltage gated sodium channels play an important role in signal transduction along neurons and muscle. These are pore forming proteins that activate in response to membrane depolarization to allow a rapid surge of sodium ions into the cytosol. Sodium channels are located along the axon, where they are responsible for the rising phase of action potential.

The identification of currents through the voltage gated sodium channels (Na_v) first began with Alan Hodgkin and Andrew Huxley, with their groundbreaking work on squid giant axon (Figure 1.1). In the series of articles published between 1939 and 1952, they described the changes in membrane permeability to sodium and potassium ions in response to electric stimulation. Hodgkin and Huxley were also the first major users of the voltage clamp technique (Hodgkin & Haxley, 1952). Another breakthrough in electrophysiology came when Bert Sackmann and Erwin Neher developed the patch clamp technique to obtain single channel recording (Neher, 1988). This technique allowed a researcher to study individual characteristics of ion channels and to see how the chemical components of the environment affect channel gating functions.

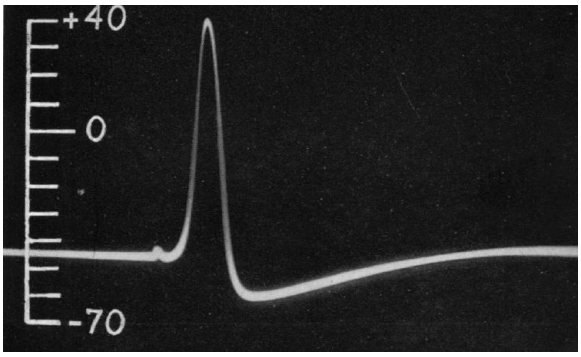

Figure 1.1. Action potential of giant squid axon, recorded by Hodgkin and Huxley (Hodgkin & Huxley, 1945)**.**

The biophysical properties of the Na_v channel have been studied extensively. The sodium channels have characteristic properties in all cells where they are expressed. Na_v channels are found in one of the three major states: active, inactive and resting (deactivated). The active state is the only ion conducting state, and only lasts for a few milliseconds. Activation is triggered by depolarization of the

membrane, and it is immediately followed by inactivation (refractory period), when the pore is occluded by the "hinged lid" on the cytosolic side and the sodium current stops abruptly (Catterall W. A., 1993). The resting state follows, when the whole channel changes conformation. The hinged lid no longer obstructs the pore but the arrangement of the channel's inner pore segments prevents the ions from passing through the central cavity. The membrane has to be hyperpolarized for the Na_v channel to transform from the refractory to the resting state (Yu & Catterall, 2003). Ion channel states are stochastic and at any given moment ion channels can exist in any of the active, inactive or resting states. As the voltage across the membrane drops, the probability of the channel switching to an active state increases. Na_v channel gates open and sodium ions move into the cytosol, promoting further membrane depolarization, which in turn activates more channels. The influx of sodium ions accelerates the rise in membrane potential and brings the action potential to its overshoot (Catterall, 2000). The overshooting action potential excites the adjoining membrane, to become a self- propagating wave which moves unidirectionally along the axon at speeds of up to 200 m/s (Hartline & Colman, 2007). The intracellular surge of sodium ions during the action potential is closely followed by a repolarizing wave of potassium ions moving out through the potassium channels. Voltage gated potassium channels work in perfect synchrony with Na^+ channels and bring about the descending phase of the action potential. By moving out of the cell, K^+ ions hyperpolarize the membrane, restoring the membrane potential to the resting state (Yu & Catterall, 2003) (Figure 1.4).

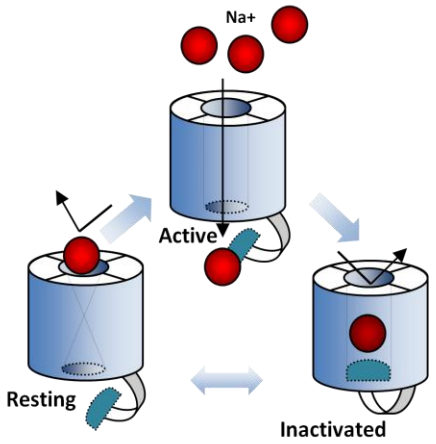

Figure 1.2. Activation states of the sodium channel.
The pore becomes permeable to sodium ions in response to membrane depolarization. The channel can spontaneously switch between resting and inactivated states, but channels can only open from the resting state.

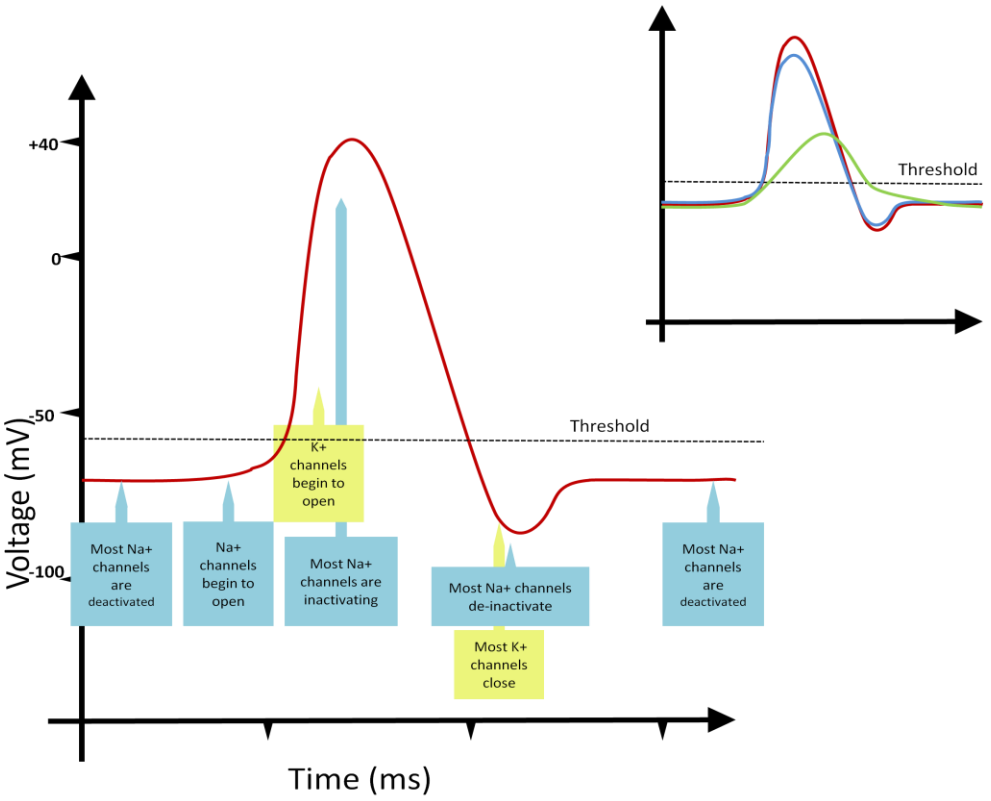

Figure 1.3. The topography of the action potential.
The combined effects of sodium and potassium currents shape the action potential. A sufficient number of Na_v^+ channels have to open for the voltage threshold to be reached and the action potential to be generated. The rectifying potassium current rises through the middle of the rising phase of the action potential, but has greater influence after the sodium channels are reduced in their contribution during the falling phase of the action potential. In the top left diagram: red depicts the action potential, the sodium current is shown in blue and the potassium current is shown in green.

$$V_{\text{Eq.}} = \frac{RT}{zF} \ln\left(\frac{[X]_{\text{out}}}{[X]_{\text{in}}}\right)$$

The Nernst equation is used to describe the resting state of the membrane in mathematical terms. V_{eq} is set by the electrochemical gradient of ion [X] which is in turn determined by the transmembrane concentration gradients and valence of the ion.

Although there are several ions that contribute to the resting membrane potential, it is almost equivalent to the potassium equilibrium potential, because potassium ions are the most permeable ion at rest (50 times more permeable than sodium ions.

A modified version of Nernst equation is the Goldman-Hodgkin –Katz equation takes into account the relative permeability of potassium, sodium and chloride ions in the establishment of the membrane potential.

$$V_m = \frac{RT}{F} \ln\left(\frac{p_K[K^+]_o + p_{Na}[Na^+]_o + p_{Cl}[Cl^-]_i}{p_K[K^+]_i + p_{Na}[Na^+]_i + p_{Cl}[Cl^-]_o} \right)$$

The letter *p* symbolizes the membrane permeability of each ion (Hille, 1975).

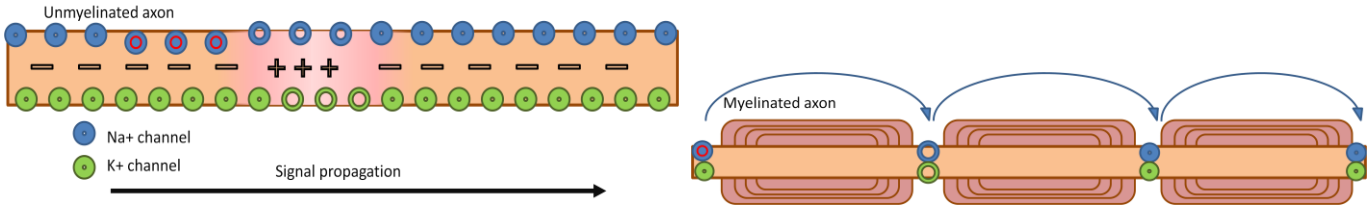

Figure 1.4. Signal propagation down the axon.
The action potential speeds down the unmyelinated axon due to the large number of ion channels distributed over the membrane. In myelinated axons the action potential propagates so quickly under myelinated regions that there is an appearance of the action potential jumping from one node of Ranvier to the next (saltatory conduction).

1.2 Neuronal components of signal transduction

To fully understand how the sodium channel works we must look at the environment in which sodium channels are operating.

Sodium channels are embedded in a network of interacting proteins *in vivo*, that traffic and target sodium channels to their proper position and stabilize Na_v channels along the axon. Among those proteins are the auxiliary sodium channel β-subunits, which are discussed later in this chapter. Ankyrin G, in combination with spectrin, binds the sodium channel at the intracellular loop between 2nd and 3rd domain, an anchoring motif that tethers channels to the actin cytoskeleton of the cell (Garrido, et al., 2003) (Figure 1.5). It has been reported that the sodium channels are uniformly inserted into the neuronal membrane, but only the ankyrin bound α-subunits in the axon initial segment (AIS) and nodal regions of the axon are retained, while the rest of the sodium channels are eliminated by endocytosis

(Fache, et al., 2004). Another important participant in ion channel localisation, Nf186, is required for maintenance of the axon initial segment (AIS) region in mature neurons. Nf186 null mice, that initially displayed normal topology in the neural AIS region, showed rapid loss of sodium channels after 4 weeks (Zonta, et al., 2011).

We know very little about the organisation of unmyelinated axonal regions, and how Na^+ channels are targeted to different membranal domains, such as the AIS. Even less is known about the targeting and localisation of sodium channels in the unmyelinated neurons of invertebrates. Although it has been shown that the invertebrate sodium channels cluster at the axon initial segment, and are expressed throughout the length of an axon, the tethering mechanism is still unknown.

In addition to neurons, sodium channels populate other electrically excitable tissues, such as skeletal muscles, cardiomyocytes, endocrine cells and glia (Catterall, Goldin, & Waxman, 2005). In humans, $Na_v1.4$ is the principal skeletal muscle α-subunit and $Na_v1.5$ is responsible for cardiac action potentials which generate contractions in cardiac cells (Yu & Catterall, 2003). Cells that are not electrically excitable sometimes express sodium channels too. For example human embryonic kidney (HEK293) cell line which is widely used for functional expression of ion channels, has been shown to display native voltage activated sodium currents (He & Soderlund, 2010).

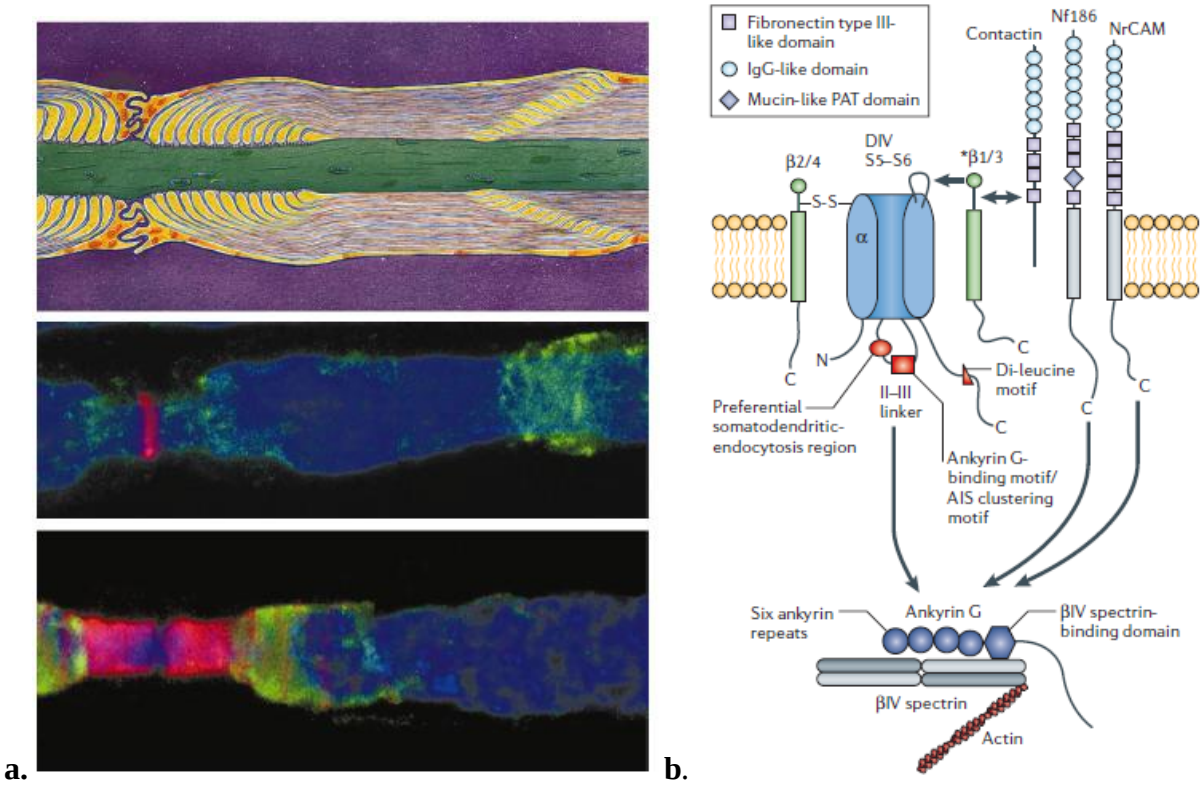

Figure 1.5. Membrane topography of the sodium channel in the node of Ranvier.
a. Localization of ion channels on the myelinated axon. Top image depicts an axon surrounded by multiple layers of myelin sheath with the small opening that encircles the axon known as nodes of Ranvier. Middle image (same fragment) shows the sodium channels (magenta) concentrated in the node of Ranvier. The lower image indicates the location of potassium channels in paranodal regions (green). Overlaid images based on laser scanning confocal micrographs of adult mouse sciatic nerve. Adapted from (Pedraza, Huang, & Colman, 2001) (Arroyo & Scherer, 2000).
b. Sodium channel α- and β- subunit associate with ankyrin, contactin, neurofascin (Nf 186) and neuron-glia cell adhesion molecule (NrCAM) to form macrocomplexes at the node of Ranvier. Adapted from (Lai & Jan, 2006).

1.3 Molecular structure of the α-subunit

Voltage gated sodium channels are members of an extensive ion channel family, which also includes calcium and potassium channels and NALCN. Sodium channel α-subunits are approximately 2000 amino acid long and 260 kDa large, heavily glycosylated, with intracellular N- and C- terminus and inter-domain linkers (Catterall, 2000). Sodium channels consist of four domains, D I-D IV, with six segments S1-S6 within each domain (Figure 1.8). The 5th and the 6th segments of each domain comprise

the pore, and a re-entrant linker that connects them (the P-loop) forms the inner lining of the pore. Located in the P-loop of each domain is the selectivity filter (SF) which, in the folded protein, takes up the narrowest part of the pore and defines the ionic selectivity of the channel. The sequence DEKA is highly selective for sodium ions (Yu & Catterall, 2003) (Catterall, 2014) (Figure 1.9).

The voltage sensing mechanism of the voltage gated ion channels includes segments S1-4 and resembles that of the Hv1 voltage-gated proton channel which does not possess a pore domain (Payandeh, Scheuer, Zheng, & Catterall, 2011). The voltage sensors consist of a pattern of positively charged residues (arginines/lysins) every third amino acid on the S4 of each domain. There are between four to six repeats that results in a positively charged band along one side of the S4 helix (Yu & Catterall, 2003). Upon change to the membrane electric field (depolarization/ hyperpolarization), it is hypothesized that the charged S4 helices slide out and in the membrane along a series of counter-charges formed by S2 and S3 segments. The sliding of the S4 segments in the voltage-sensing domain acts upon a short S4-S5 amphipathic helix running perpendicular to the membrane, which serves as a lever for movements of the pore domain spanning S5-S6, including the pore constriction (channel closure and C-type inactivation) and opening (activation) involving the inner lining of S6 residues (McCusker, Bagne, Naylor, Cole, & D'Avanzo, 2012) (Figure 1.7).

Sodium channels have a very rapid channel inactivation involving a "hinged lid" formed by the short linker (54 +/- 2 amino acids) formed between Domains III and IV. The fragment that occludes the pore is a conserved hydrophobic patch, a characteristic IFM (Ile-Phe-Met) motif that is mostly conserved in Na_v1 and Na_v2 channels (Figure 1.8).

The large size of voltage-gated sodium channels, consisting of 24 membrane segments, with many intrinsically disordered regions, precludes crystallization and determination of structural details using X-ray crystallography. Our understanding of the structures of sodium channels is derived from the known crystal structures of potassium channels (KcSA, $K_v1.2$) and the bacterial sodium channels resembling NaChBac (Yue, et al 2002), NavAb (Payandeh, Scheuer, Zheng, & Catterall, 2011) or NavRh (Zhang, et al., 2012). Both the bacterial sodium channels and potassium channels form symmetrical homo-tetramers of four identical subunits of six segments, and they are at least four times smaller than the asymmetrical eukaryotic sodium channels consisting of twenty-four segments. We have learned from the bacterial sodium channel that it possesses a wider and shorter pore than the potassium channel. In potassium channels, backbone carbonyl oxygen atoms contributed by selectivity filter residues create four positions that are optimally designed for accommodating dehydrated potassium ions

in the pore. The sodium channel has a shorter pore, with a carboxylate side chain residue projecting into the pore center which is a key residue at the pore constriction point for governing sodium selectivity (Payandeh, Scheuer, Zheng, & Catterall, 2011). The accepted model of the sodium channel selectivity filter was first proposed by Hille (Hille, 1975). According to this model, sodium ions enter the outer vestibule of the pore in a single file, fully hydrated. As the ion approaches the selectivity filter, it loses layers of the hydration shell and forms a high energy transition complex with the oxygens on the carboxylic acid residues. The sodium ion then moves further into the central cavity, regaining the hydration shell in the process (Hille, 1975). This model explains why sodium channels, despite having a larger pore than potassium channels are far more permeable to sodium then to potassium. Sodium ions are favored over potassium ions because the carboxylate side chain residue in the high field strength site partially dehydrates the waters surrounding sodium channels, and does this more rapidly and efficiently for the smaller ionic radius of the sodium ion than for the larger potassium ion (Payandeh, Scheuer, Zheng, & Catterall, 2011).

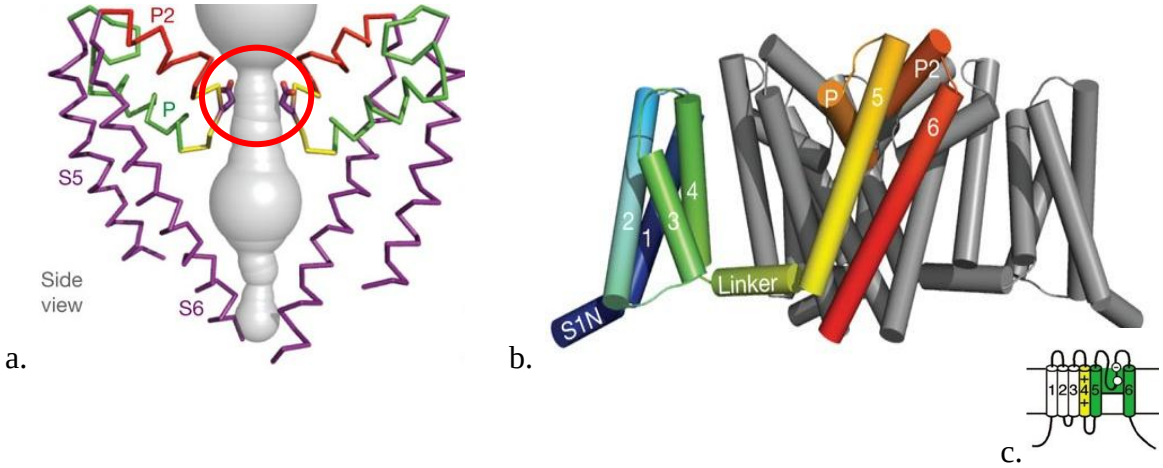

Figure 1.6. Sodium channel structure based on the bacterial sodium channel NavAb from *Arcobacter butzleri*.

a. 3D structure of the sodium channel pore based on the X-ray crystallography image. The grey rod in the middle reflects the shape of the pore. Red circle indicates the selectivity filter region. P-loop (P- and P2-helices) stabilizes cations in the central cavity. P-2 helix is found in Na^{+} and Ca^{2+} channels, but not potassium channels.

b. Location of individual segments within the channel. S1N is the cytosolic N-terminus attached to the DIS1. P refers to the P-loop. Segments 1, 2, 3 and 4 form the voltage sensing domain that comprises the outer part of the channel, while 5 and 6 form the pore lining center with the P-loop forming the innermost region of the pore.

c. One of the four subunits comprising the bacterial channel tetramer. Adapted from (Payandeh, Scheuer, Zheng, & Catterall, 2011) (Yu & Catterall, 2003).

a. 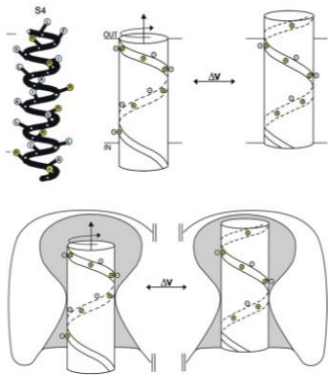

b. 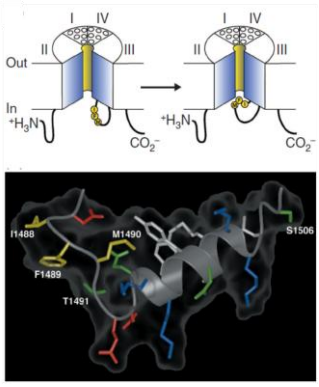

Figure 1.7. Features of the sodium channel.

a. Positively charged side chains shown as brown dots. S4 helix movement during membrane depolarization. The helix shifts upward with a clockwise rotation. This shift causes the change in conformation of the rest of the helical segments (Yu & Catterall, 2003).

b. Motif for fast N-type inactivation motif, a feature unique to sodium channels. The IFM sequence (I1488, F1489 and M1490) sits atop a rigid helix, the III-IV linker moves up to occlude the pore. The IFM motif is set in motion by the same mechanism that controls the opening of the pore which limits the channel opening to 2-3 ms. Adapted from (Catterall, 2000).

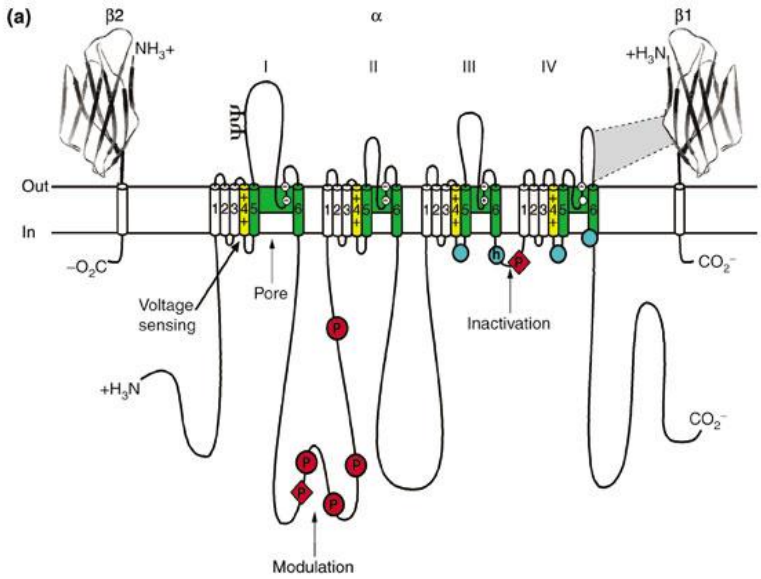

Figure 1.8. Molecular structure of the human sodium channel.

The size of the loops in the picture is proportional to the actual size of the linkers. Circled P indicates the sites of phosphorylation by cAMP-dependant protein kinase A. P in the diamond shape indicates sites of phosphorylation by protein kinase C. ψ shows the sites of glycosylation. β-subunits shown as folded Ig domains, with possible α-subunit binding site for β1. Adapted from (Catterall, 2000).

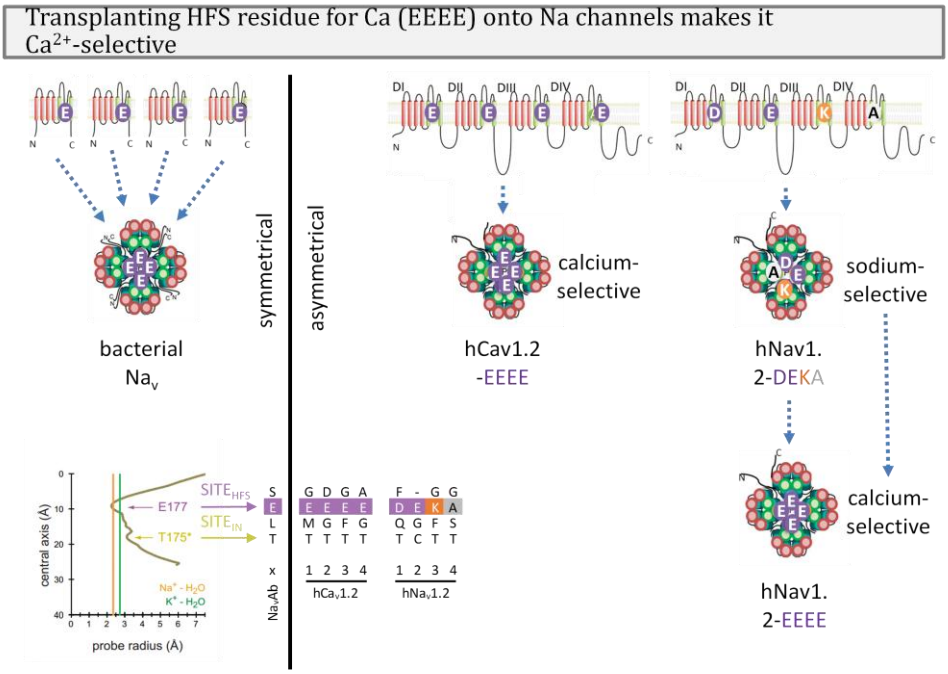

Figure 1.9. The composition of the selectivity filter defines the ionic selectivity of the pore.
Lysine in the DIII (K) is particularly important in defining sodium selectivity. Substitution with Lysine (K)→Glutamic acid (E) creates a calcium selective sodium channel (Heinemann, Terlau, Stühmer, Imoto, & Numa, 1992).

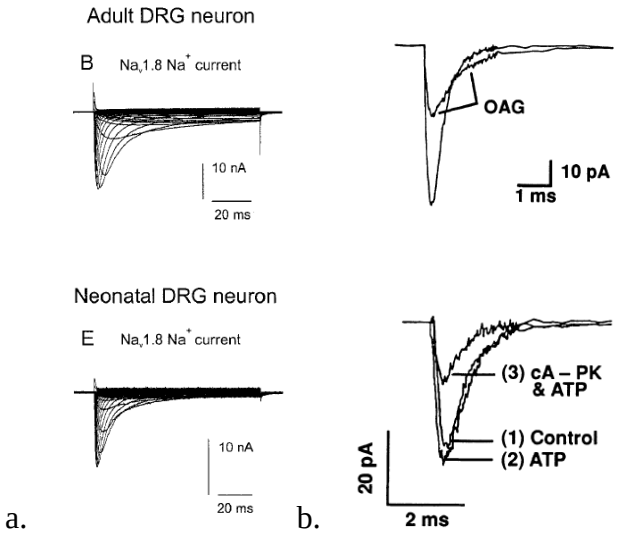

Figure 1.10. Effects of posttranslational modifications on mammalian Na_v1.
a. The effects of glycosylation on the sodium channel gating properties; neonatal dorsal root ganglia neurons contain heavily glycosylated sodium channels while in adult neuron glycosylation is reduced. While the amplitude of the peak current remains the same, the inactivation kinetics is

noticeably faster. The negative charges present on the sialic acid residues affect the dynamics of the pore (Tyrrell, Renganathan, Dib-Hajj, & Waxman, 2001).

b. The effect of phosphorylation on the sodium channel properties. Top image shows sodium current in the presence of activated protein kinase C vs. control. Synthetic diacylglycerol oleylacetylglycerol (OAG) was used to activate protein kinase C.
Bottom image shows sodium current in the presence of cAMP-dependant protein kinase (cA-PK) vs. control. Note that in both cases phosphorylation by protein kinase reduces the amplitude of the peak current. Adapted from (Tyrrell, Renganathan, Dib-Hajj, & Waxman, 2001) (Catterall W. A., 1993).

Table 1.1. Human SCN genes nomenclature

Channel	Gene name	Chromosome number	Expression
$Na_v1.1$	SCN1A	2	CNS, cardiac myocytes
$Na_v1.2$	SCN2A	2	CNS, PNS
$Na_v1.3$	SCN3A	2	CNS, PNS, cardiac myocytes
$Na_v1.4$	SCN4A	17	Skeletal muscle
$Na_v1.5$	SCN5A	3	Cardiac myocytes, skeletal muscle, CNS, gastrointestinal smooth muscle cells
$Na_v1.6$	SCN8A	12	CNS, PNS, Dorsal root ganglia, glia
$Na_v1.7$	SCN9A	2	Sympathetic neurons, Schwann cells, and neuroendocrine cells
$Na_v1.8$	SCN10A	3	Dorsal root ganglia
$Na_v1.9$	SCN11A	3	Dorsal root ganglia
Na_x	SCN7A	2	Glial cells, heart, uterus

This table is based on the data from (Widmark, Sundstrom, Daza, & Larhammar, 2010) and (Catterall, Goldin, & Waxman, 2005)

$Na_v1.1$, 2, 3, 7 and Na_x are located on chromosome 2. Except for Na_x these sodium channels are closely related to one another. They are all sensitive to nanomolar concentration of toxin produced by bacterial genus *Vibrio*, tetrodotoxin (TTX), and are prominent in neurons (Catterall, Goldin, & Waxman, 2005). $Na_v1.4$ and 1.6 which lie on chromosomes 17 and 12, respectively, exhibit 85% similarity to the chromosome 2 group and share in the high TTX sensitivity. $Na_v1.5$, $Na_v1.8$ and $Na_v1.9$ are clustered on chromosome 3 and they are highly homologous to one another but only 75% identical to the

chromosome 2 group. The Chromosome 3 grouped channels are less sensitive to TTX, with $Na_v1.8$ and $Na_v1.9$ being resistant to micromolar concentrations of TTX (Lopreato, et al., 2001).

Invertebrates have only one gene coding for Na_v1 sodium channel, but some achieved functional diversity through alternative splicing (Tan, Liu, Nomura, Goldin, & Dong, 2002). The laboratories of Dong and Baines report 15 alternative exons and 27 unique splice variants for the Drosophila *para* Na_v1 channel (Lin, Right, Muraro, & Bains, 2009) (Dong, 2007). Alternative splicing in the voltage-gated sodium channel DmNav transcript, known as *para* for its paralytic mutant phenotype generates distinct activation/inactivation patterns (Lin, Right, Muraro, & Bains, 2009). Differing variants can influence channel expression, drug resistance, kinetics and post-translational modification (Tan, Liu, Nomura, Goldin, & Dong, 2002).

The cytoplasmic linkers connecting Domains I and II and between Domains II and III are much longer (6 and 3.5 fold larger) than the 54 +/- 2 amino acids between Domains III and IV of sodium channels. For example, in snail LNav1 and human Nav1.1 and Nav1.7 channels, the I-II linker and II-III linkers, respectively are 327- 337 amino acids long and 187 -221 amino acid long. A hotbed of serine and threonine phosphorylation sites in sodium channels is located in the I-II linker, where critical sites include serine 554, 573, 576, 610, 623, 655 and 687 (Scheuer, 2011). The consequence to phosphorylation by protein kinase C (PKC) or protein kinase A (PKA) is a decrement in the amplitude of sodium currents (Yu & Catterall, Overview of the Voltage-Gated Sodium Channel Family, 2003). The proximal I-II linker contains a modified leucine zipper motif for binding of PKA anchoring protein (AKAP15), which tethers protein kinase A to the I-II linker of vertebrate sodium channels (Cantrell, et al., 2002). There is also a PKC site located in the III-IV linker (position 1506) (Catterall, et al., 2006).

The α –subunits are also glycosylated, some of them heavily. The carbohydrate content adds from 5% (Nav 1.5) up to 30% ($Na_v1.1$, $Na_v1.2$, $Na_v1.3$) to the overall mass of the protein (Tyrrell, Renganathan, Dib-Hajj, & Waxman, 2001). Glycosylation affects the voltage dependence of the steady state inactivation and acts as a developmental regulator, altering the channel kinetics during maturation (Figure 1.10). Other important functions, such as proper folding of the principal subunit and its interaction with β-subunits are also attributed to glycosylation (Tyrrell, Renganathan, Dib-Hajj, & Waxman, 2001)

The effects of these post translational modifications might appear subtle on the scale of individual channel, or individual neuron, but when applied to a community of interconnected neurons, these can dramatically alter the signalling patterns and lead to disease. Posttranslational modifications

can be tissue-specific and the channel characteristics *in vitro* might not accurately reflect its behaviour in the different signalling systems *in vivo.*

1.4 Evolution of sodium selectivity in the ion pore

Comparative analysis of basal animal lineages indicates that sodium selectivity evolved independently on at least 2 separate occasions (Liebeskind, Hillis, & Zakon, 2011). A cation channel with the first resemblances to voltage-gated sodium channels appears in *Thecamonas trahens,* which is a unicellular eukaryote before the animal-fungal split. An Na_v2 homolog is also found in the eukaryotic Opisthokonts after the animal-fungal split, such as coanoflagellates, *Monosiga brevicollis* and *Salpingoeca rosetta,* and in the simplest multicellular organisms, such as the ctenophore, warty comb jelly, *Mnemiopsis leidyi*, sponge *Amphemidon queenslandica,* and placozoan, *Trichoplax adhaerens*(Gur Barzilai, et al., 2012). The Na_v2 homologs have a DEEA or DEES (*Thecamonas spp.*) selectivity filter (Zakon, 2012).

The evolution of Na_v1 sodium channels involves the introduction of a lysine in the 2^{nd} or 3^{rd} position of the selectivity filter. Within cnidarians, the Na_v1 sodium channels have a DKEA selectivity filter, and non-trematode flatworms, like *Schmitea mediterranea* or *Dugesia japonica* have the lysine residue in the third position as a DEKG selectivity filter which in more advanced protostome invertebrates and vertebrates is a DEKA selectivity filter. Both the cnidarians DKEA and standard vertebrate DEKA selectivity filters confer highly sodium selective channels.(Gur Barzilai, et al., 2012). (Figure 1.13)

The evolution of sodium channels not only predates the evolution of nervous system, but could also be an important contributor to nervous system development (Liebeskind, Hillis, & Zakon, 2011). An ankyrin binding motif (discussed earlier on page 4) is a good example of adaptation in sodium channels during evolution. The conserved ankyrin binding motif in the II-III linker, necessary for Na+ channel clustering in the nodes of Ranvier and axon initial segment (AIS), appears before the evolution of myelin sheath (Hill, et al., 2008). Comparative analysis of anchor motifs indicates that it first appears in *Amphioxus* after the emergence of chordates (Hill, et al., 2008). This suggests that the ankyrin motif was initially used to cluster sodium channels at the AIS, where their high density facilitates the generation of action potentials. The first myelinated neurons appear in jawed fish (craniates), but the

mechanism for channel clustering using ankyrin motifs was in place before then (Figure 1.11) (Liebeskind, Hillis, & Zakon, 2011).

Several rounds of duplication of sodium channel gene occurred in vertebrates, leading to a variety of Na_v1 channels, 9 to10 in tetrapods and 8 in teleosts (Zakon, 2012). As the nervous system and other excitable tissues became more sophisticated, the sodium channel subtypes differentiated and adapted features specific for differing tissues. Despite being highly homologous, each of the ten sodium channel subtypes has unique biophysical properties, which allows diversity in their function (Goldin, 2002).

The comparison of non-vertebrate and vertebrate Na_v channel gene sequences allows researchers to speculate about the timing of chromosomal duplication that led to multiple sodium channels. It was established that the first round of duplications occurred early in the chordate history, predating the split of tetrapod and teleost lineages. The second round of chromosomal duplication occurred in parallel in those classes, followed by gene duplications within the same chromosome (Lopreato, et al., 2001). The double duplication theory is supported by the presence of a neighbor gene, HOX, which appears to have gone through the similar duplication events (Hill, et al., 2008) **(**Figure 1.12). There is a possible link between the co-evolution of homeotic (HOX) genes, responsible for the developmental patterning, and Na^+ channel genes which enabled the evolution of sophisticated nervous systems in modern vertebrates. This grouping between the differing vertebrate sodium channels and the Hox cluster include the following: $Na_v1.1$, $Na_v1.2$, $Na_v1.3$ and $Na_v1.7$ are linked with HoxD on Chromosome 2, whereas Nav1.5, 1.8 and 1.9 are linked with HoxA on Chromsome 3. $Na_v1.6$ is associated with HoxC on Chromosome 12 and $Na_v1.4$ is associated with HoxB on Chromsome 17 **(**Figure 1.12) (Widmark, Sundstrom, Daza, & Larhammar, 2010).

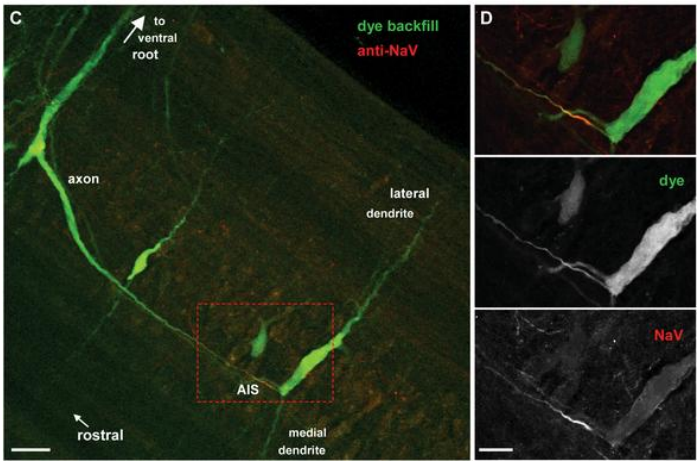

Figure 1.11. Clustering of sodium channel at the axon initial segment in Lamprey fish.
Lamprey fish have unmyelinated axons. Immunolabeling with Nav1 specific antibodies was used in combination with fluorescent dye to highlight the sodium channel clusters in the axon initial segment. Adapted from (Hill, et al., 2008).

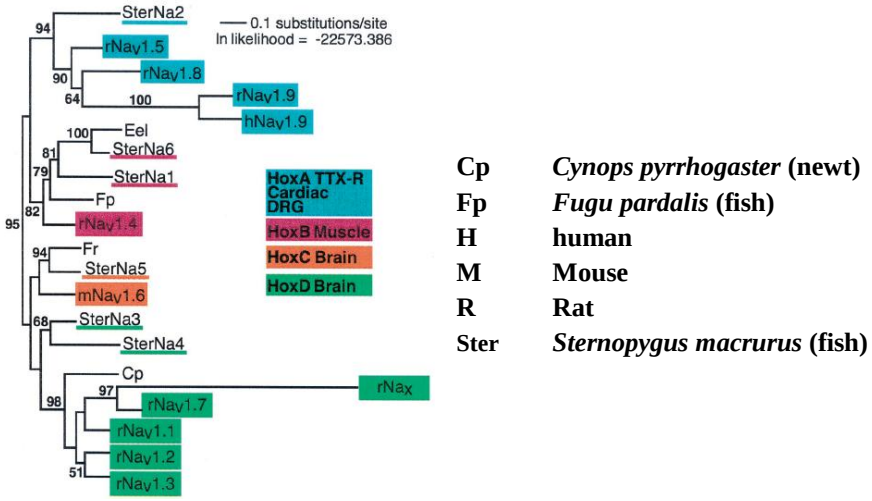

Figure 1.12. Sodium channel and Hox genes coevolving in vertebrates.
Both fish and mammalian sodium channels are linked to the 4 Hox loci, located on 4 chromosomes. Although the numbering of the teleost Na^+ channels differs from that of mammals, all the channels in both fish and mammals belong to the Nav1 group. Adapted from (Lopreato, et al., 2001)

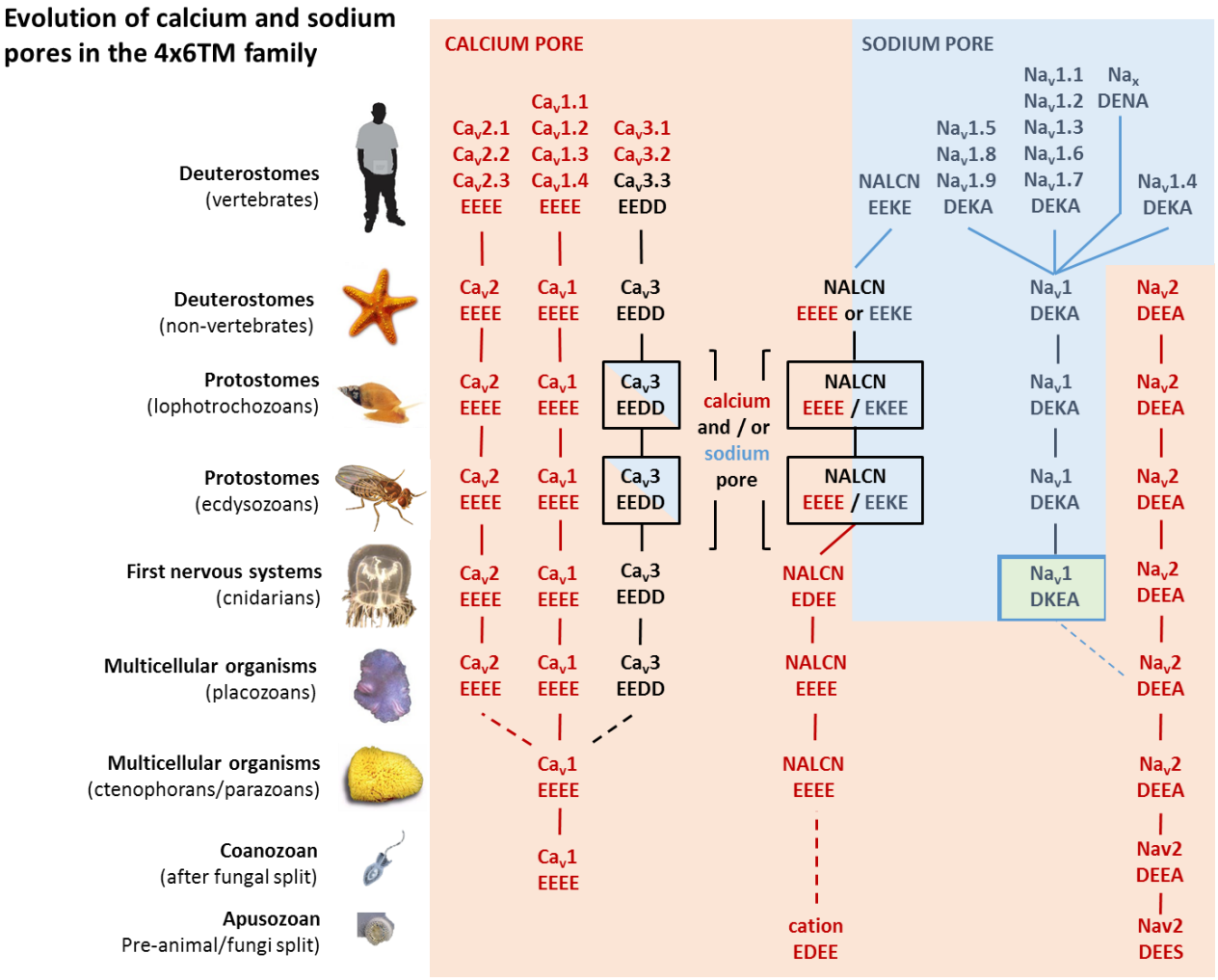

Figure 1.13. Evolution of high field strength site in calcium (Cav), sodium (Nav) and cation (NALCN) pore selectivity filters of eukaryotes.
All 4x6TM originate from single cell eukaryotes and are calcium selective channels (red color). Sodium selectivity evolved in the pores of the T-type channels, NALCN and sodium channels are in metazoans. Na_v2 channels are referred to as sodium channels since they show more structural similarity with Na_v1 group than with calcium channels, but they are mainly calcium selective.

1.5 Toxin sensitivity of α-subunits

Sodium channels are a choice target for both animal and bacterial toxins, since disabling them causes rapid paralysis. A number of toxins targeting Na_v1, derived from both bacteria and venomous animals, have been identified. Among them are tetrodotoxin (TTX), produced by *Pseudomonas* and

Vibrio species of bacteria, saxitoxin (STX) from dinoflagellate species, *Gymnodinium*, *Pyrodinium*, and *Alexandrium,* μ- and δ- conotoxin from the cone snails, as well as some tarantula and scorpion toxins (Cusick & Sayler, 2013). Small variations in toxin receptor sequences on the sodium channel can determine how susceptible the channel is to a specific toxin, and there are many examples where animals not only developed resistance to bacteria made toxins, but also used them for protection, accumulating the toxin in their bodies to deter predators. For example, some vertebrate sodium channels are highly sensitive to TTX but TTX carrying animals, like puffer fish and bivalve mollusks, have a TTX resistant copy of Na_v 1, requiring up to x100 increase in concentration to block them by TTX (Yoshida, 1994) (Twarog, Hidaka, & Yamaguchi, 1972). Toxins have been a useful tool for probing the pore structure of voltage gated channels, with the level of TTX sensitivity being widely used as a means to classify Na_v1 subtypes (Cestele & Catteral, 2000).

While neurotoxins evolved as weapons and defense mechanisms, the selective and reversible block of sodium channels can also be used for therapeutics. There are many applications for therapeutic Na+ channel agents: anaesthetics, anticonvulsants and antiarrhythmics all work by blocking ion channels pores and/or modifying gating properties. Sodium channel subtypes Na_v1.7, Na_v1.8 and Na_v1.9, which are dorsal root ganglia (DRG) specific, are a target for non-selective local anaesthetics, like lidocaine (Moldovan, Alvarez, Rosberg, & Krarup, 2013). A recently identified agent, μO-conotoxin MrVIA is able to selectively block Na_v1.8, the channel associated with nociception, without inhibiting other, TTX sensitive CNS sodium channels or calcium channels. Unfortunately μO-conotoxin MrVIA only works in murine models (Ekberg, et al., 2006).

Antiepileptic drugs, such as carbamazepine, lamotrigine and phenytoin, are channel blockers that preferentially bind channels in an inactivated state. They are non-selective and block all TTX sensitive Na+ channel subtypes (Kuo, 1998). Such drugs can be highly effective against some types of epileptic seizures. However, in other cases they can exacerbate the symptoms, by blocking the GABAergic neurons which could otherwise suppress the seizures (Catterall W. , 2014). Epileptic seizures can be caused by loss of function (such as loss of function mutations in Na_v1.1, expressed in GABAergic neurons) or gain of function (such as mutations causing increased sensitivity to voltage changes in Nav1.2). There is an ongoing effort to develop subtype specific sodium channel modulators though no such agents have been found to date (Catterall W. , 2014).

1.6 Multiple roles of sodium channel auxiliary subunits

In addition to the principal pore-forming α subunit, there are also auxiliary β-subunits associated with the sodium channels. The mammalian α-subunit can operate independently as a pore forming subunit regulated by its own voltage sensing domains, so the role of the β-subunits is sometimes overlooked. I will explain why the auxiliary subunits matter.

Sodium channels, calcium channels and NALCN all resemble each other, with 4 repeats of 6 transmembrane segments. The auxiliary ion channel subunits exhibit much greater variety in shape, size and numbers, with at least 10 unrelated gene families regulating different ion channels (Yu, et al., 2003). Vertebrate calcium channels have four β-, eight γ-, and four α_2-δ- subunits in addition to the pore forming α-subunit (Catterall W. A., 1993). The beta subunit of calcium channels is a member of the membrane associated guanylate-kinase (MAGUK) superfamily with SH3 and guanylate kinase domains, and variable numbers of PDZ domains (Arikkath & Campbell, 2003). The shared homology of calcium channel accessory β subunits extends to the earliest single cell animals to have a Ca_v1 calcium channel, the coanoflagellates (Dawson, et al., 2014). Sodium channels possess four β-subunits which are not homologous with any of their Ca_v counterparts and their lineage is limited to vertebrate species (Wollner, Messner, & Catterall, 1987). The vertebrate sodium channel beta subunits are related to the neural cell adhesion molecules (CaMs) with a V-set Immunoglobulin extracellular loop (Isom, et al., 1995).

Human β-subunits, labelled β1-4, are small glycosylated proteins (~22KDa) with an intracellular C-terminus, one transmembrane helix and a single CAM-like (cell adhesion molecule-like) Ig V-fold domain (Isom, et al., 1995). β1B is a completely soluble, alternatively spliced form of the β1gene transcript, where an intron retention containing a stop codon generates an alternative C-terminus. β1B lacks the last exon, exon 4 which contains the transmembrane domain, but still retains the extracellular CAM like immunoglobulin V-fold (Kazen-Gillespie, et al., 2000). Each pore forming α-subunit is associated with one β-subunit through a disulfide link (β-2or β-4), and another β-subunit through a non-covalent bond (β1 or β3) (Messner & Catterall, 1986) (Yu, et al., 2003). Despite the overall structural similarities, each of the β-subunits affects the Na^+ channel in a unique way. β-1 and β-3 affect the biophysical features of the sodium channel, by altering the voltage of activation and the time constant of inactivation decay(Laedermann, Syam, Petrin, Decosterd, & Abriel, 2013). β-4 in general promotes greater excitability and β1 acts in an inhibitory manner, although there are some discrepancies concerning the way the channels are affected, since both the type of the tissue where the channel is

expressed and the channel subtype affect the results (Brackenbury & Isom, 2011). While β-2 and β-4 do not appear to affect the gating functions of the sodium channel, they upregulate the surface expression of the α-subunit, by chaperoning it toward the membrane (Patino & Isom, 2010).

In addition to modulating the gating and expression of the channel, β-subunits are involved in a wide range of activities, with each one playing a unique role even though they have a rather high sequence homology to one another (Brackenbury & Isom, 2011).

The β-1 subunit has been shown to promote neurite extension in cerebellar granule cells (Davis, Chen, & Isom, 2004). Extracellular domains of different β1 subunits dimerize, causing the activation of sodium channels which in turn stimulates the localized secretion of growth promoting molecules, leading to greater neurite extension (Davis, Chen, & Isom, 2004). In addition to their self association, β1 subunits also bind other CAM-containing proteins, such as contactin, ankirin, NrCAM and N-cadherin (Leterrier, Brachet, Fache, & Dargent, 2010) (Brackenbury & Isom, 2011). β1 are also expressed in skeletal muscles, where they are likely to play a primary role in cell adhesion(Laedermann, Syam, Petrin, Decosterd, & Abriel, 2013). β1 null mice mutants experience a range of problems, which reflect deficiencies both in the development of the nervous system and muscle. Those problems include ataxia, stunted growth, seizures and up to 97% reduction in lifespan (Patino & Isom, 2010). Mutations in human β1 lead to Dravet syndrome- also known as Severe Myoclonic Epilepsy of Infancy (Patino, et al., 2009). It is a rare and catastrophic form of intractable epilepsy that manifests itself in the first year of life.

Levels of β3 subunit are high in fetal brain, and decrease after birth. β3 has overlapping functions with β1. It is likely that β1 compensates for the lack of β3, explaining why β3 null mice exhibit a normal phenotype and a normal life span. (Hakim, et al., 2008). Both β1 and β3 bind the sodium channel α-subunit in the Golgi apparatus and are believed to both affect the glycosylation of the sodium channel and ensure its proper targeting to the nodes of Ranvier and axon initial segment (Laedermann, Syam, Petrin, Decosterd, & Abriel, 2013).

Whereas β1 is found outside of the nervous system in tissues like skeletal muscle, β2 is limited to expression in neurons (Wollner, Messner, & Catterall, 1987). The extracellular region of β2 subunit contains regions homologous to contactin, also a member of CAM (cell adhesion molecule) family. Contactin is involved in formation of axon connections during embryonic development. Contactin also regulates myelination and the organization at nodes of Ranvier (Shimoda & Watanabe, 2009). The similarities between β2 extracellular region and contactin suggest a functional kinship (Isom, et al.,

1995). β2 binds extracellular matrix proteins, such as tenascin, as well as other β1 and β2 subunits (Shimoda & Watanabe, 2009).

β2 subunits are subject to cleavage by secretase family enzymes. Once cleaved, the free intracellular domain acts as a transcriptional regulator for alpha-synuclein (SNCA) genes (Brackenbury & Isom, 2011). When co-expressed with α-subunit *in-vitro*, β2 consistently increases the current density, without changing biophysical properties of sodium channels in a manner that β1 and β3 subunits do. Evidently β2 promotes an increase in the number of surface expressed channels (Isom, et al., 1995). β2 null mice are highly susceptible to seizures and have an increased sensitivity to heat (Patino & Isom, 2010), but display no visible physical abnormalities and their lifespan length is close to normal.

β4 is the most recently discovered sodium channel auxiliary subunit. β4, like β2 is expressed in excitable tissues only. Although the tissue pattern of β2/β4 expression overlaps in some parts of nervous system, other parts only express one isoform or the other. The differential expression of certain beta subunits in particular tissues is consistent with preferential association of specific α subtypes with either β2 or β4 (Yu, et al., 2003). Murine models and human patients with Huntington disease exhibit a significant reduction in β4 expression. β4 may be one of the downstream targets for the polyQ protein associated with the Huntington's disease phenotype (Oyama, et al., 2006).

The only auxiliary sodium channel subunits that have been reported outside the vertebrates are Tip-E and TEH1-4 (Tip-E homologs 1-4), identified in fruit flies (*D melanogaster*) (Littleton & Ganetzky, 2000). Tip-E mutant flies have the same paralytic phenotype as mutant flies of the sodium channel, indicating the importance of Tip-E for the expression and functional effects of the sodium channel. TipE and TipE homologs (Teh1, Teh2, Teh3, Teh4) have been identified in insects and crustaceans, but not outside of these groups within the arthropods (Derst, Walther, Veh, Wicher, & Heinemann, 2006). Tip-E and Tip-E homologs (TEH 1-4) are 65kDa glycosylated proteins, with 2 transmembrane helices, extracellular loop and cytosolic N- and C- termini, with overall similarities closest to Slo-beta or BK-beta subunit family for vertebrate big-conductance calcium-activated potassium (BKCa) channels (Li, Waterhouse, & Zdobnov, 2011). Epidermal growth factor (EGF)-like domains in the extracellular loop regions of Teh3 and Teh4 proteins are not found in Tip-E, Teh1 and Teh2 gene family members, and may be adaptations to interact with extracellular matrix components (Derst, Walther, Veh, Wicher, & Heinemann, 2006). Functional co-expression of these proteins with insect sodium channel α-subunit in oocytes leads to a sharp increase in the peak current and faster channel gating reminiscent of mammalian β1 and β3 effects on sodium channels (Dong, 2007).

Based on the functionally similar role of beta subunits with completely different structures in insects/crustaceans and vertebrates, different protein structures have likely evolved as beta subunits within different animal phyla. The co-opting of differing protein groups as beta subunits for sodium channels is different than the calcium channel beta subunits, which are homologous in all animal groups containing calcium channels including the single cell coanoflagellates (Dawson, et al., 2014). The overall common feature of beta subunits in sodium channels and calcium channels is their regulation of gating properties and expression of ion channels, but also possessing extracellular or intracellular interacting domains that are associated with development of nervous systems, (For example SH3 and GK domains, CAM-like immunoglobulin V-fold for cell adhesion and EGF-like domains) (Dawson, et al., 2014).

1.7 Lymnaea stagnalis as a model organism

Lymnaea stagnalis, the giant pond snail, is an aquatic pulmonate gastropod mollusk, found in freshwater bodies all over the northern hemisphere (Kemenes & Benamin, 2009).

Lymnaea stagnalis has been a popular model organism for neurobiologists, used for studying mechanisms behind memory formation, embryonic neuron development and simple behaviours. Lymnaea neurons are large, and form robust synaptic connections *in vitro*, which makes them especially suitable for constructing and examining neural circuits in cell culture (Syed, Ridgway, Lukowiak, & Bulloch, 1992).

The CNS of *Lymnaea stagnalis* consists of ~ 20,000 neurons in eleven ganglia forming a circle behind and atop the buccal gland. Projections from the ganglia are thick unmyelinated axons extending towards the foot, the internal organs and the external sensory organs (lips, tentacles, eyes) which are especially well innervated. The ganglia have been mapped extensively, with many individual neurons attributed to specific functions (Feng, et al., 2009)(Nakamura, et al., 1999).

A complete transcriptome analysis of the *L. stagnalis* central nervous system was completed in 2012 by a Japanese group using Next-Generation Sequencing (NGS) with an Illumina sequencer (Sadamoto, et al., 2012). . At approximately the same time, Angus Davison (UK) sequenced the whole snail genome by RAD sequencing (Dawson, et al., 2014).

The genome and transcriptome analysis reveals the evolutionary relationships of genes in *Lymnaea stagnalis* with other mollusks and vertebrates, but it also significantly simplifies the search for

novel proteins expressed in *Lymnaea* central nervous system. The snail genome and transcriptome data has greatly facilitated the identification of snail LNav1 and LNav2 sodium channel subunits, and the accessory subunits to sodium channels.

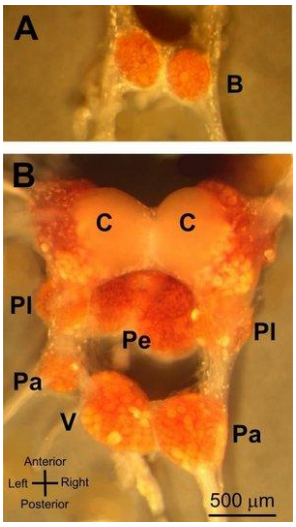

Figure 1.14. Central nervous system of *Lymnaea stagnalis* (Benjamin, 2008)**.**
C stands for cerebral ganglion, Pe for pedal ganglion, Pl stands for pleural ganglion, V/P for visceral and parietal ganglia. The top picture shows the buccal ganglia (B).

1.8 Data obtained through 499 undergraduate project on Lymnaea sodium channel LNa_v1

1.8.1 Sodium channel α-subunit from *Lymnaea Stagnalis*: sequencing

The first 0.8 kb cDNA fragment (yellow color in

Figure 1.15) of the Na_v1 sodium channel from the pond snail, *Lymnaea stagnalis* was isolated by Dr. Spafford as a post-doctoral fellow in Amsterdam in 2001 by degenerate PCR of aligned sodium channel sequences.

Two sets of degenerate primers were designed by Dr Spafford based on the known fragment and regions that are highly homologous in previously described molluscan sodium channels (See Appendix1 for molluscan channel alignment). The isolated fragments, B and D, were 533 bp and 1759 bp in size. Fragments A, C and E followed, with primers based on newly found sequences.

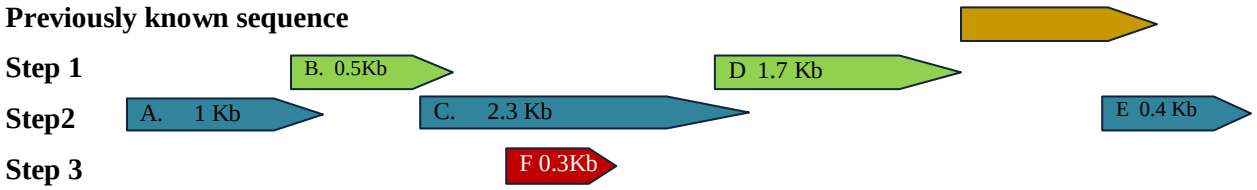

Figure 1.15.The order of fragment amplification and sequencing of PCR fragments of the *Lymnaea* Nav1 sodium channel.

The first cDNA fragment (shown in yellow color) was isolated by degenerate PCR by Dr. Spafford in 2001. In Step 1, Fragments B and D were identified, followed by fragments A, C and E spanning the full contiguous sequence of the snail LNav1 sodium channel. Fragment F was amplified to reveal the region spanning PCR sequences where the forward and reverse strands of Fragment C did not overlap.

Two sets of PCR primers were designed based on this known fragment in addition to degenerate PCR (polymerase chain reaction) primers based on flanking regions that are highly homologous in sequenced molluscan Nav1 sodium channels (See Appendix3 for molluscan Nav1 channel alignment). The newly isolated cDNA fragments isolated from snail brains by PCR were fragments B and D of 533 bp and 1759 bp in size, respectively (see Fig. 3.1, Fig. 3.2). We walked along the gene using the information from PCR fragments B and D to isolate the flanking and middle sequence of the snail Na_v1 sodium channel, dubbed fragments A, C and E (see Fig. 3.2) using PCR primers designed on the newly found sequences by PCR.

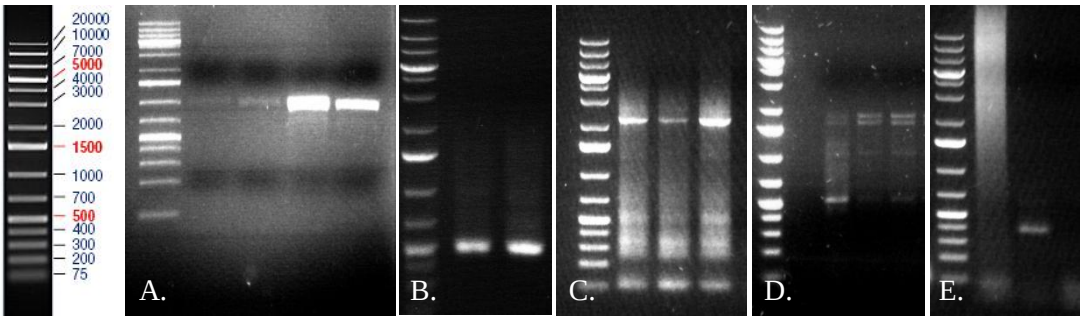

Figure 1.16 Fragments of Lymnaea sodium channel α subunit amplified by PCR.
Same gel ruler, Gene Ruler 1Kb plus (Thermo Scientific) was used for all gels. The gels are aligned in the same order the sequences are located on the α-subunit. Closely set double bands in fragment D indicate a length variation in the channel sequence.

The full-length LNa_v1 sodium channel coding sequence was found to be 6180 bp long, with an optional 174 bp deletion in the II-III linker region and two mutually exclusive exons in Domain I, S1 segment. During the final stages of sequencing, the full length cDNA sequence from transcriptome shotgun assembly (TSA), of *Lymnaea* brain was sequenced by Illumina Genome Analyzer IIx, and available on NCBI, with the full snail LNa_v1 sodium channel, identified as GenBank Accession Number: FX180203.1, published by (Sadamoto, et al., 2012). We were able to confirm the full length contig generated by PCR sequencing from brain cDNA with the published reference sequence isolated by transcriptome shotgun assembly (See list of primers, Appendix 1). The annotated amino acid translated sequence is illustrated in Figure 3.3 below. The characteristic feature that govern sodium-selective filter is the high field strength site, DEKA, where one residue is contributed by each domain in the re-entrant pore. DEKA is one of the defining features of the Na_v1 sodium channel. Figure 3.2 demonstrates that almost all Na_v1 channels from protostome invertebrates to human channels have a DEKA selectivity filter, where critically, a lysine residue is present in the third domain. The simplest organisms to have a nervous system are the cnidarians. They are classified as the simplest eumetazoans and diploblastic, with two primary germ layers in the embryo compared to three in more complex animals. The cnidarians uniquely have a DKEA selectivity filter, where the lysine is present in Domain II. Sodium currents in motor neurons of the hydrozoan *Polyorchis penicillatus* and the scyphozoan *Cyanea capillata*, demonstrate Na^+-selective voltage-gated ion currents (Anderson, Holman, & Greenberg, 1993) (Spafford, Grigoriev, & Spencer, 1996), confirming the high sodium selectivity of the DKEA selectivity filter. Transfer of the complete pore (P-)loops of the DKEA Nav1 selectivity filter onto a DEEA selectivity filter generates highly sodium selective channels out of calcium-selective ones, but it requires the full pore loop substitution not just the lysine for the complete ion selectivity transformation. Flatworms (*platyhelminthes)* have an unusual DEKG selectivity filter where glycine (G) replaces alanine (A) in the fourth domain of the selectivity filter.

Chapter 2. Materials and methods

2.1 Sequencing and cloning Lymnaea Stagnalis mRNA

2.1.1 Tissue preparation:

Lymnaea stagnalis, giant pond snails, were bred and raised in an in-house vivarium in B1-177, University of Waterloo. This system provides 20% new daily artificial freshwater, with 80% recirculating freshwater filtered by means of mechanical and biological filtration. Snails were exposed to a 12 hr: 12hr light dark cycle and were fed homegrown lettuce from seed in a growth chamber at the University of Waterloo, as well as supplemented with spirulina flakes and fish food.

In preparation to dissection, the snails were placed for 30 minutes in aquarium water with 10% Listerine which served as anaesthetic as recommended by Woodall and colleagues (Woodall, et al., 2003). Once the animals became unresponsive, the shells were carefully removed without damaging the internal organs using Vannas spring scissors.

Snails were pinned down on a resin filled plate with 10 ml 10% Listerine distilled water and dissected under a Zeiss Discovery V8 dissecting microscope. The organs were placed in 1.5ml Eppendorf microtubes and flash frozen in liquid nitrogen immediately after removal, then placed in -80 ^{o}C for storage.

2.1.2 TRIzol RNA extraction

Frozen tissues were resuspended in TRIzol® Reagent at 1ml per 100 mg sample and homogenized with sterile pestle mounted on the hand-held homogenizer. The tubes were then vortexed, incubated at room temperature for 5 minutes, and centrifuged at 4 ^{o}C, 10,000 g for 10 minutes to separate colorless aqueous phase containing RNA (top layer) from the red organic phenol-chloroform phase containing protein and lipids (bottom layer). The aqueous phases were then transferred to new tubes and 200 µl of chloroform was added to each tube. The samples were then briefly vortexed, incubated at room temperature for 10 minutes and centrifuged at 4 ^{o}C, 12,000 g for 10 minutes. The upper aqueous phases were transferred to the fresh tubes that already contained 500 µl 2-propanol in each tube. To precipitate the RNA, the tubes were centrifuged at 4C^{o}, 13,000 g for 10 minutes after 10 minutes of incubation at room temperature. The ethanol was then decanted and the pellets were washed with 70% ethanol and prepared using diethylpyrocarbonate (DEPC)- treated water. Air –dried pellets were resuspended in

DEPC Milli-Q water. The next step involved precipitation with ice cold 5 M LiCl, which was added to the samples at the volume of 86 µl. The tubes were vortexed and incubated at 4^{o}C overnight.

The next morning, RNA was pelleted by centrifugation at 4^{o}C , 13,000 g for 20 minutes, and the supernatant was decanted. The pellets were washed with 500 µl 70% ethanol in DEPC treated water, and resuspended in 200 µl DEPC Milli-Q water. To precipitate oligosaccharides, 20 µl of 2M potassium acetate, pH 5.5, prepared with DEPC treated water was added to each sample. The tubes were briefly vortexed and centrifuged at 4 ^{o}C, 13,000 g for 10 minutes. Supernatants were then transferred to new tubes which contained 600 µl of 100% ethanol and after leaving the samples in -20 ^{o}C for 10 minutes, RNA was pelleted by centrifugation at 4 ^{o}C, 16,000 g for 20 minutes. The ethanol was decanted and the pellets were again washed in 70% ethanol (DEPC) and after being thoroughly air-dried, each sample was resuspended in 50ul DEPC Milli-Q water.

RNA samples were then quantified and assessed for purity using aNanoDrop Specrtophotometer with the expected absorbance wavelength 260/280 ratio of 2.0. The samples were then stored at 80 ^{o}C until further use.

2.1.3 Reverse Transcription (RT-PCR)

To generate complementary DNA strands (cDNA) from RNA, Superscript III RT (Invitrogen) was used. This is a modified version of the protocol provided by Invitrogen. 6 µl total RNA was combined in 1.5 m Eppendorf microcentrifuge tube with 1 µl of 1µM Random Hexamer Primers, 1 µl of 10 µM dNTP and 4 µl nuclease free water. The mixture was briefly centrifuged, incubated at 25 ^{o}C for 5 minutes then placed on ice. While on ice, the following ingredients were added to the tube: 4 µl of 5x first strand buffer, 1 µl of 0.1M Dithiothreitol (DTT), 1 µl of RNAse inhibitor and 1 µl of Superscript III RT. The tubes were than incubated at 42 ^{o}C for 30 min and heated up to 85C^{o} for 5 minutes. Total cDNA was then precipitated by adding 2 µl of glycogen, 34 µl of 10 M ammonium acetate and 80 µl of 100% ethanol to the tube, followed by 1 minute of centrifugation at maximum speed (21,000 g). The pellet was then washed with 70% ethanol and resuspended in 20 µl Milli-Q water. The sample was then stored in a -20 ^{o}C freezer.

2.1.4 Sequence amplification and visualization

Total adult brain cDNA was used to determine the sequence of *Lymnaea stagnalis* sodium channel α and β subunits. Nesting primer sequences were designed using Primer3 and OligoCalc (Oligonucletide properties calculator). The primers were ordered from Eurofin MWG Operon (Table 1). Taq polymerase (Thermo-Scientific) was used for DNA amplification. The Polymerase chain reaction protocol was carried out using the protocol supplied by Thermo Scientific, however the annealing temperature and elongation time were modified each time to accommodate the appropriate conditions for different DNA fragments.

Following the polymerase chain reaction, the samples were mixed with 6x gel loading buffer (0.25% bromophenol blue, 0.25% xylene cyanol FF, 30% glycerol in DI water) loaded on 1% TAE agarose gel supplemented with 200 ng/ml ethidium bromide and placed in an electrophoresis chamber, where 110V current separated the samples into bands according to the fragment size (DNA electrophoresis). PCR gels were placed in a UV chamber, where, at 365 nm, ultraviolet light bands were visualized and/or excised from the gel for subsequent DNA extraction.

2.1.5 Gel extraction

An E.Z.N.A. gel extraction kit (Omega Bio-Tek) was used to isolate purified DNA from the agarose gel. The protocol supplied with the gel extraction kit was used.

2.1.6 Ligation

A pGEMt®-T Easy kit (Promega) which included a pGEMt vector, 2x ligation buffer and T4 ligase was used in ligation protocols. Alternatively T4 ligase and 10x T4 ligation buffer from Thermo Scientific were used.

To ensure uniform sequencing results, each DNA fragment was ligated into a pGEMt®-T Easy vector prior to sequencing. Purified PCR products were mixed with 1 µl vector and 10 µl 2x Ligation buffer in a 20 µl reaction mix. 1 µl T4 ligase was added to each mixture and the tubes were incubated in a DNA thermo cycler at 16^{o}C for 6.5 hours followed by 1 degree decrease every hour until the 4 ^{o}C was reached. The tubes were then heated up to 65^{o}C for 10 minutes to inactivate the ligase.

Alternatively, when proofreading Pfu polymerase was used for amplification, the resultant DNA strands had blunt ends, as opposed to A- overhangs generated by Taq Polymerase. To ensure proper

ligation two methods were employed successfully. One method consisted of generating A-overhangs by incubating purified PCR product with Taq polymerase in the presence of dATP for 30 min at 72 ^{o}C. The other method was to clone PCR products into PCR Blunt II TOPO plasmid (Life Technologies) with built in topoisomerase. While more expensive, this method was highly efficient and worked well when only small amounts of product were available.

2.1.7 Electrocompetent Stbl2 cell preparation

Starter cells were grown on an agarose plate overnight in a 30 ^{o}C incubator and a smaller sized colony was selected for inoculation. Bacterial culture was grown in a glass tube with 10 ml SuperBroth[1] (30 g yeast extract,10 g Tryptone powder , 5 g NaCl , per 1L dH_2O), after inoculation with the selected colony with overnight incubation in a shaker incubator at 30 ^{o}C. The next morning, the contents of the tube were transferred into 250 ml of SuperBroth and the culture was allowed to grow until OD of 0.6 was reached (Since OD above 0.5 cannot be measured accurately, the sample was diluted 1:1 with clear SuperBroth and an expected result of 0.3). After the desired turbidity was reached, the cells were cooled on ice for 30 minutes and centrifuged at 4^{o}C, 4000g for 10 minutes. The resultant pellet was resuspended in 300ml ice cold 10% glycerol, prepared and sterilised by filtering ahead of time. The centrifugation-resuspension step was repeated three more times; the first time with 300 ml, the second time with 20 ml and third time with 2 ml of 10% ice cold glycerol. The concentrated cells were then aliquoted into autoclaved PCR microcentrifuge tubes (30 µl per tube) and flash frozen in liquid nitrogen before being placed in -80^{o}C freezer.

2.1.8 Electroporation and Growth

To introduce vectors into bacterial cells for amplification, the electroporation technique was used. Electrocompetent Stbl2 cells were prepared ahead of time and kept at -80^{o}C. Eppendorf Electroporator 2510 was set to 1200V. 5 µl of circularized vector was added to 30ul frozen cells and the tube was left on ice for 15 minutes. A sterile 1 mm electroporation cuvette (VWR), chilled to -20^{o}C, was filled with a cell/vector mixture using pre-chilled pipette tips. After electroshock in the electroporator, cells were immediately transferred into microtubes filled with 500ul room temperature

[1] Although it is universally recommended to grow Stbl2 in SOC media, I found that SuperBroth works just as well, while requiring less preparation steps.

SuperBroth, and set to incubate at 30 ^{o}C on a rotating platform. Following a 1 hour incubation period, the cells were centrifuged at 3000 rcf . The pellet was resuspended in 50 µl SuperBroth and the mixture was spread on a previously prepared agar plate containing 100 µl /ml ampicillin under aseptic conditions. The bacteria were grown on agar plates overnight in a 30 ^{o}C incubator. The next day, 10 ml SuperBroth glass tubes were supplemented with the appropriate antibiotic and inoculated with colonies from the plate. The glass tubes were placed on a shaker at 30 ^{o}C and left overnight. In the morning the turbidity of the culture was assessed visually and if a sufficient amount of cells were present in the medium, DNA plasmid mini-preps were performed.

2.1.9 Plasmid isolation

Plasmid isolation protocol was adapted by A. Senatore, from (Birnboim & Doly, 1979). Plasmid isolation from the cell culture, referred to as either maxi-pre or mini-prep depending on the cell culture volume, was performed with alkaline lysis. The cell culture (Stbl 2 cell line) was incubated in SuperBroth in a shaker incubator at 30^{o}C until the appropriate density was reached(OD600 >0.6). The culture was then centrifuged at low speed to collect the cells and the pellet was resuspended in one part of physiological buffer (50 mM glucose, 25mM Tris pH8, 10 mM EDTA), and 2 parts of alkaline solution (1% SDS, 0.2 N NaOH) was added to the tube to lyse the cells. After 5 minutes of room temperature incubation, 1.5 parts of neutralizing solution (5M potassium acetate, glacial acid) was added to the lysate and the tube was briefly vortexed and centrifuged at 10000 g to separate plasmids from chromosomal DNA and the rest of the cell material.

The supernatant was collected and mixed with 0.6 volumes of 2- propanol to precipitate the plasmid DNA. The tube was incubated at -20^{o} for 15 minutes , then centrifuged at maximum speed for 10 minutes. The pellet was dried and resuspended in MilliQ water. The solution was mixed with ice-cold 5M Lithium chloride to separate the RNA out of the solution mix. The mixture was incubated for one hour at 4^{o}C and spun at maximum speed for 10 minutes. The supernatant was collected and mixed with equal amount of 2-propanol. After 10 minutes of centrifugation at maximum speed, the pellet was resuspended in 200 µl water and RNAse A was added to a concentration of 50 ug/ ml. The tube was left at 4^{o}C overnight or, alternatively at 37^{o}C for 1 hour. The incubation was followed by Phenol/chloroform extraction, where 400 µl of 50:50 phenol chloroform mixture was added to the solution and the tube was briefly vortexed and spun at 10000 rcf for 1 minute. The upper aqueous layer

was carefully transferred to a new tube, while the bottom layer was discarded. This step was repeated until there was no white precipitate in the interphase between the aqueous and organic layers. The aqueous solution was then mixed with 400 µl of pure chloroform to remove any remnants of phenol. After thorough vortexing the tube was again centrifuged for 1 minute at 10000g and the upper layer was transferred to a new tube. 2 µl glycogen, 20 µl of 10M ammonium acetate pH 5.5 and 800 µl 100% ethanol were added to the solution, the tube was vortexed and placed in -20^{o}C for 15-30 minutes. The solution was then centrifuged at maximum speed for 10 minutes to pellet the plasmid DNA. The pellet was washed with 70% ethanol and allowed to dry for 2 minutes. The plasmid was then resuspended in autoclaved Milli-Q water. The concentration of the plasmid was assessed using the NanoDrop Spectrophotometer, and restriction digest analysis was performed to ensure the presence of the plasmid.

2.1.10 Sequencing

DNA sequencing was done by the TCAG facility at the Sick Kids Hospital in Toronto. To prepare DNA for sequencing, the samples were diluted to 40 ng/µl and mixed with a primer according to specifications found at the TCAG site (http://www.tcag.ca/facilities/dnaSequencingSynthesis.html)

Sequence analysis was carried out with Sequencher® 5.1 and GeneConstruction Kit ® 4.0, with the former to evaluate an error free, full length contig, and the latter to generate and archive vector maps containing plasmid inserts.

2.1.11 Construction of the sodium channel α-subunit vector

Once a consensus sequence of the full length α-subunit open reading frame was created, and confirmed by at least 3 independently made PCR products of every cDNA segment, the coding sequence was divided into four regions; AS, SH, HE, and EX, and primers were deigned to create overlapping fragments corresponding to those regions. The inner fragments (SH and HE) contained naturally occurring restriction sites. The outer fragments (AS and EX) were engineered to have restriction sites flanking the α-subunit to facilitate the construction of a contiguous insert coding for the full length sodium channel within the polylinker of the vector.

When amplifying consensus sequences, precaution was taken to minimize exposure to mutagens and eliminate polymerase induced errors. High fidelity polymerase Pfu turbo AD (Agilent Technologies) was used for amplification to reduce the error rate. Crystal Violet (Invitrogen) was used to visualize the gel bands, instead of Ethidium Bromide and UV light, known DNA mutagens. The Blunt II TOPO plasmid (Life Technologies) was used to create constructs caring the fragments (AS, SH, HE, EX) and these fragments were then concatamerized within pIRES2-EGFP plasmid vector.

2.2 Protein Expression in HEK 293 cells

2.2.1 Expression vectors

Confirmed sequences were ligated into expression vectors pIRES2-EGFP and pIRES2 dsRED: plasmids designed for expression in mammalian cells, with a strong mammalian promoter and an internal ribosomal entry site (IRES) sequence, enabling the expression of EGFP/dsRED protein and the gene of interest in HEK 293 cells.

2.2.2 Cell Culture and Transfection

Human Embryonic Kidney (HEK) cells were grown in 10 cm flasks in DMEM medium with 10% Fetal Serum Albumin (FBS), 1% sodium pyruvate and a 0.05% Penicillin/Streptomycin combination. Each tissue culture was grown at 37^{o}C until confluent, then split 1:4. The cells were allowed to settle at 37^{o}C for 4 hours, then transfected by calcium phosphate precipitation for the purpose of both electrophysiological recording experiments and Western blotting. 600 µl of solution containing 6 -9 mg pIRES vector, 30 µl of 2.5M $CaCl_2$ and 300 µl of HES buffer (280mM NaCl, 10 mM KCl, 12 mM dextrose, 50 mM HEPES, 1.5 mM Na2HPO4) was added to the tissue culture. The flasks were left for 18 hours at 37^{o}C , then washed with 3 volumes of DHEM media and left in 6 ml media for another 2 hours, before being transferred into 28^{o}C incubator. The fluorescent protein expression of reporter proteins allowed for visual conformation of the transfection success rate. The cells were recorded/harvested 72 hours post transfection.

2.2.3 HEK 293-harvesting the protein

Harvesting and protein homogenization were carried out by a modified version of a protocol found in (Harlow & Lane, Using Antibodies: A Laboratory Manual, 1999).Transfected cells designated for Western blotting were incubated at 28^{o}C to allow for sufficient protein expression. Time between transfection and harvest was loosely based on the size of the protein (4 days for an α-subunit, 2 days for a β subunit). Prior to homogenization, MG-132 (Sigma) dissolved in dimethyl-sulfoxide was added to each flask to a concentration of 5 μM in order to suppress protein degradation. After 8 hours of exposure to MG-132, the DMEM media was removed from the flasks and the cell layer was washed 3 times with room temperature PBS pH7.4 (137mM NaCl, 2.7mM KCl, 10mM Na_2HPO_4O, 2 mM KH_2PO_4O). The tissue culture was then placed on ice and 0.5 ml pre-chilled RIPA lysis buffer (150 mM NaCl, 50 mM Tris, pH 7.4, 5 mM EDTA, 1% Nonidet P-40, 1% sodium deoxicholate and 0.1% SDS), supplemented by Sigma Protease Inhibitor Cocktail (DMSO diluted) was then added to each flask. The flasks were incubated on a rocking platform at 4^{o}C for 1 hour. The buffer/lysate mixture was then collected and centrifuged at 4^{o}C to precipitate the cellular debris. The supernatant was stored in a -20^{o}C freezer.

2.2.4 SDS-Page and Western Blotting

Protein homogenate samples were mixed with 6x Laemmli sample buffer (100 mM Tris-Cl pH 6.8, 4% w/v SDS, 0.2% w/v Bromophenol blue, 20% glycerol, 200mM β-mercaptoethanol) and heated up to 95^{o}C in order to denature the proteins. 8 to 10% polyacrylamide gel was used for SDS-PAGE electrophoresis to separate the proteins. To visualise the protein bands, gels were stained with Coomassie Brilliant Blue for 1 hour, then destained overnight in high methanol destaining solution. For the Western blotting, the bands were transferred onto nitrocellulose membrane (Whatman®), using a Mini Trans-Blot Electrophoretic Transfer Cell (Bio-Rad). For the transfer, the transfer cell was placed overnight at 4^{o}C and set at 25V. The transfer buffer was prepared fresh each time and contained 48mM Tris, 39 mM glycine and 20% v/v methanol. Once the transfer was complete, the membrane was briefly stained with Ponceau stain to visualise the bands, then placed on the rocking platform in a bath containing TBS buffer (10 mM Tris-Cl, pH7.5150 mM NaCl) to facilitate destaining. Nitrocellulose membranes containing the transferred proteins were washed two more times in TBS buffer (10 minutes each wash), then incubated in blocking buffer (TBS buffer and 5% w/v milk powder) for 1 hour. Membranes were then washed twice in TBST buffer (0.05% v/v Tween 20 in TBS) and once in TBS buffer. After the wash the membranes were incubated for 1 hour with 1/1000 diluted α -LNav1 sodium

channel specific anti-rabbit antibody in blocking buffer. Following the incubation, excess antibody was washed off the membrane twice in TBST buffer and once in TBS buffer. Membranes were then incubated for 1 hour with secondary antibody diluted 1/5000 in blocking buffer (10% w/v milk powder). The secondary antibody used was a goat anti-rabbit antibody coupled to Horseradish peroxidise (HRP), ordered from Jackson ImmunoResearch Laboratories, Inc. After washing the membrane three times in TBST, a chemiluminescence reaction was performed to detect the presence of antigen on the membrane. To induce chemiluminescence, two solutions were made in separate flasks. Solution 1 (200 µl of 250mM DMSO dissolved luminol, 100 µl of 90 mM p-cumaric in 20 ml 0.1M Tris-Cl) and Solution 2 (12 µl of 30% hydrogen peroxide in 20 ml 0.1M Tris-Cl) were mixed in the dark room and the membrane was immediately submerged in the mixture. After removing the excessive fluid, the membrane was exposed to Kodak X-ray paper for the time increments between 5 to 30 seconds.

2.2.5 Electrophysiology

The external bath solution used for whole cell patch clamp recording contained 130 mM NaCl, 2 mM $CaCl_2$, 1.2 mM $MgCl_2$, 5mM CsCl, 10 mM HEPES, 5 mM glucose, titrated to pH 7.4 with Cs OH. The internal recording solution contained 60 mM CsCl, 70 mM CsAspartate, 11 mM EGTA, 1mM $MgCl_2$, 1 mM $CaCl_2$, 10 mM HEPES and 5 mM Na_2-ATP, titrated to pH 7.2 with CsOH.

Borosilicate glass pipettes with filament (1.5 mm outer diameter, 0.86mm inner diameter) were pulled with Sutter P-1000 and fire polished with MicroForge -830 immediately prior to use. The pipette resistance was maintained at 2-4MΩ. The ground electrode was filled with 3M CsCl. Analog electrophysiology signals were sampled through a Digidata1440a A/D converter (Molecular Devices) using an Axopatch 200B amplifier (Molecular Devices) controlled through pClamp 10 software on a PC computer. HEK cells were recorded in the whole cell mode, at room temperature. Medium size, round cells with weak to medium auto-luminescence were found to produce the optimal recording.

2.3 Antigen Production and Antibody Purification

2.3.1 Antigen production and purification[2]

Two antigens for antibody production were created based on the I-II and II-III linkers of the *Lymnaea* sodium channel α- subunit. Primers were designed with restriction enzyme sites (See Appendix 1), in order to insert PCR amplified cDNA sequences into pET22b vector, which provided an in-frame 6xHistidine tag. The vectors were transformed into Rosetta TM (DE3)pLysS competent cells for protein expression. Protein production was induced by isopropyl-1-thio-β-D-galactopyranoside (IPTG) to a final concentration of 0.3 mM 5 hours prior to cell harvest. The cells were pelleted in 4^{o}C centrifuge and resuspended in PBS buffer (20 mM sodium phosphate, 300 mM sodium chloride, pH 7.4) with an addition of 25 mM imidazole. The cells were then lysed by 3 freeze/thaw cycles with subsequent sonification by Sonicator® 3000 (Giltron). The lysates were centrifuged at 4^{o}C, at maximum speed for 25 minutes, then the supernatant was collected and added to 1.5 ml of Ni-NTA agarose beads (Thermo Scientific). The lysate/bead slurry was incubated for 1 hour at 4^{o}C on a rocking platform then transferred to the gravity column. The column was washed twice with 6 ml of 25 mM imidazole in PBS pH7.5, then 3 more times with 6 ml of 45mM imidazole in PBS pH 7.5 to wash out the unbound proteins. The Histidine tagged proteins were then eluted from the column with 250 mM imidazole in PBS pH 7.5. The eluted proteins were then separated in the SDS-PAGE gel and the bands containing I-II and II-III linkers were excised. The proteins were then extracted from the gel with the use of electroeluter (Bio-Rad) fitted with 10kDa caps. Concentrations of the isolated proteins were established using Nanodrop ND-1000. The final concentration was found to be 11.74 mg/ml for I-II linker and 24.38mg/ml for II-III linker of LNav1 sodium channel. The proteins were stored in -80^{o}C until they were used for antibody production.

2.3.2 Antibody expression [3]

For LNav1specific antibody production, two New Zealand White (NZW) rabbits were ordered from Charles River and housed in the Central Animal Facility in the University of Waterloo. Freund's

[2] This project was done by Neil (Hsing –Tse) Hsueh, a 499 project student in Spafford laboratory. The Methods described above were taken from Mr Hsueh's BIOL 499 Senior Honours Thesis Project, "Production of a polyclonal antibody against a *Lymnaea stagnalis* sodium channel".

[3] The injections and the blood collection were performed by Martin Ryan, the Departmental Technician in Biology department, University of Waterloo.

adjuvant- both complete and incomplete- were ordered from Thermo Fisher Scientific. The rabbits were allowed to acclimatise for 3 weeks prior to peptide injections. For the first antigen injection, 75 mg of antigen was mixed with complete Freund's adjuvant. For each subsequent injection, same volume of incomplete Freund's adjuvant was used. The emulsion was mixed using 2 glass syringes connected by a double-hub needle. The mixing process began 10 minutes prior to injection and continued until the emulsion became viscous. Each immunogen had a designated needle and set of syringes. 10 ml blood was taken from each rabbit prior to each injection and used for serum extraction. Overall 4 injections were performed, each 20 days apart, before the animals were exsanguinated. The serum collected prior to the first injection was labeled `pre bleed` serum and used as a negative control. The serum samples collected after subsequent injections were used to test the progress of antibody production. After the final bleed, 150 ml blood was harvested from each animal.

2.3.3 Serum preparation

Centrifuge tubes filled with 10 ml animal blood was left at 37^{o}C for 1 hour, mixed with glass rod to separate the clot from the walls of the tube and left overnight at 4^{o}C. The next morning the serum (the liquid fraction) was decanted into a fresh tube and centrifuged at 6000g for 10 minutes. The serum was tested both against the antigen and the clone of LNav1 α-subunit raised in HEK cells in Western blots. Serum aliquots of 500 µl were stored at -20^{o}C for further use.

2.3.4 Antibody purification

Polyclonal antibody separation from blood serum was done using the SulfoLink Immobilization Kit (Thermo Scientific). Four serum aliquots (2ml) were thawed until the samples reached room temperature. The serum was then mixed with 17.8ml MilliQ water and 0.2 ml 1M Tris pH 7.5 to the final volume of 20 ml and filtered through a 0.45 µm syringe filter. The Sulfolink column was washed 4 times with one volume (2 ml) of TBS buffer. One volume of sample was added to the column and it was then incubated on a rocking platform at room temperature .Following 15 minutes of incubation, the column was centrifuged to remove the flow through. This step was performed nine more times until 20 ml of sample had passed through the column. The resin was then washed twice with one volume TBS buffer, then the antibody was eluted with 2 ml acidic elution buffer (0.1-0.2M glycine-HCl , pH 3.0) into a microtube containing 100 µl neutralising buffer (1M Tris-HCl, pH 8.5). The elution step was repeated

three times and all fractions were collected. Antibody purity was tested with SDS-PAGE gel. Antibody activity was tested against the antigen, the clone of LNav1 α-subunit raised in HEK cells and snail brain lysate by Western blotting. The purified antibody was aliquoted into 25 µl samples and stored in a -80^{o}C freezer.

2.4 Co-Immunoprecipitation

2.4.1 Snail organ homogenate preparation

RIPA buffer was used initially to lyse snail organs, before it was substituted with a more gentle CHAPS buffer (30mM Tris-HCl pH7.5, 150 mM NaCl, 1% v/w CHAPS from Thermo Scientific) which is better suited for co-immunoprecipitation experiments. Twenty snail brains were extracted from adult snails (see section 2.1.1 for details). The brains were submerged in 400 µl buffer (20 µl per brain), supplemented with 4 µl protease inhibitor cocktail (Sigma-Aldrich). The sample was incubated on ice for 10 minutes, and a mini pestle was used to grind the tissue. After another 10 minutes on ice, the sample was centrifuged at 4^{o}C 10000 g for 10 minutes; the supernatant was collected and used for downstream applications.

2.4.2 Pre –clearing step

A pre-clearing step was performed on the lysate samples to eliminate proteins that unselectively bound antibodies with a protocol adapted from (Harlow and Lane, 1999). For this step, pre-bleed serum (serum collected from the same animal prior to antigen injection) was added to the lysate in a 1:20 ratio (95 µl lysate, 5 µl serum). The mixture was incubated on a rocking platform at 4^{o}C for 1 hour. SAC (Staphylococcus aureus Cowan strain) was used as a source of protein A. 100 µl of fixed SAC (Sigma-Aldrich) was centrifuged at 10000g for 30 seconds and the pellet was resuspended in 100 µl CHAPS buffer by mixing the pellet with the pipette tip. The sample was centrifuged again and the buffer removed. The SAC pellet was resuspended in lysate/serum mixture. The resulting slurry was incubated on ice for 30 minutes, then centrifuged at 10000g for 15 minutes at 4^{o}C. The supernatant was transferred to a new microtube.

2.4.3 Purification of α/β subunit complex

The supernatant collected in step 2.3.3 (~500 µl) was mixed with the LNa_v1 α-subunit specific antibodies. For the antibody source, both final bleed serum (1 µl) and Sulfolink purified antibody (5 µl) were used and they both produced the same results. The sample was incubated on ice for 1 hour. Meanwhile, 100 µl of protein A agarose beads in saline buffer (Sigma-Aldrich) was centrifuged and resuspended in CHAPS buffer in a 1:10 ratio. The lysate-antibody reaction was added to the protein A suspension to a total volume of ~1.5 ml and the sample was incubated at 4^oC on a rocking platform. Following the incubation, the agarose beads were collected by brief centrifugation and washed three times with CHAPS buffer. After complete removal of CHAPS buffer with the last wash, the protein complexes were eluted from the beads by adding 50 µl of 1x Laemmli sample buffer to the pellet, heating the sample to 85^oC for 10 minutes and collecting the supernatant. The sample was then loaded onto the SDS-PAGE gel directly to analyse the results of co-immunoprecipitation. Negative controls used in α/β complex purification included snail foot tissue (qPCR indicates that snail foot tissue does not express LNa_v1 α-subunit) and lysed HEK cells transfected with LNav1/pIRES2 EGFP vector (expresses LNa_v1α but not β).

2.4.4 Preparation of sample for Mass Spectrometry

Once the candidate band was localised, the purification of LNa_v1 α/β subunit complex was repeated, but this time precautions were taken to avoid keratin contamination. The working surfaces, including the SDS-PAGE rig and glass plates were wiped with 100% ethanol, a new lab coat was obtained and sterile15 cm Petri plates with closed lids were used for staining and destaining. The band excision was performed in the laminar fume hood with a new sterile scalpel blade. The gel band was submerged in 40 µl of 1% acetic acid in Milli-Q and shipped to SPARC BioCenter (Sick Kids Hospital) for trypsin digest analyses and determination of protein size and sequence using electrospray ionization and tandem mass (ms/ms) spectrometry.

Chapter 3. Sodium channels LNa$_v$1 and LNa$_v$2: Results, Analysis and Discussion

The contig of the newly sequenced LNa$_v$1sodium channel was converted into an amino acid sequence and functionally important regions of the channel were identified. Those include twenty four transmembrane domains, four conserved voltage sensor motifs, fast inactivation motif MFM and selectivity filter with characteristic inner and outer sodium selectivity rings (Figure 3.1).

```
MEEETVERTPFRLFTRESLFNIERRIAEEEAAKHAEKVKPESDDEDDDDASQNEETLKPNPKLEAGRKLPPSLEDYPREYIGKP
LEDLDEFYHNQKTFVVLNKDKAIFRFSATNAIFLLSPFNPIRRTAIYILTHPGFSLLVMLTILVNCASMAITSWTPPPYVEHIF
LGIYTVEAFIKTLSRGFILKPFTYLRDPWNWLDFFVISIAYMTMAIKSLGNLSALRTFRVLRALKTISVIPGLKTIVGALLEAV
RRLRDVMILTIFVLSIFALVGMQLYSGSLRRKCIKNYRIFYGANISHDEWWEWVNNESNWRTDHYNEIQVCGNNSGAGQCGNNT
FNGTAEYECLPGIGKNPNFDFTSFDNFGMALLCAFRLMTQDYWESLYRLVLRAEGMAHCLYFVLVIILLGSFYLVNLILAIVAMS
YDETQKQDQADAEEEAAERQEEEARKEALSIMTKSPSNSSWNNDFFAGVRTAGDKAEEKERLSLTSDHSATSAHLKPSRLNQKR
HSLSLPGSPYIHRRNSRGSQYSWRKPVPTAKRSPYCPDRQPLVHHTLENLPLPFADDSAAVTPSSEDLCNFSFIRNMPNGRRFS
FASQRRPDGTGRSGSRRSSFASNHSRASRTSRGSGQGDRTKTQTLLNFKKGKVPDVVLDKSKLDDDQDSVSSGGSGHCPEKDKA
SESNPFLSNTPGGPNVEMKDVMVLKDILDQASGHRRSFVSMASIQQKTMKDIMWKYFCTWDCNPNFQKLQRLVSLFIMDAFVDL
FITVCIVVNTLFMAMDHYNMDKNLQDISSQANEVFTAIFAAEAFLKILAMSPVVYFKDGWNIFDSLIVALSLMELSMKELPGLS
VLRAFRLLRVFKLAKSWPTLNMLIAIVARTMGALGNLIIVLAIVIFIFAVMGQQLFSTHYAIYLYKELDNGTKVYDIDNMPRWN
FNDFLHSFMIVFRVLCGEWIESMWWCHKAAGWPCVPFFLLTYIIGNLVVLNLFLALLLSSFGGESLSRSESADEPNKIAEAIDR
FKRFGNWVKVKIIVCIKVKLQRQKNWRPSVPPSKLPELNGKENAFGDGTVIAMEKTPDDFPDGAMEPDDCFCYSLTKRCTWCLV
IEKPPIGRAWWALRCFMYRLAEHRYFDTFIIVMILLSSCALALEDAYLHEKPLLKEILEYMDKVFTVIFIVEMLVKWFAFGFKT
YFTDAWCWLDFCIVMLSIMMLMADMMASADGHGGGKMGAMRSIRTLRALRPLRAVSRWEGMRVVVNALFKAIPSICNVLLVCLV
FWLIFGIMGVQLFNGKFHACVCENGTRCEPDVIPNRTVCELQGYNWTNAQINFDNVIAAYLALFQVATYKGWVDIMNNAIDARE
IGVQPKREENIYSYLFFVLFIIFGSFFTLNLFIGVIIDNFNSQKKKAGGSLEMFMTDDQKKYYNAMKRMKSKSPQKSIPRPKYK
LAALVFDITTDQKFDIVIMIIIILNMLTMMFEYEDMSKQMKDILGIFNLVFITIFTAECVLKLFGLRWYYFKVPWNVFDFIVVV
LSIMASSLDEFEDSFFISPTLLRVIRVFRVGRVLRLVKSAKGIRTLLFSLAVSLPALFNIGLLLGLVMFIYAIMGMNFFQGYPQ
TFGMDDAFNFDTFLSSFILLFQMCTSAGWSDVLNALISPCPPTGSCSHYNKATLYLATYLIISFLVVVNMYIAVILENFSQATE
DVQQGLTPDDFDMYYEKWEKYDPKATKYIPLDQLSDFVDYLEEPLRLPKPNHFILVKLDIPICEGDKCYCRDILDALTKNFLGT
SETADIPIKETDKEKEEYTPISSTLRRQKEHYAARIIQKAYRNYKGLTISEVSYGHEDVMDSYSQDNDDDRDSGGSSGRNLDKS
FPSPPSSYKSDKKPPENGTKEKKSEDSSKKAKDKKDKGKDKKAKSDKKDDGKKKKDASKPPNGLSKTTRSKESAAITLIMKRTV
ELGPDSGVVA
```

Figure 3.1 Open reading frame of LNav1 α-subunit.
The protein sequence has been analyzed with ExPasy(SIB Bioinformatics Portal) to reveal 24 transmembrane segments (in turquoise color) grouped into four repeat domains. The voltage sensing 4th segment of each domain carries a string of positively charged amino acids (in purple). The components of the selectivity filter are shown in yellow. Shown in red is the rapid N-type inactivation motif. Dark grey indicates the sites of splice variations.

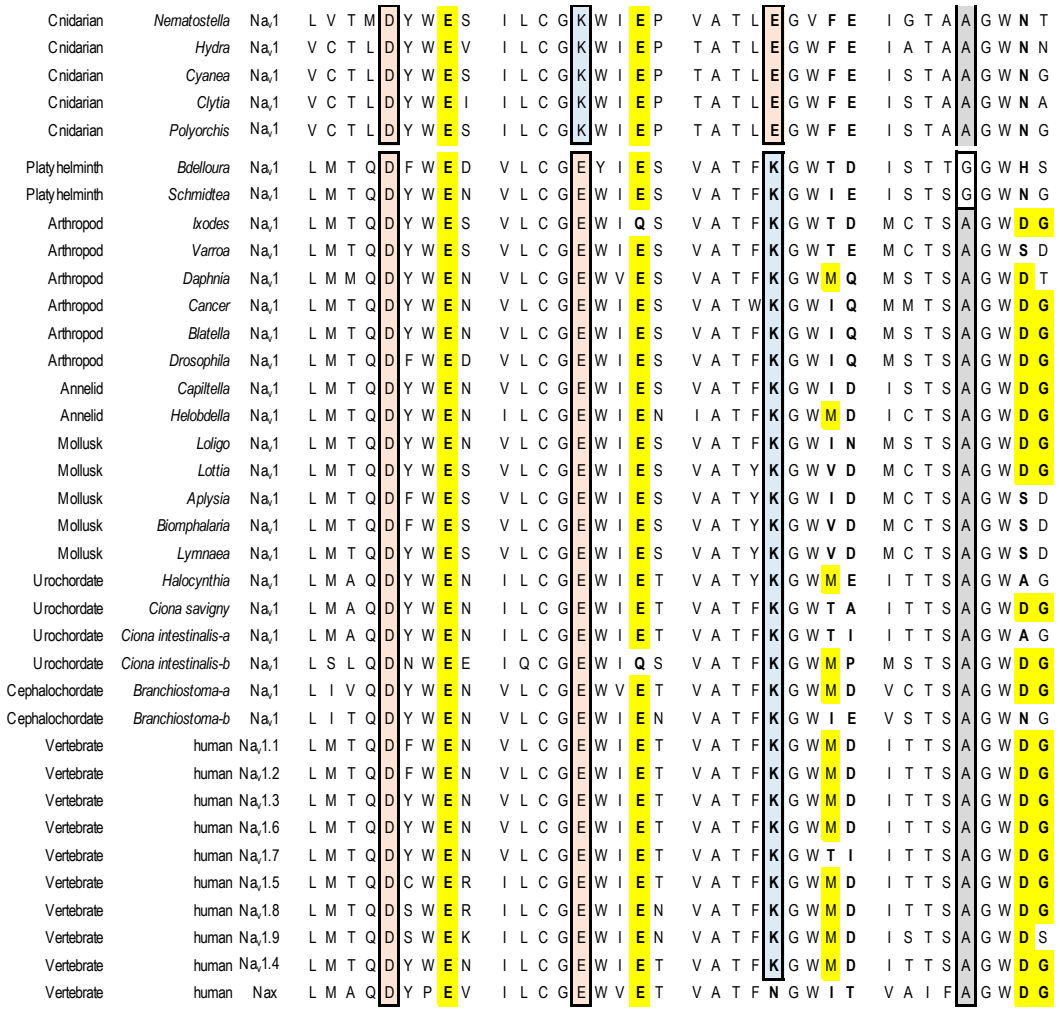

Figure 3.2 Selectivity filter of the sodium channel Na_v1.
Pore loop selectivity filter residues of four domains of Na_v1 contribute to the characteristic DEKA the ion selectivity filter, characteristic of most Nav1 sodium channels. Downstream of DEKA there is a EEDD consensus sequence which forms the outer ring of the selectivity filter and together with other residues highlighted in yellow is known to be involved in TTX sensitivity(Catterall W. A., 2005).

The full alignment of *Lymnaea* Na_v1 amino acids sequences with highly homologous channels identified from other mollusks is shown in Appendix 3 (Alignment 1) and a comparison with representatives of the closest homologs of human sodium channels (Nav1.1 and Nav1.7) are shown in Appendix 3 (Alignment 2).

3.1.1 Splice variants found in α-subunit

3.1.1.1 Mutually exclusive exon in LNav1 sodium channel α-subunit coding for Domain I, segment 1.

Mutually exclusive exons were identified coding for Domain I S1 domain, coded as exon 4a and exon 4b, and these are found side by side in *Lymnaea* genomic sequence provided by Angus Davison (University of Nottingham) (Liu, et al., 2013). See Appendix 4. Genomic region 1 for the sequence of LNav1 from *Lymnaea stagnalis*.

Exon 4a: 78 bp of novel sequence found by PCR cloning:

GGTTTTAGTCTTTTGGTGATGCTGACCATTTTAGTAAACTGCGCCTCTATGGCCATAACTTCGTGGACACCCCCGCCC Exon 4b:

75 bp of novel sequence identified in published *Lymnaea* transcriptome, GenBank Accession # FX180203.1

TTGTTTAGTTTGACTGTTATGATCACCATCATCACCAACTGTGTCTTTATGGCTCGCGCTGAAAATCCGCCAGAA

Exon 4a is one amino acid longer then 4b.

Amino acids:

```
4a    G F S L L V M L T I L V N C A S M A I T S W T P P P
4b    L F S L T V M I T I I T N C V F M A R A E N _ P P E
```

Lymnaea LNav1 sodium channel was aligned with genomic regions for exons 4a/4b of Nav1 sodium channels from closely related species *Biomphalaria glabrata* (pulmonate freshwater snail), *Aplysia californica* (California sea hare) *Lottia gigantea* (giant owl limpet) *and Loligo bleekeri* (spear squid) along with human sodium channels (Figure 3.5). The alignment analysis indicates that homologous, mutually-exclusive exons 4a/4b are identifiable in other molluscan Nav1 sodium channels.

Gastropod snails, *Lymnaea*, *Biomphalaria*, *Aplysia* have both exons 4a/4b but *Lottia* sodium channel α subunit, otherwise highly homologous to *Lymnaea*, posesses only exon 4b, which suggests possibly that exon 4b variant is ancestral to exon 4a isoform. Splice variations in this region are not found in non-molluscan species to date.

The functional difference between these two variants is unknown, but since it codes the region spanning the first of 24 segments, it may facilitate membrane insertion or trafficking. We have not succeeded in cloning an LNav1cDNA with exon 4b yet.

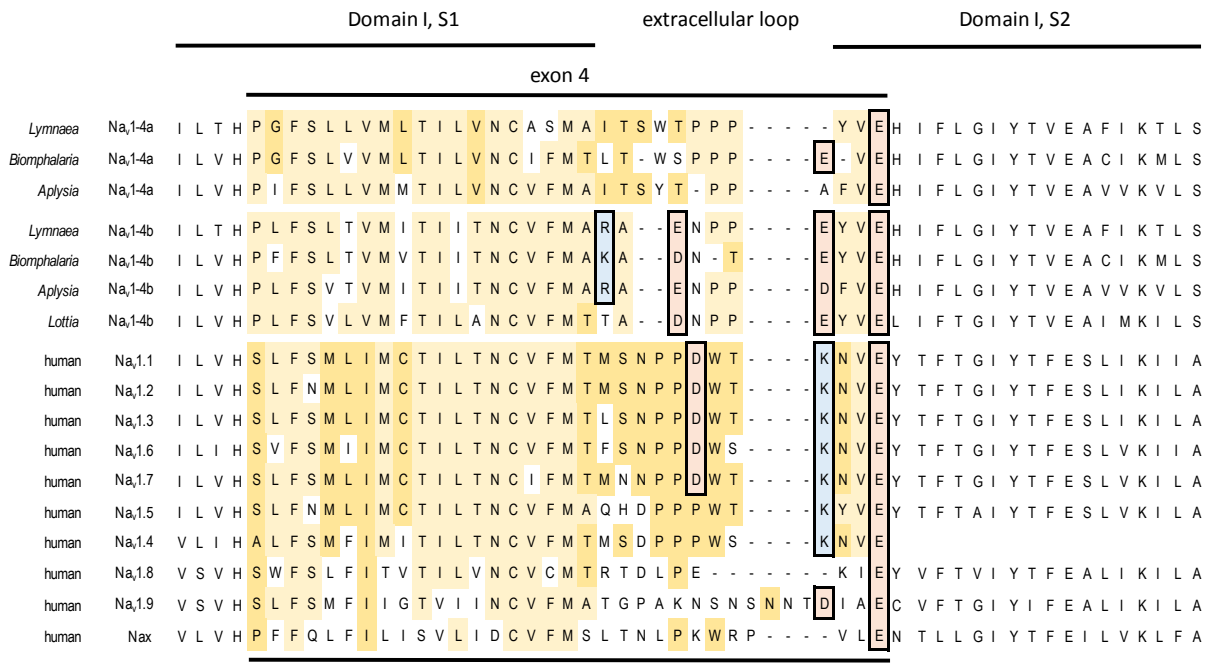

Figure 3.3. Alignment of the mutual exclusive exon 4a/4b splicing in Domain I, segment 1 of molluscan sodium channels, compared to the homologous exon region in human Nav1 channels.

Exon 4b differs in possessing two to three extra charged amino acids that are missing in exon 4a. These extra charges could be connected to the functional differences associated with expression of the two exons.

3.1.1.2 Optional exon in II-III linker region (optional exon 21) found in LNav1 sodium channel α-subunit

The optional exon region is 174 bp long and translates into 58 a.a. and is inserted at a phase 0 splice site where the exon splices into the reading frame without disturbing the reading frame.

The optional exon 21 is found in the distal portion of the II-III cytoplasmic linker, upstream of which is an ankyrin binding motif found only in vertebrate Nav1 channels that promotes clustering of Nav1 channels at nodes of Ranvier of myelinated vertebrate axons.
This exon possesses an unusually high amount of serins, some of them conserved among different molluscan species (Figure 3.4).

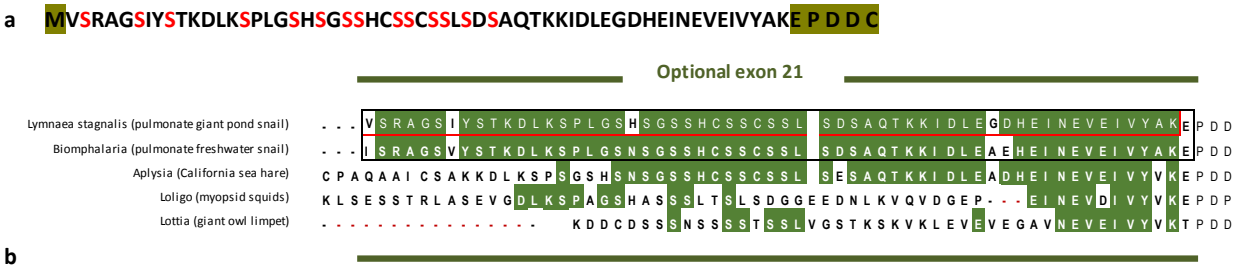

Figure 3.4 Optional exon 21 in molluscan and human sodium channel α-subunit.

a. The amino acid sequence of optional exon 21(adjacent exons shown in green). There are 14 serines concentrated in the 35 a.a. stretch of the exon (red).
b. Optional exon 21 is conserved among gastropods *Lymnaea*, *Biomphalaria* and *Aplysia* but only the distal part of it is conserved in more distant mollusks *Loligo* (squid) and *Lottia* (limpet snails). Two serines are conserved among all gastropods compared, while 5 more are somewhat conserved.

LNav1α /pIRES clones both with and without the II-III fragment were made. They are referred to as LNav1α (-) and LNav1α (+).

3.1.2 The construction of the full length α-subunit clone

Once we had confirmed the reference mRNA sequence of the snail LNav1 sodium channel, we split up the snail Nav1 channel coding region into four equal parts, put together with unique restriction sites into mammalian expression vector pIRES2-EGFP fitted with an adaptor to accommodate the four unique restriction sites (See Appendix 1Table 5.2. Primers for full length α-subunit contig construction in pIRES vector for primer sequences). The adaptor consisted of two self-annealing 50 bp linker sequences

spanning XhoI and XmaI overhang and containing four internal restriction sites for cloning, MluI, SpeI, HindIII and EcoRI:

XhoI overhang MluI SpeI HindIII EcoRI XmaI overhang

TCGACCCAAACGCGTCCAAACTAGTCCAAAAGCTTCCAAGAATTCCCAAC

GGGTTTGCGCAGGTTTGATCAGGTTTTCGAAGGTTCTTAAGGGTTGGGCC

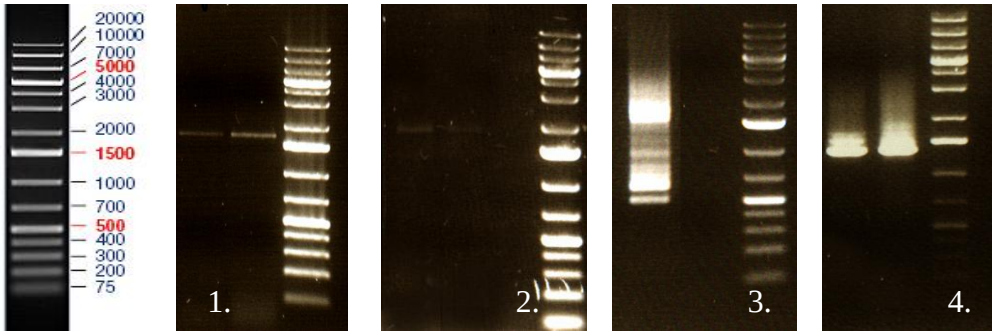

Figure 3.5. Amplification of four overlapping fragments coding for the LNa$_v$1 α- subunit. Overlapping cDNA fragments amplified with unique restriction sites : 1.MluI-SpeI, 2.SpeI-HindIII, 3.HindIII-EcoRI, 4.EcoRI-EcoRI[4]. The level of PCR amplification varied with differing PCR primer sets but all PCR products were successfully ligated into TOPO Blunt vector and transformed to collect sufficient amount of cDNA inserts for construction of the final full length Nav1 α-subunit cDNA clone. See the sequence of the full length LNav1α in Appendix 2. See the vector map of pIRES2 –EGFP with LNa$_v$1 insert below.

[4] The direction of the Fragment 4 insertion into EcoRI site was confirmed by control digest with KpnI, XhoI.

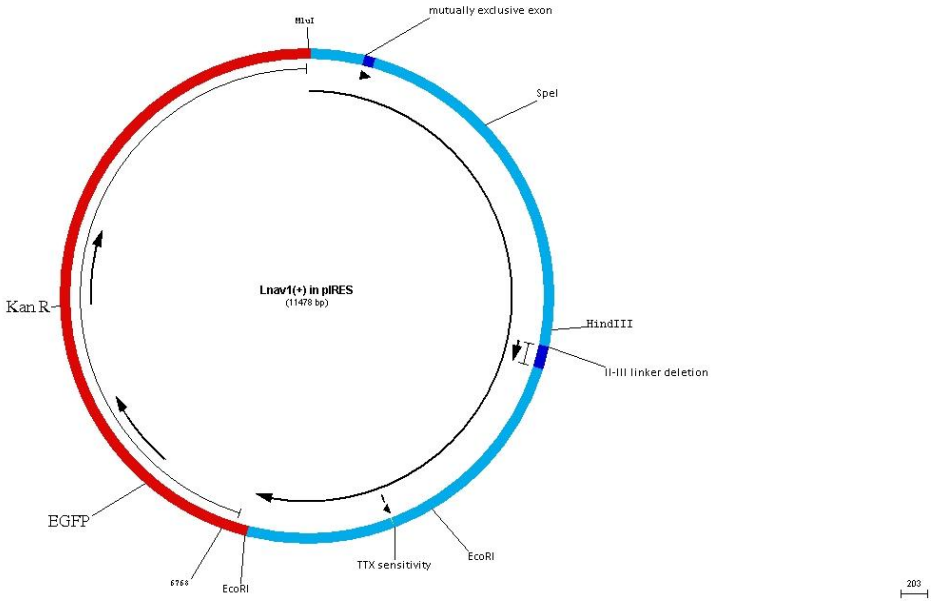

Figure 3.6. Vector map of pIRES2 –EGFP with LNa$_v$1 insert.

The electrophysiological recordings of HEK cells transfected with LNav1α – both with (+) and without (-) optional exon 21, with exon 12a, failed to demonstrate any sodium current above ~100 pA, that could be accounted above the low level of contaminating, native human Nav1.7 α-subunit that has been detected in HEK-293T cells. Attempts to record the snail LNav1 channel in combination with co-transfected human Na$_v$1 channel beta subunit homolog β1[5] and *Drosophila* beta subunit homolog, Tip-E[6] did not generate any positive results either.

Although we did not obtain expression characteristics of the snail LNav1 α subunit, there were a number of things we identified about the expressed gene. qPCR analysis revealeds that the *Lymnaea* Nav1 is limited to the brain and is not expressed in internal organs. We have not yet separated different sensory organs to assess whether Nav1 is also present in sensory organs such as lips, eyes and tentacles.

[5] The clone of human B1 was generously donated by Lori Isom`s Laboratory.
[6] The clone of Tip E along with the clone of rat beta1 was graciously provided by Ke Dong`s laboratory.

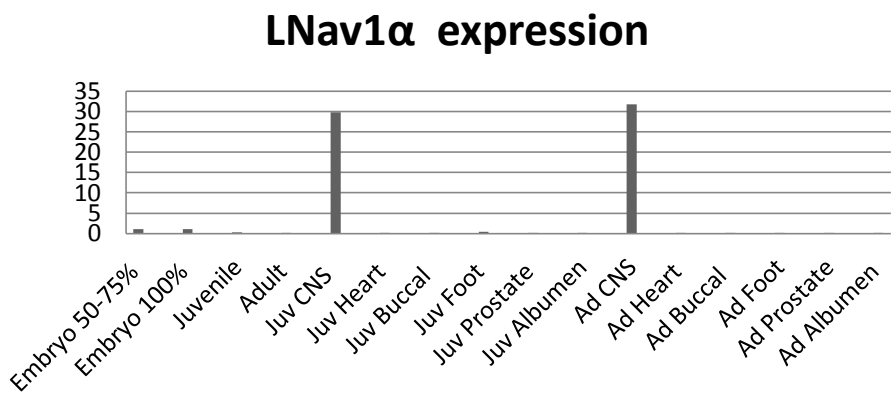

Figure 3.7 Quantitative PCR analysis of *Lymnaea stagnalis* internal organs for the presence of LNa_v1[7].

Expression of LNa_v1 in internal organs and whole animals at various developmental stages (embryo, juvenile, adult) were analyzed with qPCR. 50%- 75% embryos taken 5-6 days after the egg mass was deposited. 100% embryos were taken when the snails were fully formed inside the eggs, just prior to hatching: 10-11days after the egg mass was deposited. The state of the snail embryonic development and maturation was based on the schedule established by (Nagy & Elekes, 2002).This diagram demonstrates the prevalence of Na_v1 in the brain, both adult and juvenile but not anywhere else.

The sequences of the two major variants of LNa_v1 α subunit were submitted to GenBank and received the following accession numbers:

LNav1 exon 4a + KM283185 (coding for LNav1 exon 4a and + optional exon 21)

LNav1 exon 4b + KM283186 (coding for LNav1 exon 4b and + optional exon 21)

3.2 Analysis of calcium selective sodium channel LNav2

In parallel with cloning a sodium selective Na_v1 channel, I was attempting to sequence and analyse the expression of the snail calcium-selective Na_v2 channel. This is a more ancestral version of a sodium channel, found in a simple single cell eukaryote, before the fungal-animal split (*Thecamonas trahens*) to most invertebrate phyla but notably absent in vertebrates. The Nav2 channel has been associated with sensory systems.

I used primers designed by Dr Spafford (see Appendix 1). The PCR primer sequences were originally based on homologous regions in genomic sequences spanning Nav2 channel exons in other

[7] The qPCR was performed by A. Senatore as part of his research on T-type calcium channels.

gastropod snails, *Lottia*, *Aplysia* and *Biomphalaria*, and later compared with *Lymnaea* genomic sequence once the first cDNA fragments were isolated from PCR reactions. After the initial success of finding N-terminal sequence in mRNA from snail tentacles, I was not able to find a fully expressed LNav2 in any of the snail organs that were tested. The project of cloning LNa_v2 was therefore abandoned in favor of other research directions.

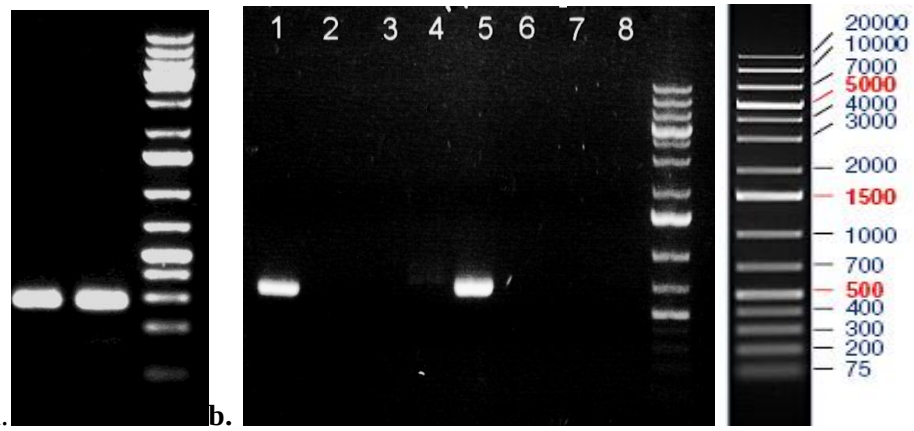

c.

MSEMKIVPLAFRPFTEESH
KALLEREAELNQRDLHRAR
HAQDAHLVDGELKFGSQED
EDTLPPENPDLKEGNALTK
AYGRFPNRLLGCPIEEIDP
GIRDKFVVIGSRFGKKFIY
RFTATKSLFILAPWHSLRR
LTLRIATNQFFDLCIFLTI
IVNCVFLAVPYLPIAENIE
YLFLAIYTLECIIKIMARG
FVTHKHTYLFDPWNWLD

d.

MSEMKIVPLAFRPFTEESHKALLEREAELNQRDLHRARHAQDAHLVDGELKFGSQEDEDTLPPENPDLKEGNALTKAYGRF
PNRLLGCPIEEIDPGIRDKFVVIGSRFGKKFIYRFTATKSLFILAPWHSLRRLTLRIATNQFFDLCIFLTIIVNCVFLAVP
YLPIAENIEYLFLAIYTLECIIKIMARGFVTHKHTYLFDPWNWLDFIVIVTAYMTIVLQLVSQEMTVGNLQGLRTFRVLRA
LKTVSIVPGLKTMVSALLRAFKMLFEVILLTFFCLMVFAMFGLQIYMGAFRNKCVMNVTGYVENPSQTYDDYYAKWIRNPD
KWHQADGEYIICGNLSGSGTCPDSYICLAGIGDNPRFGYLSFDHFGWALLSCFQLITLDFWEDIYNKAIRATGPWNVIFFI
IVIFFGSFYLINLMLAVVSMSYEEEAADELIDPDIGALEGQVIDRNCDCCERWMCLYIPFLKMQNHFYVFVSDPLFDLIIT
FCIFINTLFLSLEHHNQSSTLTTTLTVSNIIFTCVFILEAFCKIIGLGKYYFMVGWNIFDLVIALASLLDLGLEQVDGLNV
LRTFRLLRVFKLAQSWPTMRLLLTIIVSTLGALGNLCLILCIVIYIFAVIGLQLFRTQYTAENFGKDGVPRWHFKDFYHAM
LMIFRVLCGEWIEPLYDCMKASSELCMVVFLPALVFGNFIVLNLFLALLLNAFASDSLDKHRESSTERSKLMEGFDRLQQL
FCCCFTCPNGKVGPAGNTTQNASQGEADADSLNDTAFGRNWHLFRVFIKRIVDHRFFELCVLIMILGSSLSLAFEDIYLYQ
RPTMMYVLGICNITFSVLFTIEMILKWIGLGLTEYFTNFWTILDFFIVFISLLGLIGDYIGLGSVAAFRSLRTLRSLRPLR
AISRWQGMKIVVNALMNAIPAIINVLLVCMVFWLIFSIMGVQFFKGRFYKCKNTTSLTVFDASVVPNKNVCLAVGGAWENS
NVNFDNSAVGFLALFQVATFEGWMEVMRDAVDSTSVTNLYAYLYFIVFIVFGSFFSLNLFIGVIIDNFNVLKKRYEGSYLD
AFLTQSQRNYYNTLKKLGKKKPQKTIKRPKNKFQLFFYNLSMSSKFEISIVLLIFCNMVNMAVEHYHESGAVTDGLEMINL
LFTAVFTLEAVVKILGLRHHYFRFLWNLFDFTIVTVSLFAELFNFVMDNLFVTPTLLRVIRVFRIGRILRLIKGAKGIRKL
LFALIISLPAIFNIGALLFLIMYMYAIIGMSSFIHVRVNGVMTEIINFQTFGNSFMLLLRLATSAGWNDILEALLISPPYC
NPNFYTLPDGTMKESVYGDCGTPYLAIPYMVSYIIIVWLIVINMYIAVILENFSQAHEQEEVGITEYDFDMFYVTWEKYDP
LATQFIKFDQLANFVGDLEQPLQIPKPNEIALVSFNIPIMEGEKMHCLDILIALVRNVLSDVEESEELKTLKEQMEAKFAE
NFPARVNITVKSSTLQRKKEDVAARTLQRAWRSYKAHKAMRNITALAVQLKIRKAGNAGLRSRSEAIRNLDTNLTSALTYF
NNRDPNANPESSDMNVSENALSRQIQVKTMSEISSPASQQPSKVHTEPL

Figure 3.8. PCR amplification of snail sodium channel LNa_v2 fragment and sequence of a full-length amino acid contig formed out of snail genomic sequence .

a. A 280 bp amino terminus encoding region spanning the start codon of snail LNav2 was amplified from juvenile snail central nervous system cDNA and sequenced. The 280 bp fragment is contained in Exon 1 in the genomic region of LNav2, identified in *Lymnaea* genome sequence available from Angus Davison (Liu, et al., 2013).

b. Using newly designed primers, a 650 bp amino terminal encoding fragment including region downstream of the first fragment was isolated from eye (1) and tentacle (5) tissue. The fragment spans

the first two exons 1 and 2, thus confirming that the source of the amplified sequence in eye and tentacle mRNA but not genomic DNA, which could have been the source of the first 280 bp fragment.

c. Amino acid sequence of the amino-terminus fragment. Exon 1 and exon 2 shown respectively, in grey and yellow. (See Appendix 4, Genomic region 2).

d. Proposed sequence of Nav2 formed by contiguous spliced exons identified from genomic DNA. The transmembrane domains are shown in blue, Voltage sensors are indicated in purple and ion selectivity pore is highlighted yellow. The proposed hinged lid motif (AFL) responsible for fast inactivation in sodium channels is shown in red. The hydrophobic region analysed to find the transmembrane regions was performed with ProtScale in ExPASy (SIB Bioinformatics Resource Portal) and TMPred(Hofmann & Stoffel, 1993).

The Nav2 sodium channel has been cloned and expressed from German cockroach *Blatella germanica* and fruit fly *Drosophila melanogaster* (Zhang, et al., 2013) as well as sea anemone *Nematostella vectensis* (Gur Barzilai, et al., 2012). It is a calcium-selective sodium channel, with a DEEA selectivity filter which lacks the lysine in the pore that confers sodium selectivity. Replacement of the pore-loop from Domain II not just including the lysine residue in DKEA will generate a sodium selective channel out of the calcium selective one.

Below is the comparative alignment of the pore loop sequences of invertebrate Nav2 channels. Most of the Nav2 channel sequences have DEEA in the pore selectivity filter, except notably the simplest one, *Thecamonas* which has a DEES selectivity filter. The alignment of full length molluscan Na_v2 homologs is illustrated in Appendix 3 (Alignment 6).

The genomic contig of the LNa_v2 exon sequence was submitted to GenBank and received the accession number 282660.

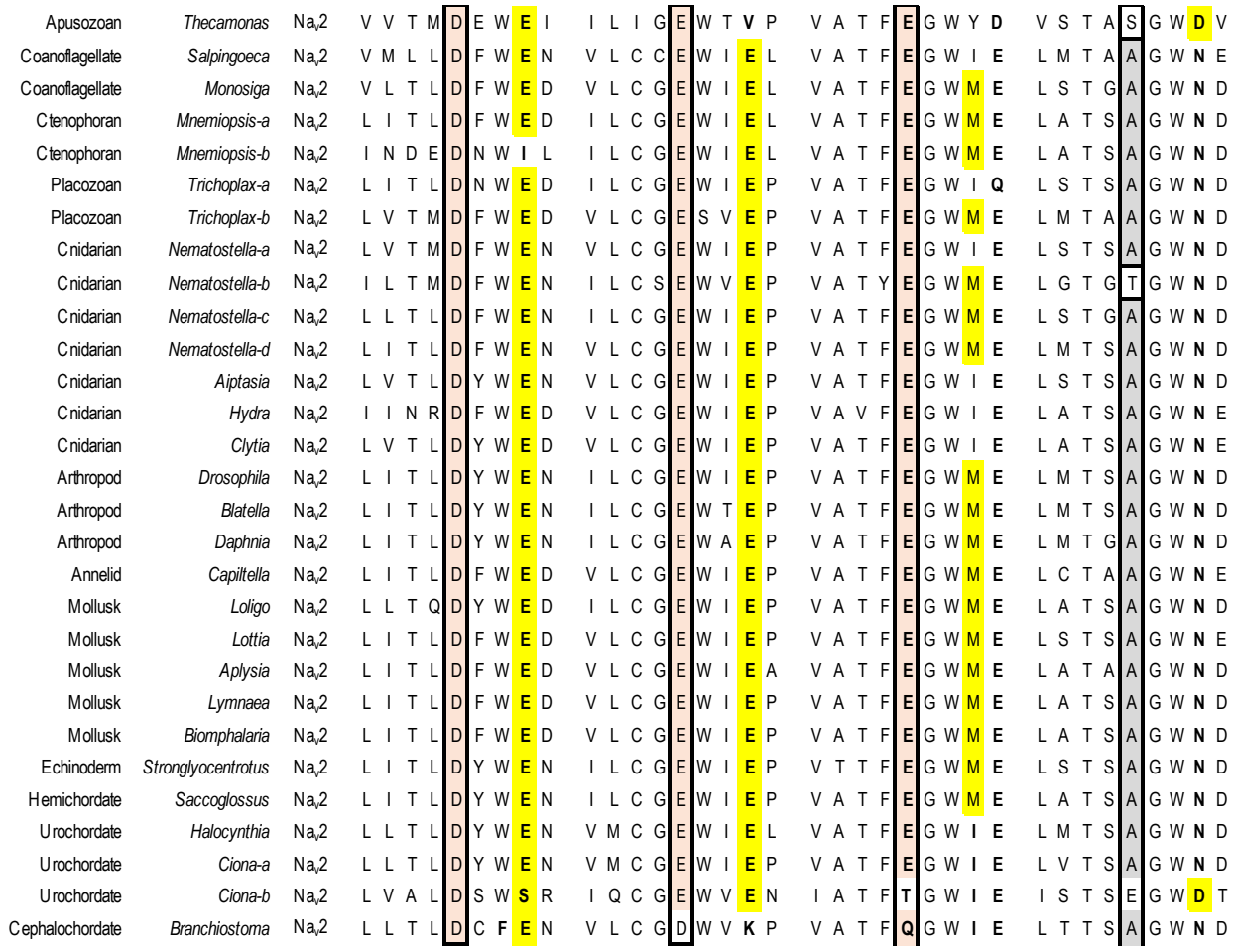

Figure 3.9. **Alignment of pore selectivity filters residues in calcium-selective Na_v2 channels**
The inner, high field strength (HFS) site in selectivity filters is boxed. The outer ring is highlighted in yellow color. Nav2 channel HFS site is typically DEEA. There is a variations in the apusozoans (pre-animal fungi/split) with a DEES pore. Cephalochordate, *Branchiostoma* is DDQA, and there are unusual DEET and DETE pore of second Nav2 isoforms from *Nematostella* and *Ciona*.

3.3 Notable features from the gene structure of snail LNav1 and LNav2 channels

3.3.1 Conserved voltage sensors

All voltage-gated ion channels including 1x6TM potassium channels, and 4x6TM channels like sodium channels (Nav1 and Nav2) as well as calcium channels (Cav1, Cav2 and Cav3) and NALCN have voltage-sensing S4 segments. The human Na_x, which is not voltage sensitive, contains mutations in DI and DIII voltage sensor regions, which are almost identical in other sodium channels in different species. The homology of the S4 region is evidence for the conservation of voltage sensitivity associated with most Na_v channels.

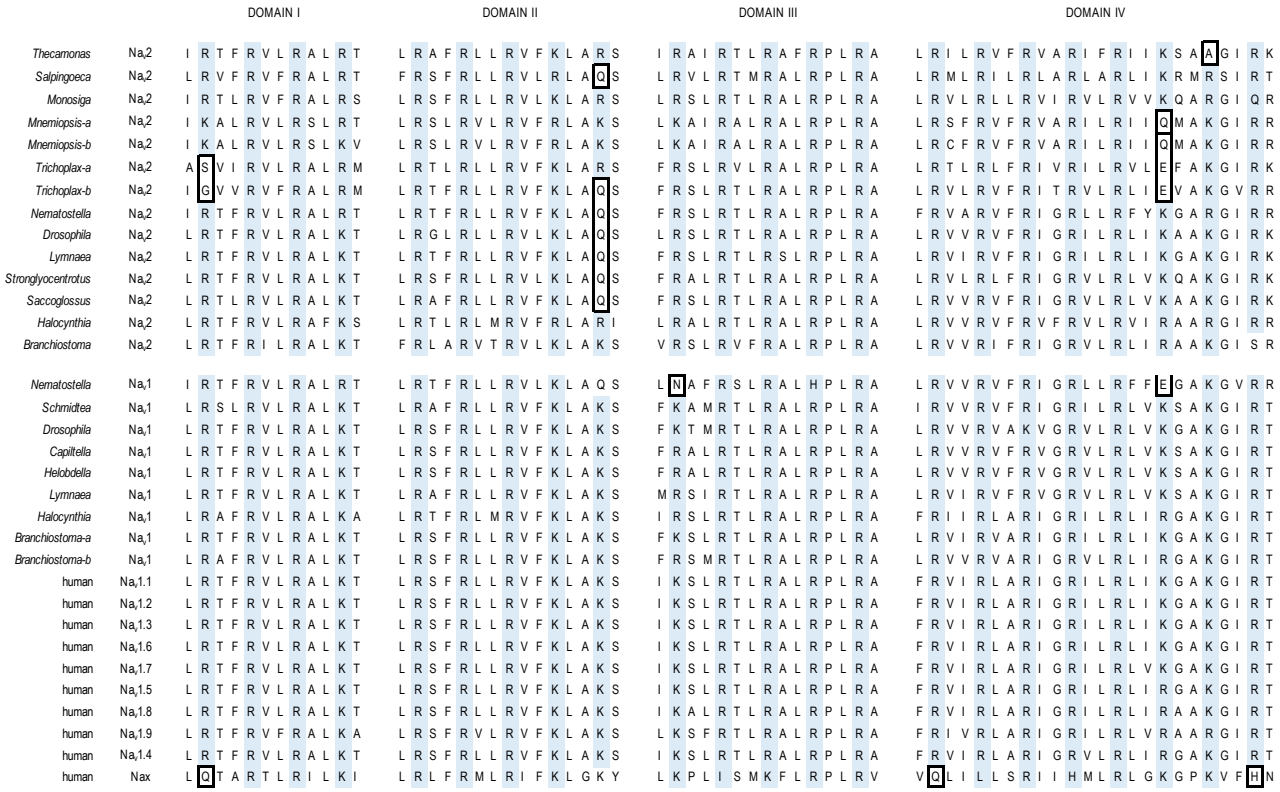

Figure 3.10 Alignment of voltage-sensing S4 segments containing positive charges (R/K) every third amino acid in Na_v1 and Na_v2 channels.

Positive charges every third amino acid in S4 segments lie on one side of an alpha-helix. Voltage-sensing for ionic channels conferred by sliding helix rotating outwards upon membrane depolarization and operating through a lever action of the amphipathic S4-S5 linker, drive opening of the channel pore domain.

3.3.2 Conserved fast inactivation motif in the III-IV linker of sodium channels.

The rapid inactivation motif located on the III-IV linker serves as a putative hinge-lid responsible for rapid N-type inactivation characteristic of sodium channels (Catterall, 2000).

It consists of three key hydrophobic amino acids, which often form the sequence IFM, but V, L, and A substitutions are also possible. See full alignment in (Appendix 3 Alingment 4).

Cnidarians	*Nematostella*	Na_v1	F L L
Platyhelminth	*Schmidtea*	Na_v1	M F M
Arthropods	*Drosophila*	Na_v1	M F M
Annelids	*Capiltella*	Na_v1	M F M
Annelids	*Helobdella*	Na_v1	M L M
Mollusks	*Lymnaea*	Na_v1	M F M
Urochordate	*Halocynthia*	Na_v1	I F M
Cephalochordate	*Branchiostoma-a*	Na_v1	L F M
Cephalochordate	*Branchiostoma-b*	Na_v1	L F M
Vertebrate	human	$Na_v1.1$	I F M
Vertebrate	human	$Na_v1.2$	I F M
Vertebrate	human	$Na_v1.3$	I F M
Vertebrate	human	$Na_v1.6$	I F M
Vertebrate	human	$Na_v1.7$	I F M
Vertebrate	human	$Na_v1.5$	I F M
Vertebrate	human	$Na_v1.8$	I F M
Vertebrate	human	$Na_v1.9$	I F M
Vertebrate	human	$Na_v1.4$	I F M
Vertebrate	human	Nax	I F I

Coanoflagellates	*Salpingoeca*	Na_v2	V L L
Coanoflagellates	*Monosiga*	Na_v2	L F L
Ctenophorans	*Mnemiopsis-a*	Na_v2	V L L
Ctenophorans	*Mnemiopsis-b*	Na_v2	V L L
Placozoan	*Trichoplax-a*	Na_v2	L F M
Placozoan	*Trichoplax-b*	Na_v2	I L L
Cnidarians	*Nematostella*	Na_v2	I F L
Arthropods	*Drosophila*	Na_v2	V F L
Mollusks	*Lymnaea*	Na_v2	A F L
Echinoderms	*Stronglyocentrotus*	Na_v2	M L L
Hemichordates	*Saccoglossus*	Na_v2	M F L
Urochordate	*Halocynthia*	Na_v2	A F L
Cephalochordate	*Branchiostoma*	Na_v2	I F L

Figure 3.11. Key triplet residues forming the hinged lid associated with fast N-type inactivation of sodium channels.
Snail LNav1 and LNav2 have "MFM" and "AFL" motifs, in lieu of the "IFM" motif in human Nav1 channels.

3.3.3 Conservation of eight core cysteines in extracellular turrets of all 4x6 cation channels

All known four domain cation channels (Nav2, Nav1, Cav1, Cav2, Cav3 and NALCN) possess eight core cysteines shared in the extracellular turret regions. Between S5 segment and the pore loop (S5P region), Domain I has four cysteines and Domain III has two cysteines. Domain IV has two core cysteines in the region between the pore loop and the S6 segment (PS6 region). These cysteines are likely fundamental for the integrity of 4x6TM ion channel types, supporting the P-loop structure.

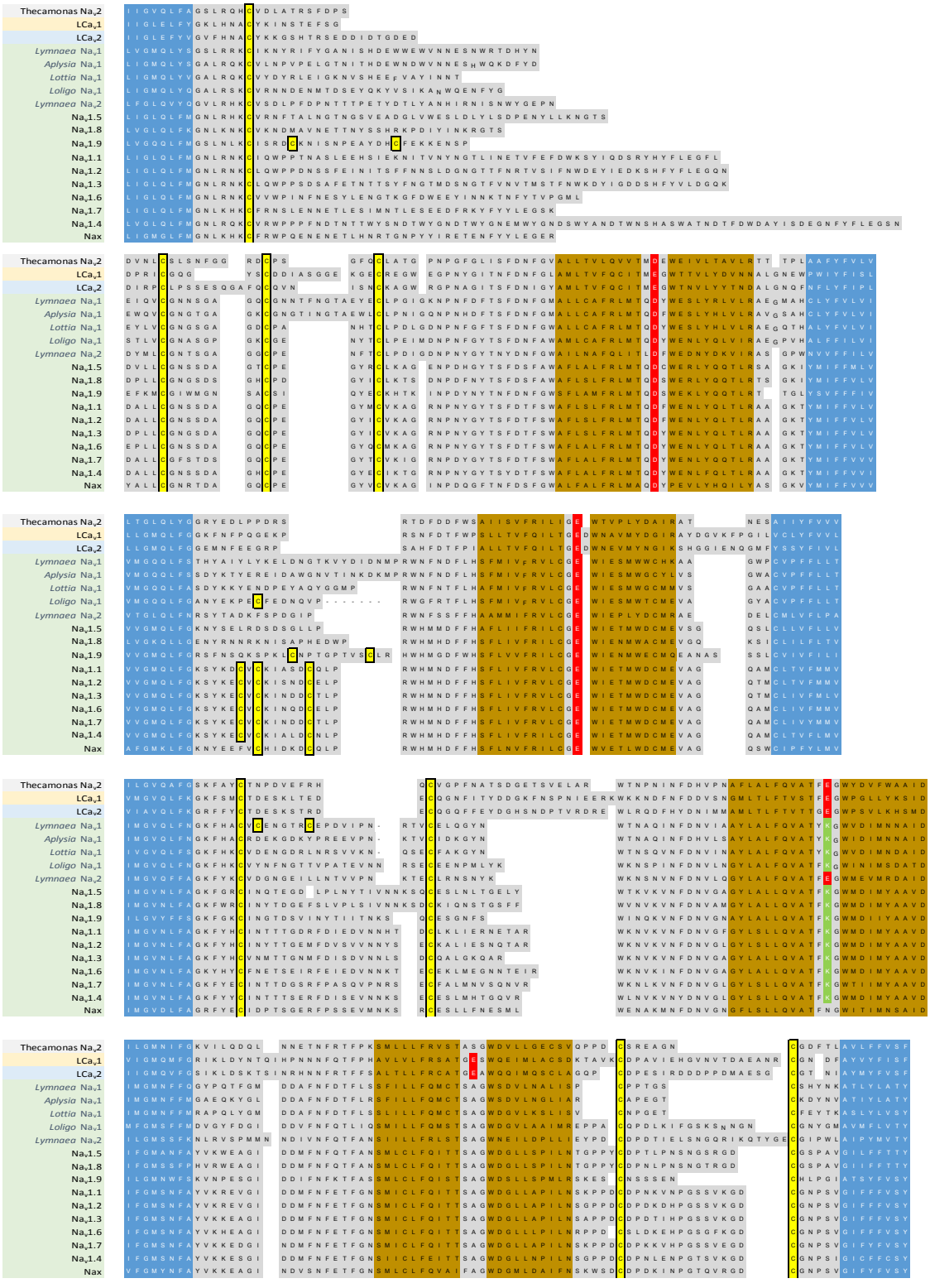

Figure 3.12 Extracellular S5P and PS6 turret regions of Na$_v$ and other channels.

Illustrated in the alignment are *Thecamonas trahens* Nav2, *Lymnaea* Cav1, Cav2 and all human Nav1 channels. The segments are shown in blue and the pore loop regions are shown in brown. Deviated from

the core 8 cysteines are 2 or 3 extra turret cysteines in some human Na_v channels in Domain II S5P turret. $Na_v1.9$ has two extra cysteines in Domain IS5P. Lymnaea Na_v1 has two extra cysteines in Domain III S5P turret.

3.3.4 Conserved PDZ binding motif in ion channel C-termini.

PDZ domains are widespread, conserved sequence motifs preserved in most eukaryote species. PDZ domains are between 80 and 90 amino acids long with a tertiary structure of a six stranded beta sandwich with 2 alpha helices(Ranganathan & Ross, 1997). These structures were named after proteins PSD-95 (PSD stands for postsynaptic density), the Drosophila septate junction protein Discs-large, and the epithelial tight junction protein ZO-1(Sheng M. , 1996), and they are found in most signaling proteins, where they are involved in protein-protein interaction (Lee & Zheng, 2010). By analyzing a total of 72 PDZ domains corresponding to 2,998 ligands, Tonikian and colleagues suggested that there are 16 classes of PDZ domains, which are defined by the sequence of the C-terminal motifs that they associate with (Tonikian, et al., 2008). The analysis of the C-terminal tails of sodium and calcium channels reveals that human and molluscan Na_v1 channels have differing C-terminal motifs that can be grouped according to their overall relatedness. Chromosome 2 sodium channels Nav1.1, Nav1.2, Nav1.3, Nav1.6 and Nav1.7 mostly end in a "K", whereas molluscan Na_v1 channels have a different motif ending in a "V". All Ca_v2 calcium channels have a conserved C-terminal "C". Interestingly, the most ancient sodium channel (Na_v2) and the most ancient Ca_v channel (Ca_v1) both have a similar C-terminal "L", that suggest a common regulatory mechanism of different channels through interaction with PDZ domain containing proteins.

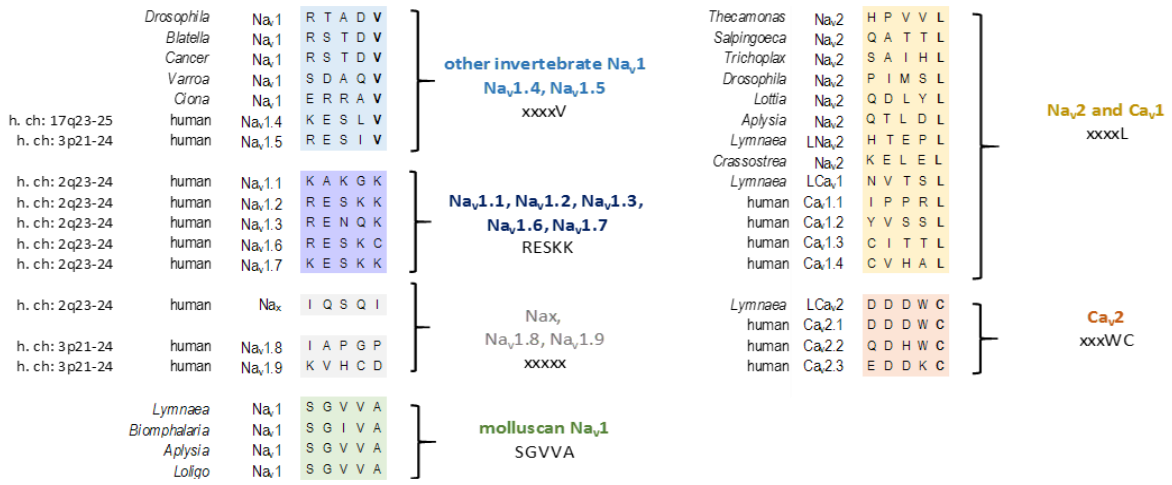

Figure 3.13 Groupings of sodium and calcium channels according to apparent C-terminal PDZ binding motifs.

3.3.5 Conserved C-terminal IQ motif

Both sodium and calcium channels possess a single C-terminal calmodulin binding IQ motif (Van Petegem, Lobo, & Ahern, 2012). Through electrophysiological experiments (Kung, et al., 1992) shows the importance of Ca^{2+} calmodulin modulation on the calcium dependant potassium and sodium currents in *Paramecium* and other early eukaryotes.

Ca_v2 channels have a calcium-dependent facilitation that involves calmodulin association with the C-terminus, but the IQ motif is not completely conserved. Na_v1 channels on the other hand, possess a conserved C-terminal IQ motif, but the regulation of Na_v1 channels by calmodulin is variable. There is no calcium-calmodulin regulation of cardiac $Na_v1.5$ channels, while currents generated by brain $Na_v1.2$ and skeletal muscle $Na_v1.4$ channels are regulated by calcium (Feldkamp, Yu, & Shea, 2011). $Na_v1.4$ channels bear a fast calcium regulation as measured by the rapid kinetics of Ca2+ photorelease into the cytosol. Transplanting the $Na_v1.4$ carboxy terminus onto Ca_v1 channels recreates the Ca^{2+} regulation of sodium channels in calcium channels (Ben-Johny, et al., 2014).

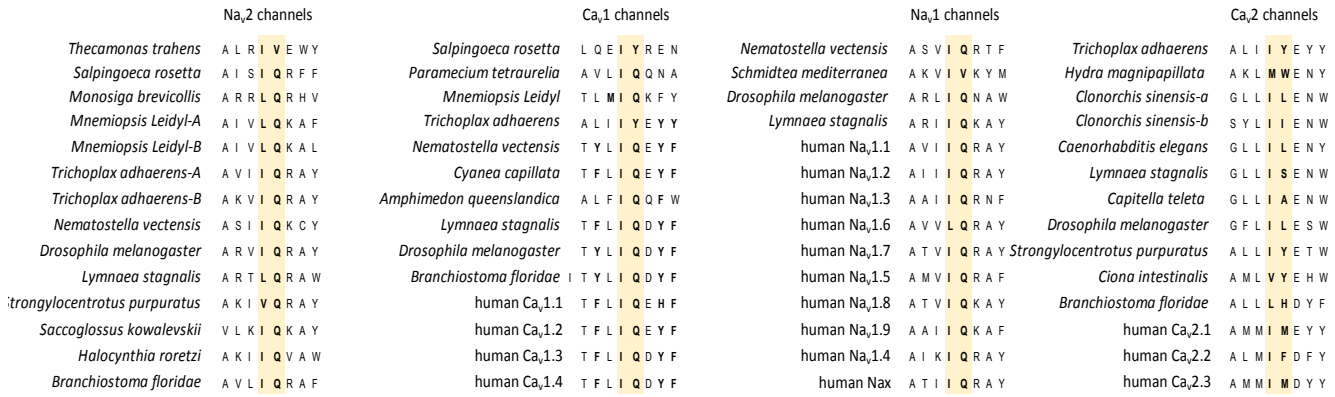

Figure 3.14 Comparison of the IQ motif among eukaryotic ion channels.
The IQ motif is conserved in Na_v1 and Ca_v1 channels but shows variations in Na_v2 and Ca_v2. In molluscan Na_v2 the IQ motif is represented by LQ sequence.

3.3.6 Cytoplasmic I-II linker of LNa$_v$1 is most homologous to nervous system-specific human sodium channels such as Na$_v$1.

Snail LNav1 sodium channel shows no overall amino acid sequence similarity across the full-length 2007 amino acid protein, for any one of the ten Nav1 sodium channels. However, the comparative alignment of human and snail channels (especially the I-II linker region) suggests that snail LNa$_v$1 does resemble the TTX-sensitive, neuronal sodium channels on human chromosome 2, linked to Hox D: Nav1.1, Na$_v$1.2, Na$_v$1.3 and Na$_v$1.7. LNa$_v$1 also somewhat resembles Nav1.6, which is structurally similar to these other sodium channels located on chromosome 2, but is located on chromosome 12, and linked to Hox C. Snail Na$_v$1 is not found outside the brain, so it is not surprising that it is less similar to skeletal muscle specific sodium channel, Nav1.4 (chromosome 17), linked to Hox B, or heart-specific (Nav1.5) or Nav1.8 or Nav1.9 which are peripheral nervous system specific channels, linked to Hox A (Lopreato, et al., 2001).

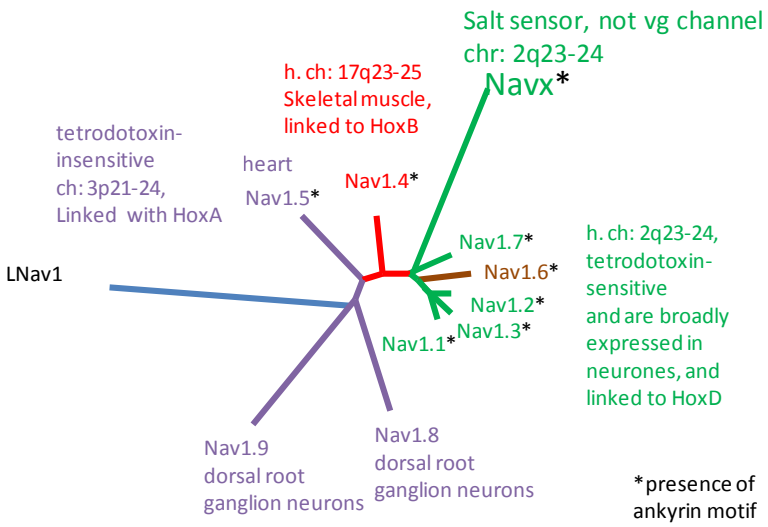

Figure 3.15 Overall structural relationship between LNa$_v$1 and the ten human sodium channels.

The unrooted phylogenetic tree represents the degree of homology among human sodium channels and the snail sodium channel. Different colors refer to different localization of the channel genes on different human chromosomes (h.ch). Na$_v$1.1, Na$_v$1.2, Na$_v$1.3, Na$_v$1.7 are found on Chromosome 2 (green). Na$_x$ is also on Chromosome 2, but is a highly modified sodium channel, that is reported to serve as a salt receptor in the hypothalamus. Na$_v$1.6 is found on Chromosome 12 (brown) and resembles the cluster of Na$_v$ channels on Chromosome 2. Na$_v$1.5, Na$_v$1.8, Na$_v$1.9 are clustered on human Chromosome 3(purple). Na$_v$1.4 is found alone on Chromosome 17 (red).

As mentioned above, the similarity of snail LNav1 channels to human nervous system specific channels is evident in the more divergent cytoplasmic regions, such as the I-II cytoplasmic linker. Exon 11, in particular, contains two conserved protein kinase A regulatory sites (serine: 573 and 623) and a protein kinase C regulatory site (serine 576). These are shared amongst snail LNa$_v$1 and human Na$_v$1.1, Na$_v$1.2, Na$_v$1.3, Na$_v$1.7 and Na$_v$1.6 channels, but not other mammalian sodium channels (Na$_v$1.5, Na$_v$1.8, Na$_v$1.9, Na$_v$1.4). Phosphorylation at these serine residues reduces the peak current of mammalian neuronal sodium channels (Cantrell, et al., 2002), and may be an ancient feature shared amongst invertebrate and vertebrate neuronal sodium channels (See Appendix 3, Alignment 3).

3.3.7 Cytoplasmic II-III linker sequence of LNa_v1 channel shows little homology with human Na_v1 channels, where a sodium channel ankyrin binding motif is located.

The cytoplasmic II-III linker, unlike the I-II linker, is highly divergent in snail LNa_v1 channels compared to human Nav1 channels. The divergence appears to relate to the evolution of the II-III linker in vertebrates. Axon initial segments and nodes of Ranvier in myelinated axons contain dense clusters of sodium channels, which underlie the evolution of fast signaling in vertebrates (Hill, et al., 2008). Key to this evolution is the ankyrin-spectrin based membrane structures. Ankyrin-G participates in localization of all known AIS components, such as voltage-gated sodium channels, potassium channels that modulate sodium channel activity, 186 kDa neurofascin, a L1 CaM that directs GABAergic synapses to the AIS and beta-4 spectrin, which stabilizes axon initial segments (Hedstrom, Ogawa, & Rasband, 2008). Moreover, ankyrin G is required to form microtubule bundles at the axon initial segment (Lai & Jan, 2006).

The evolution of ankyrin binding motifs in L1 CaM is found in all bilateral organisms including *C. elegans* and *Drosophila* (Bennett & Lorenzo, 2013). Voltage-gated Na_v1 sodium channels only acquire an ankyrin-binding motif in cephalochordates like *Branchiostoma* (*Amphioxus*), while KCNQ2/3 channels followed with gaining of an ankyrin-binding motif later in jawed fish (Pan, et al., 2006). True myelination appears in jawed fish, so the ankyrin binding motif likely evolved for clustering sodium channels in AIS before their appearance in clustering sodium channels in nodes of Ranvier (Hill, et al., 2008). The distal II-III linker contains optional, 58 amino acid exon 21 downstream of the chordate ankyrin binding motif. The function of the optional exon 21 in the II-III linker of snail LNav1 channels is unknown, but it appears to be a conserved optional exon found in all molluscan channels (Appendix 3, Alignment 4).

3.4 Discussion

3.4.1 Characterization of the *Lymnaea* sodium channel gene LNa_v1.

In this thesis I set out to characterise the pore forming α-subunit of the *Lymnaea* sodium channel which serves to generate the upstroke of the action potential in snails and all metazoan species. Sodium channels are found in all animals with nervous systems, including the basal cnidarians, but are absent in more simple multicellular organisms, such as the placozoan (*Trichoplax adherens)*, the sponges

(*Amphimedon queenslandica)*, and the ctenophorans (*Mnemiopsis leidyl)* (Liebeskind, Hillis, & Zakon, 2011).

As expected, in the pond snail, *Lymnaea stagnalis* we found a single gene coding for the Na_v1 sodium channel and it spans 31 exons and codes for a full length channel with a 2007 amino acid sequence. We identified several conserved domains that are expected to be important for different aspects of sodium channel activity and expression. We also compared highly divergent regions of the channel which allowed us to gain insight into both the evolutionary relationships of this protein and its functions within the invertebrate nervous system.

3.4.2 The dual evolution of sodium-selectivity of the Na_v1 channel in the brain and the Cav3 sodium channel outside the brain in invertebrates.

We only found LNa_v1 localized to the snail central nervous system. It is not found in appreciable amounts in any other tissues including, glands (prostate, albumin) or muscle or the heart. It has also been reported that the equivalent *Drosophila* Nav1 channel is also limited to the nervous system, so it is likely the case that sodium-dependent action potentials involving Na_v1 channels don't exist outside the brain in invertebrates. The Spafford lab has shown that the snails like other invertebrates generate sodium-selective T-type channels by alternative splicing in exon 12. These alternatively spliced T-type channels are notably expressed within the snail heart (Senatore, Guan, Boone, & Spafford, 2014). It would mean that the sodium permeant T-type channel replaces the highly tissue specific Nav1 sodium channel genes expressed outside the brain, such as $Na_v1.5$, a primary cardiac channel and $Na_v1.4$, as a predominantly muscle channel.

From their localization patterns, snail Na_v1 channels are most homologous to the human channels expressed in neurons in the chromosome 2 locus which contains $Na_v1.1$, $Na_v1.2$, $Na_v1.3$, and $Na_v1.7$ channels and Nav1.6, localized on chromosome 12.

This closer homology of LNa_v1 sodium channels to the chromosome 2 and 12 mammalian sodium channels is evident in the most divergent regions of sodium channels, such as the I-II linker. Three consensus phosphorylation sites include serine 573, 576 and 623, all harbored in exon 11, that are commonly shared between snail and the chromosome 2 sodium channels and Nav1.6. Phosphorylation by PKA and PKC dramatically reduces the sodium channel peak amplitude without affecting other gating properties and the surface expression of sodium channels, leading to an overall reduction in neuron excitability *in vivo* (Catterall, 1993). Dampening of sodium channel activity by phosphorylation

in Nav channels appears to be a conserved evolutionary feature between mammalian and invertebrate neuronal Nav1 channels.

3.4.3 The localization of invertebrate sodium channels along the axonal surface

The II-III linker of mammalian sodium channel shows little homology with LNa_v1 II-III linker. This region is directly involved in channel localization and serves as a binding point for the cytoskeleton structures that keep sodium channels clustered at the nodes of Ranvier and on the axon initial segment. Differences in the axonal organisation of the sodium channels between myelinated mammalian neurons and unmyelinated invertebrate neurons would partially explain the divergence in the II-III linker region. Mammalian Na_v 1channels have a highly conserved II-IIIL anchor motif that binds ankyrin G- an adapter protein that tethers the channel to the spectrin-actin complex(Lai & Jan, 2006). It is a 9 amino acid sequence $\frac{V}{A}$ P $\frac{I}{L}$ A X X E $\frac{S}{D}$ D where X are random amino acids.

This ankyrin G binding motif is found in basal chordates, including the urochordates (ascidians) and jawless fish (hagfish and lampreys), where it likely serves to support clustering of sodium channels at the axon initial segment (Hill, et al., 2008). Myelination first appears within the craniates of vertebrates which includes all the bony fish and contemporary sharks (gnathostomes) and most basally, in a placoderm ancestor (Hill, et al., 2008) (Bullock, Moore, & Fields, 1984). The ankyrin G motif promotes the localization of Nav channels clustered at the nodes of Ranvier in myelinated axons of craniate vertebrates (Fache, et al., 2004).

The snail sodium channel does not have the anchor motif and there is little information available about the axonal distribution of the sodium channels in invertebrates. Myelination though, isn't strictly a vertebrate innovation, since many invertebrate lineages have myelinated axons (internodes) and nodes, like nodes of Ranvier, whose structure resembles vertebrate axons. The examples of myelinated invertebrate axons are found in crustaceans (malacostraca, including cecapod shrimp and copepods) and annelids (polychaetes and oligochaetes) (Hartline & Colman, 2007).

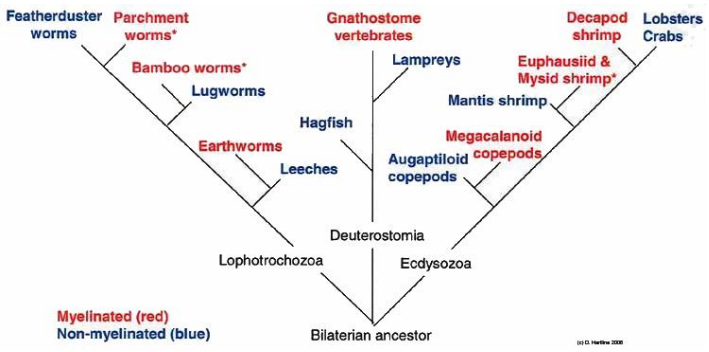

Figure 3.16. Evolution of myelin sheath in bilateria.
Taxa that are reported to have myelin sheath are shown in red. Animals with unmyelinated neurons are shown in blue. Taxa marked by asterix have suspected myelin structures that have not yet being confirmed by electron microscopy (Hartline & Colman, 2007).

We can speculate that the molluscan sodium channels spread along the axon with an especially high concentration at the AIS(Hill, et al., 2008). The mechanism for axonal localization of snail channels has not been found yet, although the II-IIIL region appears to be a likely target for any possible anchor –like proteins. The string of charged amino acids at the distal end of the optional exon 21[8] in the II-IIIL (N E V E I V Y $\frac{A}{V}$ K) is conserved among all known molluscan channels, but not in human channels and seems like a potential candidate for ankyrin –like protein binding. Another candidate region for protein-protein interaction is located on the C-terminal end immediately posterior (7 residues in Na_v1 and 8 residues in Na_v2) to the DIVS6. It is conserved both among Na_v1 and Na_v2 sodium channels. A high degree of homology indicates functional significance, though no known motifs were identified.

Mollusc Nav1	E	D	V	Q	Q	G	L	T	P	D	D	F	D	M	Y	Y	E	K	W	E	K	X	D	P	K	A
Mollusc Nav2	E	E	V			G	I	T	I	X	D	F	D	M	F	Y	V	X	W	E	X	Y	D	P	X	A
Human Nav1.1	E	E	S	A	E	P	L	S	E	D	D	F	E	M	F	Y	E	V	W	E	K	F	D	P	D	A

[8] In molluscan sodium channel alignment the optional exon is exon 17. When aligned with human channels the exon numbers are based on the human sodium channel gene.

3.4.4 The evolution of TTX insensitivity in *Lymnaea* Na_v1 channel and other Na_v1 sodium channels.

Tetrodotoxin is a highly potent pore blocker of Na_v1 sodium channels and is produced by bacteria, mostly *Vibrio alginolyticus* which exists symbiotically with many discovered hosts including puffer fish and other fish species, turbellarian flatworms, blue-ringed octopus (Hapalochlaena), western newt (Taricha), toads (Atelopus), sea stars, angelfish, polyclad flatworms, arrow worms (Chaetognaths), several ribbonworms (nemerteans) and xanthid (horseshoe) crabs (Soong & Venkatesh, 2006). TTX serves as protection against predators and is also used by predators to subdue prey. TTX can pass through cell membranes so that all tissues are exposed to it, and thus both predator and prey have developed mutations in the Na_v1 sodium channel pore for TTX resistance. TTX is found in gastropod snails too (Hwang, Tai, Chueh, Lin, & Jeng, 1991). TTX poisoning due to ingestion of marine, gastropod snails is widespread throughout Japan, China, Taiwan and Europe and it is believed that the marine snails accumulate TTX from eating animals that contain the TTX producing bacteria, such as starfish or pufferfish (Yoshida, 1994).

It is probably because of the chronic exposure to TTX, that gastropod snails, like the freshwater pond snail *Lymnaea stagnalis* have high insensitivity to TTX. Where TTX sensitive Na_v1 sodium channels are blocked in the low nanomolar range, action potentials in snail neurons are resistant to upwards of tens of micromolar levels of TTX (Soong & Venkatesh, 2006).

Evolutionary adaptations in the sodium channel pore for TTX-resistance has allowed a population of garter snakes *Thamnophis sirtalis* in the Willow Creek district to survive and feed on its toxic prey, the newt *Taricha granulosa*, which have extremely high levels of TTX in their skins. Sodium channels in garter snakes in a Bear Lake district are sensitive to low nm concentrations of TTX, whereas the same garter snakes in the Willow Creek district, are insensitive to TTX in the tens of micromolar range (Geffeney, Brodie, Ruben, & Brodie, 2002). Peter Ruben and colleagues have shown that Domain IV pore helices of Nav1.4 sodium channels are altered in the locales of species of *Thamnophis sirtalis* garter snakes. In particular a DG to NV conversion in pore helix 2 alters TTX sensitivity from a 50% block at 44 +/- 4.2 nM to 12,000 +/- 2000 nM (Geffeney & Ruben, 2006). In a similar fashion, TTX insensitive gastropod snails from *Lymnaea*, *Biomphalaria*, and *Aplysia*, also have a similar mutation of the DG pair of residues to an SD configuration. Mutation of the Domain IV SD residues in unique insect *Varroa destructor* to DD leads to the creation of high TTX sensitivity as long as a Domain III pore residues are modified too.

The DG pair of residues in Domain IV pore helix 2 is not altered in TTX sensitive species, such as the atlantic squid (*Loligo*) or fruit fly *Drosophila*, and the mammalian Nav1 sodium channels.

Once we have successfully expressed snail LNav1, we can address whether changes to the DG pair of residues in the pore helix of snail channels is responsible for its TTX insensitivity in exactly the same manner that Willow creek district *Thamnophis* garter snakes have TTX insensitive channels.

There are differences in TTX sensitivity of mammalian Na_v channels with TTX-sensitive (blocked by nM concentrations) channels and TTX-resistant channels (blocked by uM concentrations). The cause of the differences in TTX-sensitivity in mammalian channels is different than that which creates the highly TTX insensitive channels described above, and involves a particular aromatic residue (tyrosine or phenylalanine) (position 401) in the outer pore of Domain I in Na_v1.1, 1.2, 1.3, 1.4. This aromatic residue is altered to a cysteine or serine in Nav1.5, and Nav1.8 and Nav1.9 channels which provides the TTX resistance of mammalian channels.

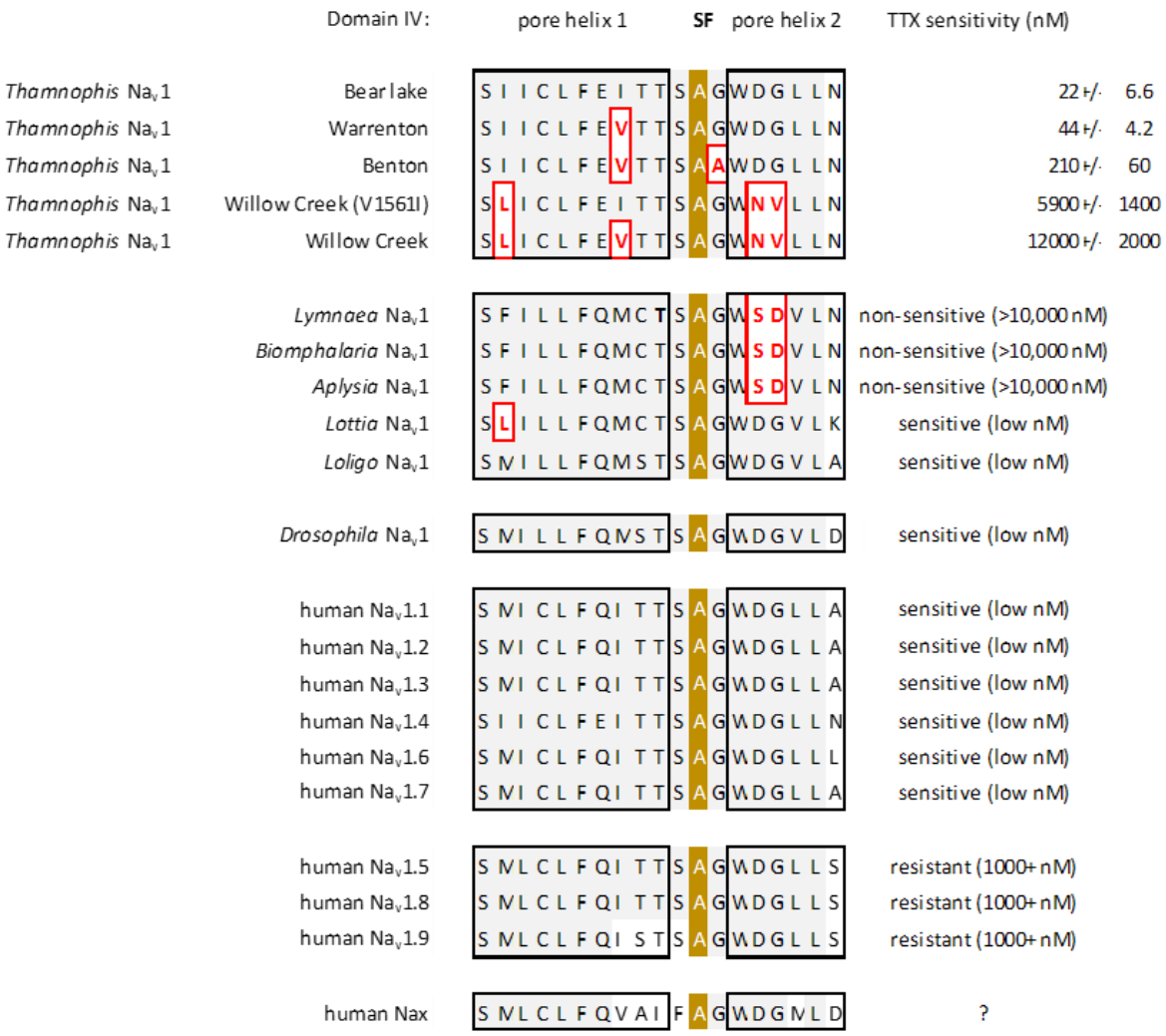

Figure 3.17 Residues responsible for tetrodotoxin resistance/sensitivity of sodium channels. Here we can see the residues responsible for TTX resistance in molluscan and snake sodium channel, but not mammalian sodium channels, whose mechanism for TTX resistance is located in the different region. Shown in yellow is the forth domain part of the selectivity filter motif DEKA. The boxed regions that flank the selectivity filter form 2 helices and with the red letters representing amino acids responsible for TTX resistance. SD residues (molluscan sodium channels) that substitute for DG residues render the channel TTX-insensitive. Mutation in the same location in garter snakes (DG to NV) also increases resistance to tetradotoxin. DG residues are therefore likely to be essential in for tetrodotoxin binding in the pore of the sodium channel.

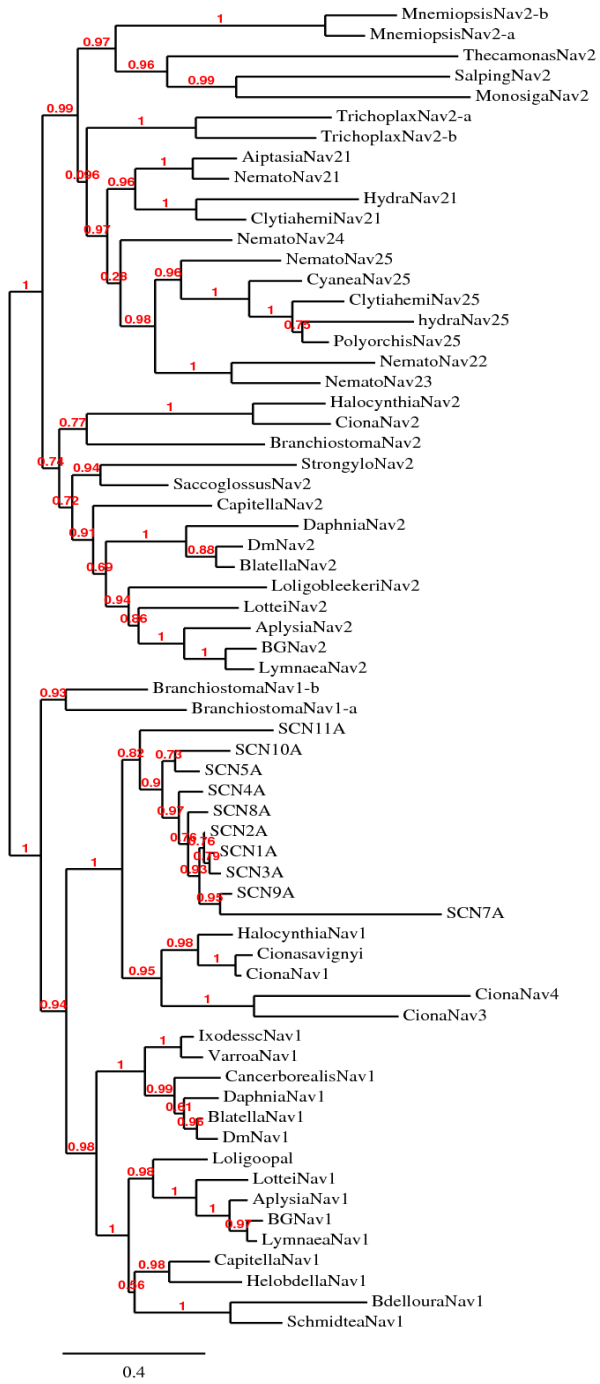

Figure 3.18 The comparison of *Lymnaea* Na_v1 and Na_v2 against the sodium channel sequences of other organisms.

Maximum likelihood phylogeny of Na_v1 and Na_v2 sodium channels, with bootstrap scores above branches. Due to high homogeneity of sodium channel across the species, alignment of the sodium channels helps establishing the evolutionary relationships between the species.

3.4.5 Characterization of the LNa$_v$2 channel gene.

There is a second, more ancestral sodium channel gene that is located in invertebrates, but lacking in vertebrates. It was dubbed "DSC1" or "*Drosophila* Sodium Channel 1" in fruit fly; later the first expression of a homolog of this gene was obtained from german cockroach and termed BSC1 or "*Blattella* Sodium Channel 1" gene. The notable feature of this channel is that it is highly similar in sequence to the invertebrate Na$_v$1 channels, but displays a DEEA selectivity filter in place of the conserved Na$_v$1 DEKA sodium-selectivity filter. Expression of Na$_v$2 channels from *Drosophila*, *Blattella* and the cnidarian, *Nematostella* in *Xenopus* oocytes confirm that Nav2 channels are calcium-selective channels (Zhang, et al., 2013) (Gur Barzilai, et al., 2012). Mutant DSC1 channels in *Drosophila* suggest that Nav2 channels are involved in sensory systems, like olfaction, and are also associated with the stress response, as knockout animals have a distinct jumpy phenotype that is intensified by heat shock and starvation (Zhang, et al., 2013).

We found a partial mRNA transcript coding for the N-terminus of snail LNa$_v$2 using cDNA derived from snail tentacles and eye spots, but we were not able to amplify any snail LNa$_v$2 fragments from cDNA isolated from heart and brain. Our PCR data supports the assertion that Nav2 channels have limited expression outside of sensory systems, and has limited to no overlap in expression with brain-specific Nav1 channel in snails. This is also consistent with the available *Lymnaea* brain transcriptome, which has a full length LNav1 sodium channel, but there isn't a single fragment of the LNav2 channels. We can put together almost the full contig of 25 exons of LNav2 from available genomic DNA sequence.

We have yet to put together a full length clone of snail LNav2 for expression but others have characterized the expression of Na$_v$2 homologs. Ke Dong's lab has expressed Nav2 channels from german cockroach (*Blatella germanica*) and fruit fly (*Drosophila melanogaster*) and the Moran lab has expressed Na$_v$2 sodium channels from the cnidarian nervous system, starlet sea anemone, *Nematostella vectensis*, From this work, it appears that invertebrate Nav2 channels express without requirement of additional auxillary beta subunits(Gur Barzilai, et al., 2012).

Remarkably, the only successful expression of invertebrate Na$_v$1 sodium channels comes from different arthropod Na$_v$1 channels expressed *in vitro* by Ke Dong (Michigan State University), including

Drosophila melanogaster (fruit fly), *Aedes aegypti* (mosquito) *Blattella germanica* (german cockroach) and non-insect arthropod, varroa mite (*Varroa destructor*)(Lin, Right, Muraro, & Bains, 2009).

Full length invertebrate Na_v1 and Na_v2 clones express poorly in human HEK-293T cell lines and more successful expression is found by mRNA injection of run-off transcripts and expression in *Xenopus* (frog) oocytes. The absence of expressible invertebrate Na_v1 channels outside of arthropods may be the requirement of auxiliary beta subunits, identified as Tip-E in insects, which is required for functional expression of *Drosophila para* Na_v1 channels (Warmke, et al., 1997). Another possibility for poor expression of invertebrate Nav1 channels in human cell lines is the importance of replacing the divergent II-III linker of snail LNa_v1 with the human $Na_v1.7$ counterpart containing the ankyrin G binding motif that is a requirement for trafficking human Na_v1 channels to axon initial segments and nodes of Ranvier. HEK-293T cells were originally described as being derived from embryonic kidney cells, but their transcriptome reveals a more neuronal lineage.

3.4.6 Common conserved domains in LNa_v1 and LNa_v2

The presence of the calmodulin binding IQ motif in both LNa_v1 and LNa_v2 implies that the snail sodium channels, like many other ion channels are subject to regulation by intracellular calcium. Experiments in unicellular eukaryotes with a conserved IQ motif demonstrated that sodium channels lose their activity rapidly when the cytosolic concentration of calcium is low. The activity can be restored by introducing Calmodulin $–Ca^{2+}$ complex but not by the presence of higher calcium concentration alone (Kung, et al., 1992).

The PDZ domain, a conserved C-terminal region found in multiple membrane proteins is responsible for protein-protein interaction. The distal part of the PDZ domain located on the carboxy tail is responsible for specific binding partner recognition. Morgan Sheng proposed that the PDZ domain plays a role in the clustering of ion channels on the neuronal surface (Sheng M. , 1996). Since different carboxy tail sequences imply different binding partners, we can presume that SGVVA from LNa_v1 and HTEPL from LNa_v2 would not bind the same ligands (See Figure 3.13 for PDZ motifs of different ion channels).

Chapter 4. Sodium channel auxiliary subunit LNa$_v$B

4.1 Putative auxiliary snail sodium channel subunit: results

4.1.1 LNa$_v$1 specific polyclonal antibody

To recapitulate the expression features from snail LNa$_v$1 α-subunit i*n vitro*, we needed to express sodium channel specific β-subunits from snails. Since pond snail genomes and transcriptomes do not contain any gene resembling the four human sodium channel β- subunits or insectal auxiliary subunits (Tip-E or TEH genes), we were aware that we would have to use a different method than homology cloning to find a snail sodium channel beta subunit. In subsequent sections of this results chapter, I will outline how we generated a bacterial fusion protein coding for cytoplasmic regions of the snail sodium channel (the antigen), which was then injected into rabbits to generate snail Na$_v$1 specific antibodies. The antiserum was used to fish out the sodium channel protein complex from the *Lymnaea* brain.

4.1.2 Making the antigen

Bacterial fusion proteins were designed by Dr Spafford and constructed by Neil Hsueh, a 499 project student. The target areas were I-II and II-III linker of the α-subunit. The I-II linker was intended to be universal for all the α-subunits, while the II-III linker was specifically designed to target the LNav1α (+) variant. An in-frame C-terminal His tag on the vector pET22b vector was used to purify the bacterial fusion proteins on a nickel column. (See Appendix1. Table 5.3).

NavI-II L, size = 25.1 kDa

SSFGGESLSRSESADEPNKIAEAIDRFKRFGNWVKVKIIVCIKVKLQRQKNWRPSVPPSKLPELNGKENAFGDGTVIAMEKTPDDFPDGAMEPDDCFCYSLTKR
CTWCLVIEKPPIGRAWWALRCFMYRLAEHRYFDTFIIVMILLSSCALALEDAYLHEKPLLKEILEYMDKVFTVIFIVEMLVKWLEHHHHHH

NavII-III L, size = 11.5 kDa

SRAGSIYSTKDLKSPLGSHSGSSHCSSCSSLSDSAQTKKIDLEGDHEINEVEIVYHHHHHH

Induction of bacterial expression of fusion proteins in Rosetta bacteria produced visible protein bands illustrated on a SDS-PAGE gel (Figure 4.1).

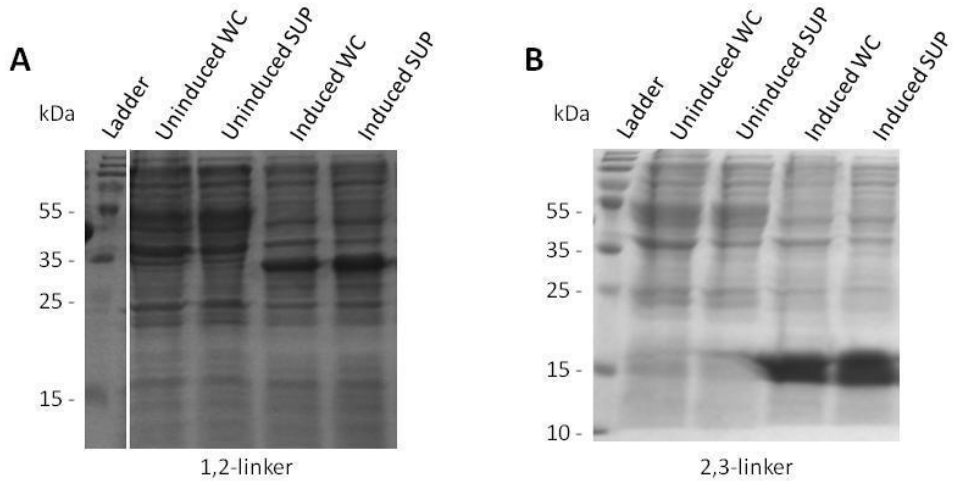

Figure 4.1 Expression of fusion protein[9]

Both whole cell lysate (WC) and supernatant (SUP) were compared for fusion protein presence before and after induction with IPTG. The thick protein band at present at 35 kDa (1,2-linker gel) and 15 kDa (2,3-linker gel) in the IPTG induced lanes is the fusion protein. The presence of the protein both in whole cell and in supernatant indicated that the proteins are water soluble.

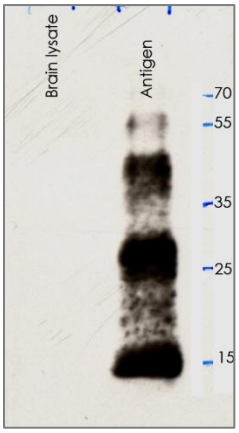

Figure 4.2 Western blot of II-III linker polyclonal antibody.

Antibody binds the antigen well but the lack of the band on the brain lysate lane indicates that the antibody does not bind the proteins in the snail brain.

4.1.3 Antibody production

At the time of antibody production, the LNav1 with exon 21 (+) channel that would generate the II-IIIL antigen to serve as a positive control for the II-IIIL polyclonal antibody, was not available and testing

[9] Images taken from: H.T Hsueh(2013) Production of a polyclonal antibody against a *Lymnaea stagnalis* sodium channel,

the II-III L against the brain lysate produced negative results (Figure 4.2). The II-III L antibody was purified but never tested further. The universal I-II L polyclonal antibody alone was used for all downstream applications, and referred subsequently as the LNav1α-specific antibody.

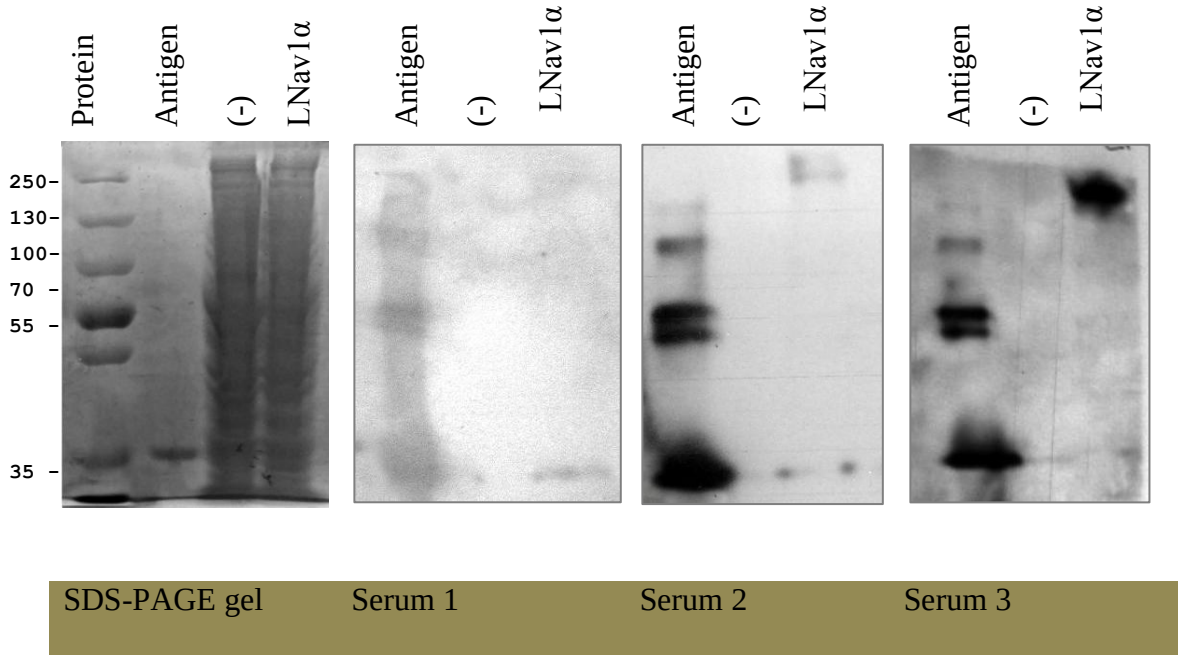

Figure 4.3 Testing of an LNav1 specific antibody using Western Blotting.
Gradual increase in the affinity with every boost of antigen in rabbits of the polyclonal $LNa_v1\alpha$ antibody resolved using SDS-PAGE. Coomassie stained gel (left gel) is a duplicate of the gel used for Western blotting (right three gels).The serums are numbered according to the number of antigen injections complete before a test bleed. Pre-bleed is not shown since no visible bands appeared on the membrane. The antigen serves as positive control while the HEK cell lysate serves as negative control. . The substantial antibody staining of HEK cells expressing the LNav1α subunit (serum 3) demonstrate the potency and specificity of the rabbit antiserum for the LNav1 sodium channel.

Western Blotting with the LNav1α antibody demonstrates that the antibody is highly specific for the expected 260 kDa LNav1 alpha subunit expressed in HEK-293T cells and the original fusion protein antigen. It also shows that HEK-293T cells will express the cloned LNav1 sodium channel, although we are unable to find expressible sodium currents after transfection.

The rabbits were terminally bled (exsanguinated) after the fourth boost with antigen and incomplete adjuvant cocktail, and the polyclonal antibody was purified from the antiserum with the antigen on a SulfoLink column, and then tested against expressed LNav1 in transfected HEK cells and in *Lymnaea* brain homogenates.

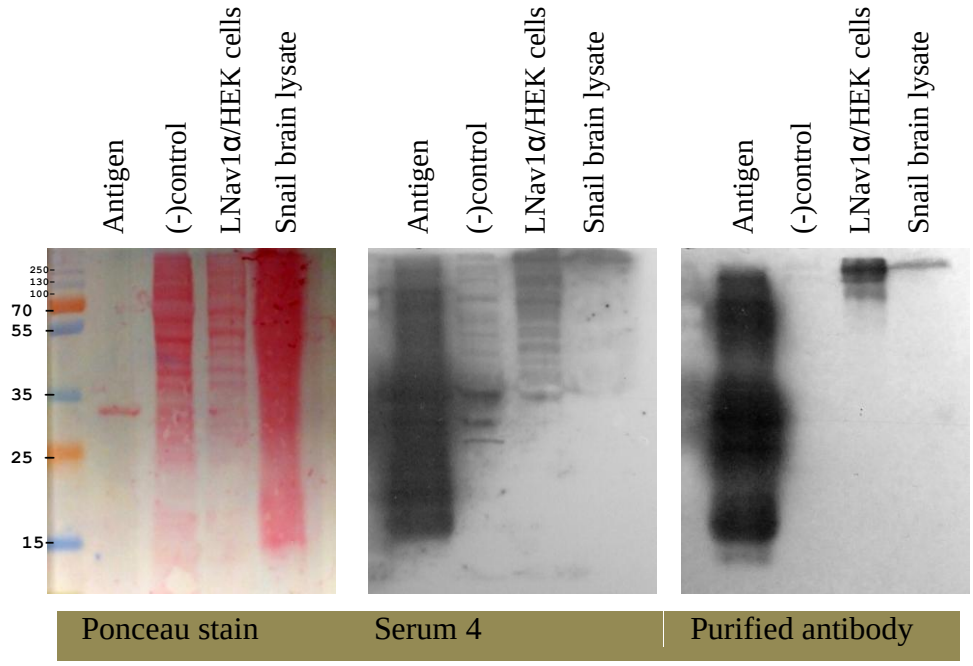

Figure 4.4 Comparison of LNa$_v$1 *α*-subunit affinity between final bleed serum and purified antibody.

Western blot, Left (Ponceau general protein stain), Middle (tested with terminal antiserum #4) and right (testing with purified antibody) with original bacterial antigen, untransfected HEK-293T cells, HEK cells expressing LNav1 and snail brain lysates. For the sake of consistency, the same amount of antigen was used in this gel as in gels used to test serums 0, 1, 2 and 3 illustrated in Figure 4.3. Terminal bleed antiserum (#4) indicates some background binding in both negative control and transfected HEK cells expressing LNav1α lanes (middle gel), but the background improves dramatically after purification of the polyclonal antibody .Multiple bands in transfected LNav1α subunit in HEK-293T cells may occur because of degradation of the large sized channel protein during membrane purification.

4.1.4 Co-Immunoprecipitation

The purified polyclonal LNav1 sodium channel antibody was used to fish for an LNav1α subunit associated accessory subunit. For the lysis buffer, I originally chose RIPA (RadioImmunoPrecipitation Assay) buffer, a fairly strong buffer recommended for extracting membrane proteins. After an attempt using RIPA lysis buffer was unsuccessful, I switched to a milder buffer, CHAPS cell extraction buffer, which contains less harsh detergents and is better suited for co-immunoprecipitation experiments (Harlow & Lane, 1999).

The polyclonal antibody was cross-linked to protein A sepharose beads with glutaraldehyde. Differing protein homogenate samples were poured over the antibody-coupled beads, washed with buffer and the remaining protein bound to antibody beads was loaded for SDS-PAGE analyses. SDS-PAGE was loaded with differing samples to resolve whether there was a unique protein band appearing only in a lane containing a snail brain protein complex. We expected a band in the range of 30 to 40 kDA, which corresponds to approximate sizes for *Drosophila* TIP-E and human sodium channel beta subunits.

A number of negative controls (lanes A to F, Figure 4.5) were used to ensure confidence that a positive result associated with a unique protein band (lane G, Figure 4.5) on an SDS-PAGE gel was specific to sodium channel complexes in snail brains. No positive control was available, except that we knew that the LNa_v1 polyclonal antibody bound with high and selective affinity for LNa_v1 sodium channel protein expressed in HEK-293T cells and in snail brain homogenate.

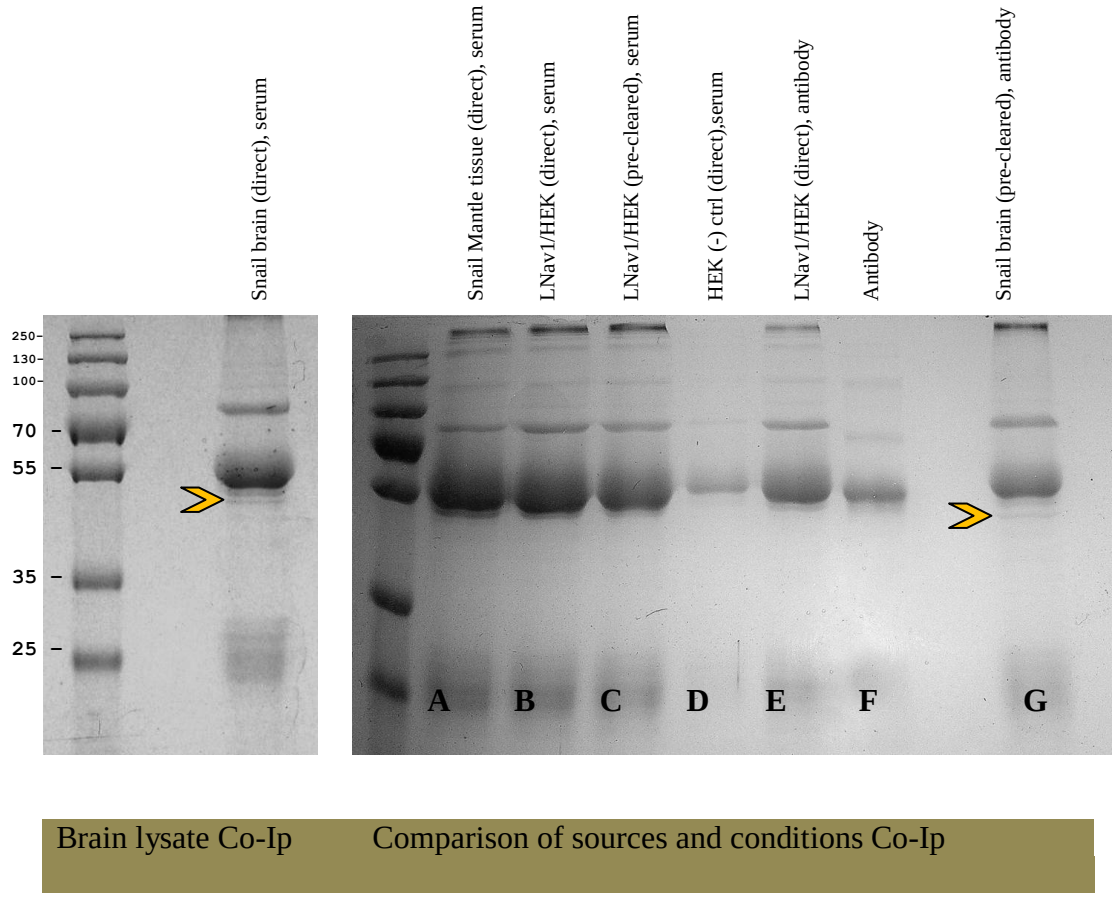

Figure 4.5 Isolating the β subunit using LNa$_v$1 specific antibody.
SDS-PAGE gels were run that contained protein samples with snail mantle (lane A) versus snail brain homogenate (G). Control HEK cells (lane D) vs. transfected HEK cells with LNav1 channel (lanes B, C, E). Protein homogenates that were pre-cleared with general rabbit serum bound to protein A (SAC)[10] and without pre-clearing the protein homogenate (lanes A, B and E). Lane F contained polyclonal antibodies alone bound to beads without protein homogenate. A comparison was also made between rabbit anti-serum containing (Lanes A, B, C, D and the gel on the left), and polyclonal antibody purified against the bacterial fusion protein antigen before binding to beads (Lanes E, F, G). The unique band in snail brain homogenate bound to the antibody-bound LNav1 complex is at roughly 47 kDa (lane G) and is not seen in any of the control lanes (A to F).

Snail mantle tissue was lysed and prepared as a protein homogenate in the same way as the snail brain tissue. Comparison between snail mantle tissue homogenate (lane A) and brain homogenate (lane G) allowed for identification of unique protein bands localized specifically to brain, the only organ

[10] *Staphylococcus aureus Cowan* I strain (SAC) is a relatively cheap source of protein A that is recommended by (Harlow & Lane, 1999) for a preclearing step.

where LNav1α-subunit is expressed, according to our previous qPCR transcript profile analyses for LNav1 channels from different snail tissues.

Homogenates of HEK-293 cells transfected with the α-subunit, both pre-cleared and not pre-cleared, were compared to see if the pre-clearing step eliminates any visible bands. Pre-clearing however, in our case had no obvious effect on removing contaminating proteins that could interfere with visualization of the protein of interest (lane B versus lane C, Figure 4.5). Most of the visible bands are likely due to non-specific proteins in the antiserum such as albumin, and the polyclonal immunoglobulin G antibodies themselves (molecular mass ~150 to 170 kDa) which are comprised each of two light chains (23 kDa) and two heavy chains (~50 kDa). The LNa_v1 sodium channel α-subunit is not visible on Coomassie stained gel and is only detectable by Western blotting with specific LNav1 specific polyclonal antibody. Using the comparative approach, especially comparing LNa_v1 channels transfected in HEK cells (lane E, Figure 4.5), snail mantle homogenate (lane A, Figure 4.5), and snail brain homogenate (lane G, Figure 4.5), a unique protein band of ~47 kDa, a possible accessory β subunit homolog, was only visible on the brain lysate sample (lane G, Figure 4.5).

4.1.5 Identifying the amino acid sequence of the putative β-subunit of LNa_v1

The unique ~47 kDa protein band was cut out of the SDS-PAGE gel and sent to the SPARC BioCentre at the SickKids Hospital in Toronto, where protein sequences were determined. The protein band was digested by trypsin enzyme into fragments which underwent electrospray ionization (ESI) that ionizes the liquid containing protein fragments at high voltage and sprays the liquid as an aerosol to separate the protein fragments by liquid chromatography. ESI was coupled with tandem mass spectrometry (MS/MS) for protein sequencing, where resulting peptide sequence tags are compared to a translated protein database. We generated a translated database from the published *Lymnaea* brain transcriptome shotgun assembly (TSA), (Sadamoto, et al., 2012).

Mass spectrometry is highly sensitive to contamination, and despite being careful to maintain sterile conditions, the highest number of peptide sequence tags matched human keratin (162 peptides in six proteins). The greatest hit for a non-human protein was 8 peptides that matched a protein we dub, LNavbeta1, translated from the *Lymnaea* brain transcriptome (see Table 3.1). These eight peptides cover 31% of the expected 32.6 kDa protein.

Table 4.1. Protein sequence tags identified by ESI tandem mass spectrometry (MS/MS), that code for a novel *Lymnaea* protein, LNavbeta1.

Peptide	Unique	-10lgP	Mass	ppm	m/z	Z	RT	Scan	#Spec	Start	End
K.SPYFGFSNYLANTR.C	Y	80.13	1635.7681	3.6	818.8943	2	44.08	13132	1	53	66
R.LADQSNIYVK.S	Y	63.20	1149.6029	3.6	575.8108	2	27.62	7626	1	43	52
R.GFQVQISAVR.Y	Y	58.03	1103.6088	3.7	552.8137	2	35.55	10217	1	142	151
R.FTYVLPPGR.N	Y	33.90	1048.5706	-2.2	525.2914	2	37.10	11081	1	118	126
R.TDGSVTARGFQVQ(+.98)ISAVR.Y	Y	26.41	1891.9751	1.9	946.9966	2	54.84	16324	1	134	151
R.ATDNLLR.A	Y	19.94	801.4344	3.7	401.7260	2	1.04	471	1	273	279
A.DQSNIYVK.S	Y	17.82	965.4818	3.3	483.7498	2	26.81	7362	1	45	52
R.YYQTSPDYYRPSQHLDRIPILYFLFEAQAALNKA.A	Y	15.44	4091.0581	7.6	1023.7795	4	50.14	15074	1	233	266

We then used the TBLASTN algorithm (Basic Local Alignment Search Tool, National Center for Biotechnological Information (NCBI), National Institute of Health (NIH), Bethesda, MD) to find candidate transcripts that were close homologs to the translated $LNa_v\beta1$. Another three homologous proteins, members of the CUB domain family were found after the analysis of the Lymnaea transcriptome, termed $LNa_v\beta2$, $LNa_v\beta3$ and $LNa_v\beta4$. Searching the protein sequence tag database resulting from the ESI MS/MS of the isolated protein band, revealed two peptide hits for $LNa_v\beta3$ and $LNa_v\beta4$ (Table 3.2 and Table 3.3). The finding of multiple close homologs in the *Lymnaea* transcriptome that were isolated from the original protein gel band provides confidence in identified $LNa_v\beta$ subunits as candidate accessory subunits for LNa_v1 channels, with differing protein sequences, with common regulatory domains for associating with LNa_v1 channels.

Table 4.2. Overview of protein sequence tags identified by ESI MS/MS mass spectrometry

Protein Group	Protein ID	Accession	-10lgP	Coverage (%)	#Peptides	#Unique	PTM	Avg. Mass
4	2428	**LNavb1**	152.64	31	8	8	Y	32.612 kDa
NA	NA	**LNavb2**	NA	0	0	0	NA	42.4 kDa
6	2433	**LNavb3**	21.26	6	1	1	N	27.729 kDa
7	2434	**LNavb4**	20.24	3	1	1	N	40.076 kDa

Table 4.3. Protein sequence tags identified by ESI MS/MS mass spectrometry that code for a novel *Lymnaea* protein LNavbeta3 and LNavbeta4.

	Peptide	Unique	-10lgP	Mass	ppm	m/z	z	RT	Scan	Start	End
LNavβ3	S.DDNSCAWDKLCISNVK.F	Y	21.26	1809.8025	1.9	905.9102	2	41.15	12112	94	109
LNavβ4	I.DIGAQSYGLIK.S	Y	20.24	1163.6187	4.8	582.8194	2	41.75	12340	43	53

Below are the amino acid sequences of putative peptides for LNavbeta1 through LNavbeta4, with grey areas indicating oligo-peptides identified by ESI MS-MS.

>LNavb1 (32.6)

MMRCGALTVLAGAWLVFAGGHVIDKRQAIFPNLVLCVDSEARLADQSNIYVKSPYFGFSNYLANTRCQLTLRSGADPLTVSVQFDAFDLELEARACSSDSLCVGGVQFCGNWQVN
QRFTYVLPPGRNFTLVFRTDGSVTARGFQVQISAVRYDYQPTLITSGGVGSSSGGVQTQLLSYNGDYEHTYQDKCAVDADGGFWNDQTTPYYYNGNSSFADLWRGQASPRDPFT
DT RYYQTSPDYYRPSQHLDRIPILYFLFEAQAALNKAAFKRGRATDNLLRAYDASGGRAINYKK

>LNavb2 (42.4 kDa)

MMGVYVLATLLSVWLVCTGAHVIDKRQASYSNLALCQDTAFSIGAYSNLYVKSPNYGFGNYQDSTRCNLVLQSGSETLFITVRFDVVELEYNLECVFDSICVGGYKFCGPNWAANKE
YSFIIPANRTFTLDFKTDGSVTGRGFQLFITASPFTGQTALTPVGGVGSSNNSLQVDYLTYSSNYSDTYQDKCRIDNYGGNGYYQTSPNYYTDNPWYYQTSPNYYTDNPWYYQTSPN
YYTDYYQTSPNYYTNYPWYYQTSQNYYTDNPWYYQTSQNYYTDYPWYYQTSQNYYTDYPWYYSTSHSPNYYTDYPYYYNTSPDRRTDSTFLLYSLYEALSSLSQANFDIQTAVQHL
QRAIAHVDGSVARKK

>LNavb3 (27.73 kDa) (missing the C-terminal end)

MTTVKLLSILAGVFLIPCAAHVVRRQTPTPVVELCNGSQSNVVDIGDKSIGIVRTANFSASNYKDNTRCNVILRTQGQALIVSIYFRSFDVESDDNSCAWDKLCISNVKFCGVWPTSRT
FDYVVPANNTFTLDLQTDTSVTARGFELQISAVEYKGVAVTYPSGGFGSAYERLIFSTLNSTNQTGYADKCKDNIGATFSYYKFSAPNYVYSSWVLQNASSSKAASLNTTTPSSNLTAT
RPLN TTTPSSNLTTTRP

>LNavb4 (40.08 KDa) (missing the C-terminal end)

MFILRLLTVLAGALLVTNANVVRRQTSSQVVELCNGSTKSLIDIGAQSYGLIKSPGFGQRNYPNNVACKATLRTQNQPLIINLQYNYFSLEYESQSCSYDRLCVSGVQYCGGWSSNYNY
EYVVPAYSTFTLDFRTDSSVTDSGFQIAASARAYNGEAIAVATGGVGTNSGRVTYSSPYLNTYYDACAPSSSDPAYNKDTASVYYSWMGQDNLYNLTSTQSWSAYYNTTNYPYYNTT
YYPYNTTYHPYYNTTYYPYNTTYYPYYNTTYYPYNTTYYPYYNTTYYPYNTTYYPYYNTTYYPYNTTYYPYYNTTYYPYNTTYYP YYNTTSYPYYNTTSYPYYNTTSY

The novel β-subunit sequences were submitted to GenBank and the following accession numbers were assigned to them:

LNa_vB1 : LNavbetas.sqn LNavbeta1 KM282656
LNa_vB2 : LNavbetas.sqn LNavbeta2 KM282657
LNa_vB3 : LNavbetas.sqn LNavbeta3 KM282658
LNa_vB4 : LNavbetas.sqn LNavbeta4 KM282659

4.1.6 Secondary and tertiary structure of the LNa_vB proteins

The protein secondary structure of LNavβ1-4 was analyzed using Phyre-2 a protein fold recognition algorithm (Kelley & Sternberg, 2009). The Phyre2 server compares the input sequence with homologs of known three-dimensional (3D) structure, the so-called template-based homology modeling or fold-recognition. A recurring structure – a beta sandwich with a jelly roll fold motif of about 110 amino acids, recognized as a CUB domain, was found in all four proteins. Two CUB domains were identified in $LNa_vβ1$ and $LNa_vβ3$, while a single CUB domain followed by recurrent motifs was found in $LNa_vβ2$ and $LNa_vβ$ 4(Figure 4.6). The evolutionarily conserved CUB domain (standing for complement C1r/C1s, Uegf, Bmp1) is found almost exclusively in extracellular and plasma membrane associated proteins, many of which are developmentally regulated.

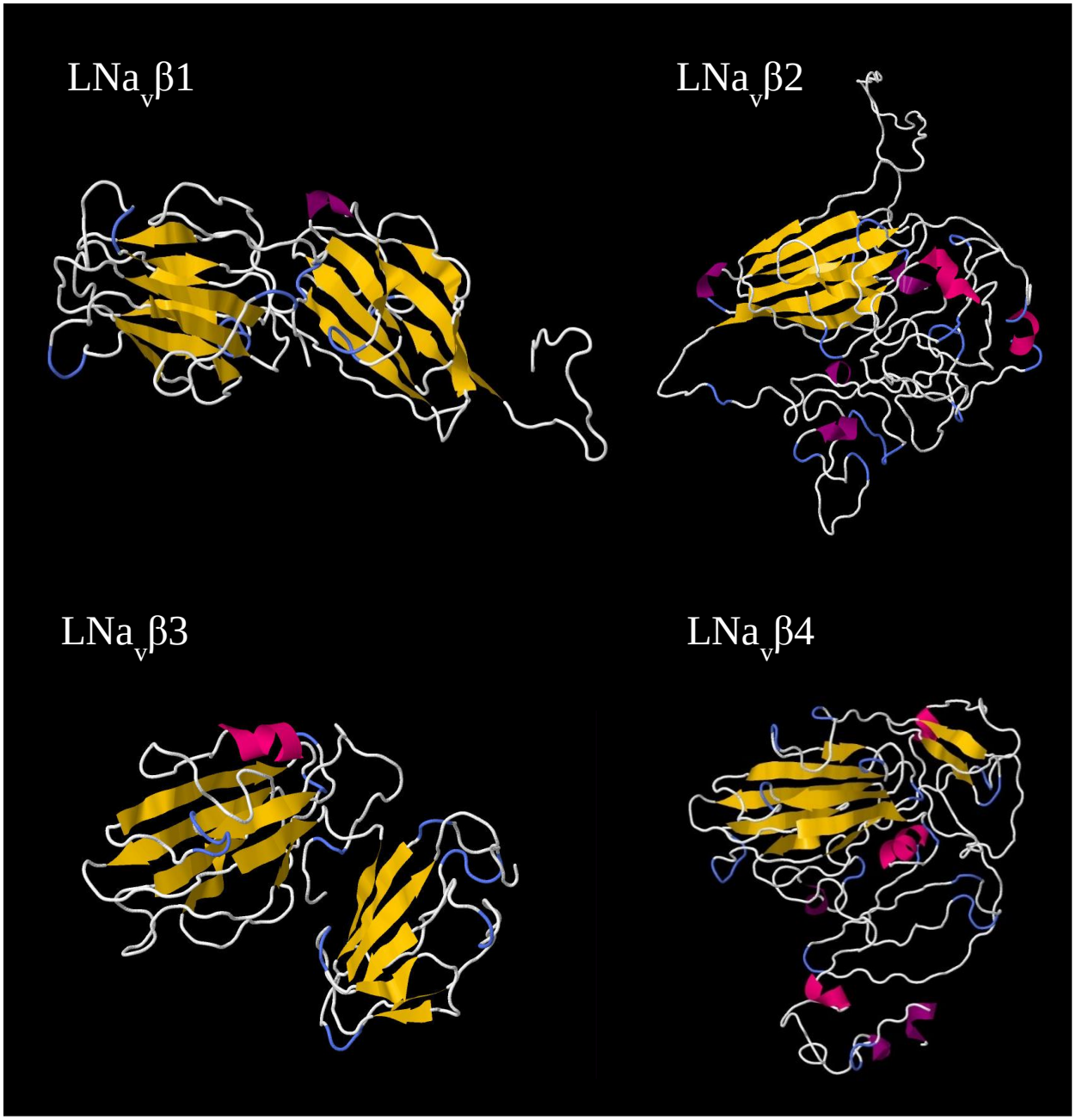

Figure 4.6. Structures of sodium channel beta subunits.
Structures of LNavβ1, β 2, β3 and β4, generated by homology modeling using Phyre2 protein fold recognition server. LNavβ1 and β3 have two predicted CUB domains compared to one CUB domain predicted for LNavβ2 and β4.

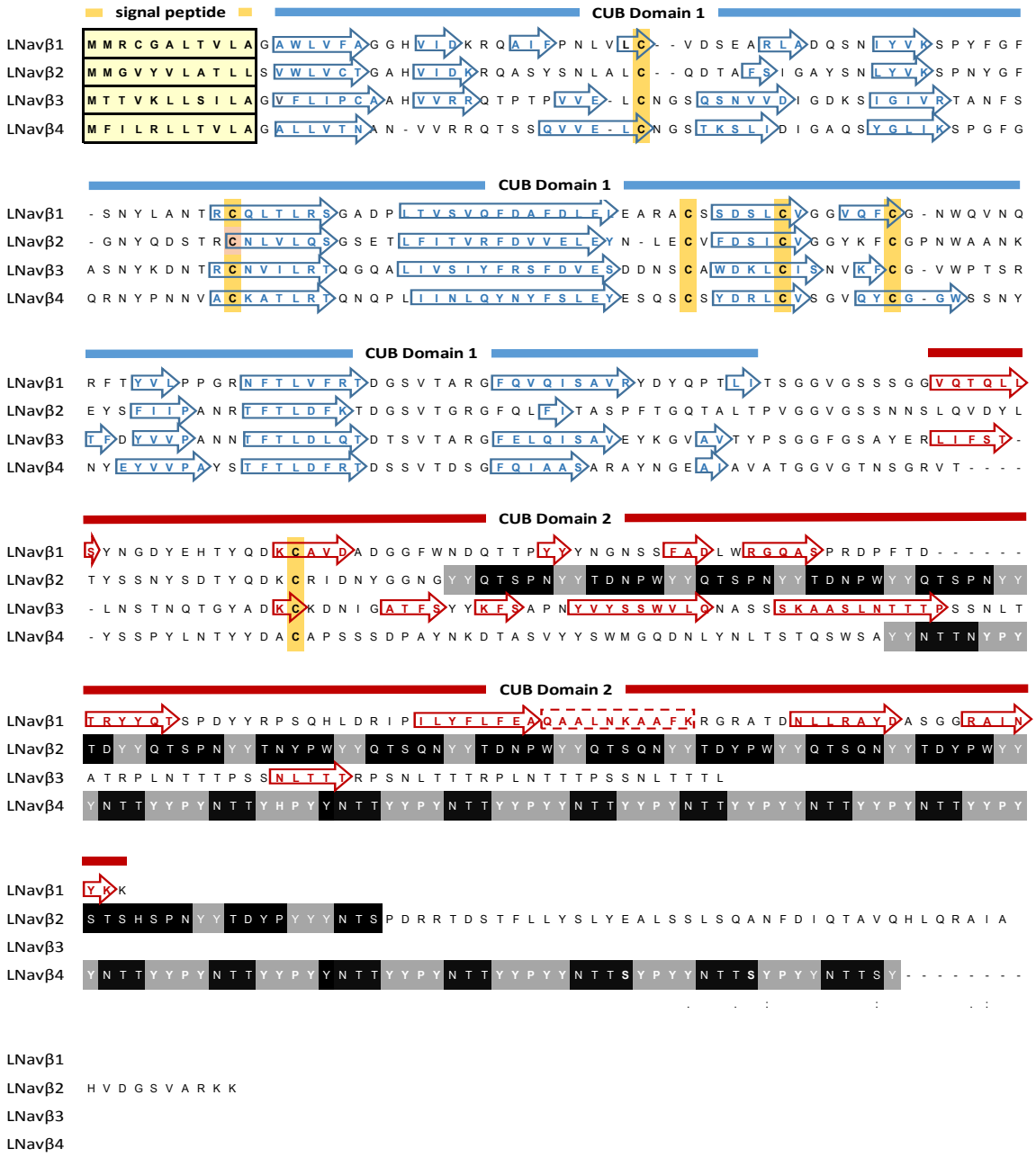

Figure 4.7. Alignment of putative Lymnaea sodium channel β-subunits with predicted secondary structure derived from the Phyre2 algorithm.

There is a high degree of homology between signal peptide domains and the first CUB domain of all four subunits. Six conserved cysteines (shown in tan color) form three disulfide bonds (1-6, 2-5, 3-4) according to DiANNA 1.1 (unified software for Cysteine state and *Disulfide Bond* partner *prediction* (http://clavius.bc.edu/~clotelab/DiANNA/)). The red squares show four possible glycosylation sites.

The extracellular repeat sequences in $LNa_v\beta2$ have 7 repeats of mostly "YY-QTSPN-YY-TDNPW", and $LNa_v\beta2$ has "YYPY-NTT" repeated at least 16 times. There are extracellular repeats in $LNa_v\beta3$ too, of "TTT-PSSNL". The full length cDNA is known for $LNa_v\beta1$ and $LNa_v\beta2$ and identifiable in the *Lymnaea* transcriptome and/or *Lymnaea* genome. The complete 3' end of the $LNa_v\beta3$ and $LNa_v\beta4$ sequence is not known because of the large number of repeat sequences that can't easily be matched and identified across multiple genomic contigs. The repeat sequences are reminiscent of coiled coil structures in which two to five alpha-helices are coiled together in a super coiled structure like the strands of rope. Coiled coil domains are found in a diverse array of proteins, from transcription factors like c-Fos and c-jun, to motor proteins like myosin, dyneine and kinesin, to skeletal proteins such as α-keratin (Burkhard, Stetefeld, & Strelkov, 2001).

4.1.7 Homologs of LNa_vB in other closely related species

We TBLASTN searched in available databases (NCBI, JGI and others) for similar $LNa_v\beta1$ subunit homologs amongst known genomes available in gastropod snails besides pond snail *Lymnaea stagnalis*, which includes *Biomphalaria glabrata* (pulmonate freshwater snail), *Aplysia californica* (California sea hare, a marine snail) and *Lottia gigantea* (giant owl limpet). We were only able to definitely confirm a set of $LNa_v\beta1$ homologs in the most closely related pulmonate freshwater snail, *Biomphalaria*. It is likely that gastropod snails outside of pulmonates, as well as other mollusks, and differing animals in other phyla, have unique beta subunits. The restricted distribution of the pulmonate snail $LNa_v\beta1$ subunits within freshwater pulmonate snails, is similar to the unique Tip-E and the four TEH subunit homologs identified in *Drosophila melanogaster* which have a restricted distribution to insects and crustaceans, but are not present within other arthropods, such as the chelicerates (Li, Waterhouse, & Zdobnov, 2011).

We evaluated the structural relationships amongst pulmonate snail $LNa_v\beta$ subunits in a phylogenetic tree generated by protein amino acid sequence alignments using phylogeny.fr (Dereeper, et al., 2008)

$LNa_v\beta1$ and $LNa_v\beta2$ are closest homologs to each other in *Lymnaea*. *Biomphalaria* also has similar $LNa_v\beta1$ and $LNa_v\beta2$ homologs but has three genes, a $BgNa_v\beta1$ and two very closely related genes, $BgNa_v\beta2a$ and $BgNa_v\beta2b$.

$LNa_v\beta3$ and $LNa_v\beta4$ are more distant to $LNa_v\beta1$ and $LNa_v\beta2$ in *Lymnaea* and *Biomphalaria* also have $BgNa_v\beta3$ and $BgNa_v\beta4$ homologs that contain similar long extracellular repeat sequences. See full alignment of *Lymnaea* and *Biomphalaria* auxiliary sodium channel subunits in Appendix 3, Alignment 5.

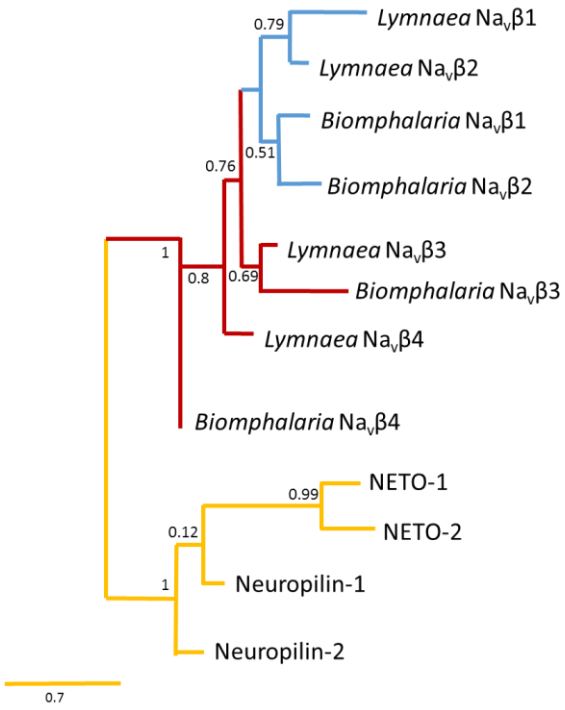

Figure 4.8. The Gene tree of the four sodium channel beta subunits from pulmonate freshwater snails, *Lymnaea* and *Biomphalaria.*
Snail LNa$_v$β subunit homologs are homologous to neuropilin (1 and 2) and NETO-1/NETO-2, which also have two CUB domains. Neuropilins and NETO proteins are illustrated as outgroups in the gene tree. Neuropilin are co-receptors for semaphorins, which are responsible for axon guidance during the development of the nervous system in vertebrates. NETO proteins are kainate receptor auxiliary subunits. Tree generated by Phylogeny.fr website (Dereeper, et al., 2008)

4.1.8 Comparison of snail accessory β-subunit with other members of the CUB family.

CUB domain containing proteins are known to be involved in neuronal related functions, including developmental patterning, axon guidance, neurotransmitter and receptor mediated endocytosis, and notably, act as auxiliary subunits to ligand gated ion channels.

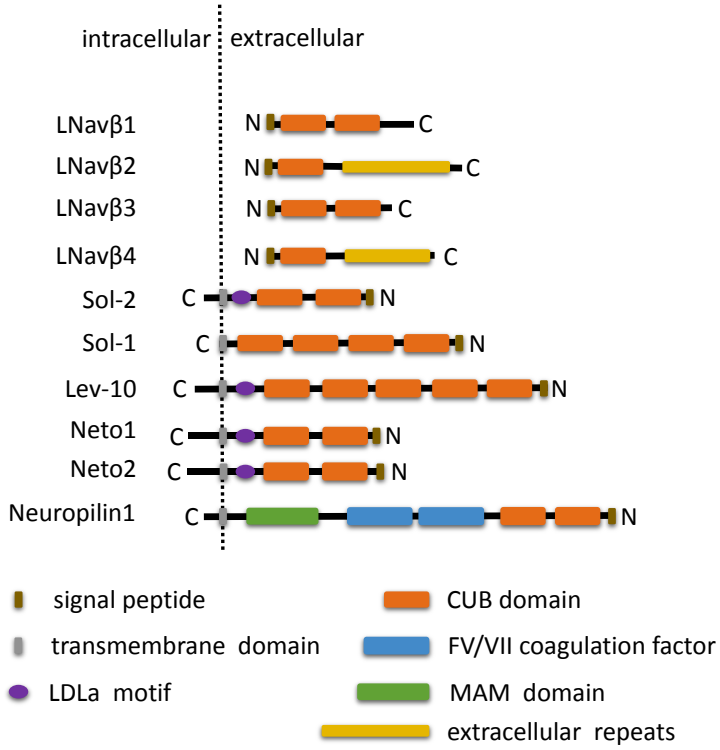

Figure 4.9. Members of the CUB domain family.
Neuropilins have the CUB domain structure that is most homologous to that of $LNa_v\beta$ proteins, while NETO and Sol show overall structural similarity to $LNa_v\beta$ in possessing two CUB domains.

The most closely related human CUB domain proteins that were recognized by the Phyre2 protein folding prediction program were neuropilin-1 (NRP-1) and neuropilin-2 (NRP-2). Neuropilins are co-receptors for class-3 semaphorins, which are responsible amongst other things for axon guidance during the development of vertebrate nervous systems (He & Tessier-Lavigne, 1997).

Sol-1 and Sol-2 that are found in the nematode *Caenorhabditis elegans* and contain two CUB domains serve as auxiliary subunits to ionotrophic AMPA glutamate receptors (iGluRs) that are not (N-methyl-D-aspartate) NMDA receptors. Sol-1 was so named because of a conserved amino acid that when modified generates a "lurcher" ataxic mouse. Sol-1 was identified as a "**S**uppressor **O**f **L**urcher" in a screen of modifiers of genes that suppressed the "lurcher" phenotype of iGluR-1 (Zheng, Mellem, Brockie, D., & Maricq, 2003). Sol-1 affects

iGluR gating but not localization of receptors to synapses. Sol-1 slows receptor desensitization and speeds recovery from desensitization, similar to the effect of NETO (NEuropilin and TOlloid like-1) proteins on mammalian ligand gated channel receptors. Mammalian Neto1 and Neto2 auxiliary subunits coassemble with NMDA receptors (NMDARs) and kainate receptors (KARs) to modulate their gating, and possibly regulate trafficking of these receptors to the membrane (Ng, et al., 2009)

Another CUB domain protein in *C. elegans*, Lev-10, is required for clustering of levamisole-sensitive acetylcholine receptors (L-AChRs) at the nematode postsynaptic membrane of neuromuscular junctions (NMJ). Loss of Lev-10 does not functionally modify the gating of receptors like Sol-1 or mammalian NETO subunits, but causes the complete loss of receptors at synapses (Gally, Eimer, RichmondJ.E., & Bessereau, 2004). Many CUB proteins, including Sol-2, Lev-10, Neto-1 and Neto-2 have a low density lipoprotein class A (LDLa) domains adjacent to the membrane that is lacking in the snail $LNa_v\beta$ subunits (Gaboriaud, Thielens, Bally, & Arloud, 2011).

The putative $Na_v\beta$ subunits from pulmonate snails, *Lymnaea* and *Biomphalaria* are likely soluble proteins, with the first eleven amino acids predicted to form a signal peptide that is post-translationally cleaved. There are no predicted transmembrane domains in $LNa_v\beta$. All the CUB domain containing proteins (neuropilin-1, neuropilin-2, Sol-1, Sol-2, LEV-10, NETO-1, NETO-2) described above have a single-pass transmembrane domain, but at least some of these proteins have soluble versions that are functional. Both Neuropilin-1 and Neuropilin-2 have truncated and secreted form of splice variants, while the presence of a soluble Sol-1 CUB domain partially rescues the function of GLR-1 ionotrophic receptors (Ng, et al., 2009). A truncated, soluble form of LEV-10 is able to cluster the L-AChRs at NMJs and restore synaptic currents. Lev-10 is associated in a complex with Lev-9 and OIG-4, that are required for clustering L-AchR, but Lev-9 and OIG-4 are completely soluble, secreted proteins (Gally, Eimer, RichmondJ.E., & Bessereau, 2004). It is also pertinent that one of the human sodium channel beta subunit splice isoforms, $Na_v\beta1B$, retains an intron that creates a secreted β-subunit without a transmembrane domain (Brackenbury & Isom, 2011).

The lack of transmembrane domains of snail β-subunits therefore may not be particularly unique.

It has recently been found that a subset of CUB domain family, dubbed cbCUB domain proteins, have the ability to bind calcium (cb stands for calcium binding). A calcium binding site is located among the linkers that connect the β sheets and presents a conserved sequence of Y-E-D-D with the residues distanced 6 to 27 amino acids from one another (Gaboriaud, Thielens, Bally, & Arloud, 2011). We have identified the conserved calcium binding motif in the first CUB domain of four *Lymnaea* LNavβ subunits (See Figure 4.10) as well as *Biomphalaria* (See Appendix 3, Alignment 5). All putative β-subunits have this motif with the adjacent conserved residues that are characteristic of cbCUB domain family. Neuropilin CUB domains are also alleged to be calcium binding, as well as *Drosophila* tolloid and human TTL1(tolloid-like 1) (Gaboriaud, Thielens, Bally, & Arloud, 2011).

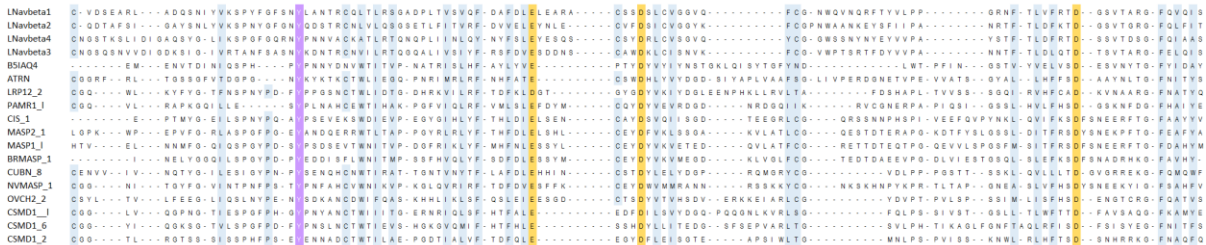

Figure 4.10. Calcium binding CUB domain alignment.
Tyrosine residue is shown in purple, and acidic residues E D D that are involved in coordination of Ca^{2+} ion are shown in yellow. Alignment is based on (Gaboriaud, Thielens, Bally, & Arloud, 2011) with *Lymnaea* CUB domains on top.

4.1.9 Cloning of the putative accessory β subunit for the analysis of its functional regulation of sodium channels.

We PCR amplified the full $LNa_v\beta1$ sequence from mature snail brain cDNA, and constructed clones with a bicystronic vector pIRES DS red. Positive clones containing the insert were identified by insert PCR amplification from bacterial template. (See Appendix B, vector map 2 for the map of LNavB1/pIRES DS red

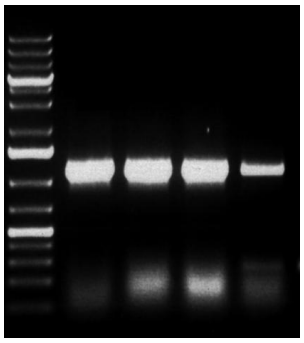

Figure 4.11 $LNa_v\beta1$ colony PCR.
Colony PCR with pIRES specific primers was performed to ensure the vector contains the insert of expected size. The gel shows all four colonies that were tested, contained the $LNa_v\beta1$ sequence. Once isolated, the plasmid was sequenced to ensure no mistakes were found in the sequence.

HEK 293 cells were transfected with primary and auxiliary subunits of sodium channel LNa_v1 to evaluate the functional effect of the $LNa_v\beta1$ as a regulator of the Nav1 α-subunit. We were able to confirm positively transfected LNa_v1 (4a+ variant) by the emission of green fluorescence of cells, and the co-expression of $LNa_v\beta1$ by the emission of red fluorescence of cells

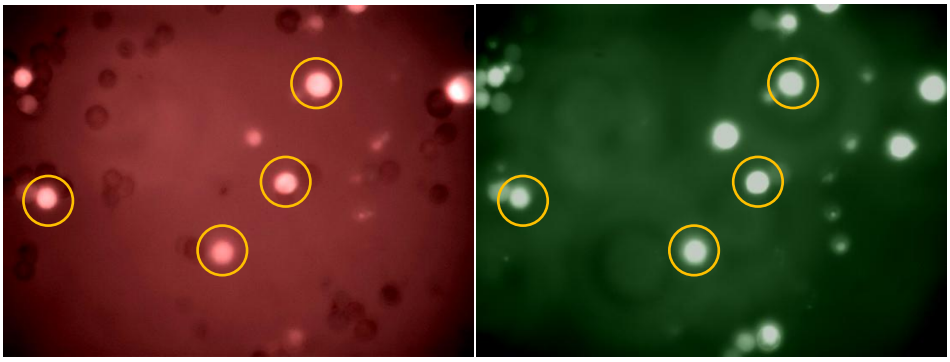

Figure 4.12 Co-transfection of LNav1.a(+) and LNavβ1 in HEK cells.
The outlined cells exhibit both green and red fluorescence.

I tested various combinations of the α-subunit (snail LNav1, and human Nav1.7), and β-subunits (snail LNa_vB1, Drosophila Tip-E and rat beta1 subunit), and evaluated sodium channel properties in whole cell patch clamp electrophysiological recording of transfected HEK-293T cells. Transfected sodium channels express poorly in HEK-293T cells and there are also contaminating native human Nav1.7 currents expressed in HEK cells, mostly in the 100-400 pA range (He & Soderlund, 2010). We were unable to confirm the expression of the *Lymnaea* Na_v1 sodium channel above the levels of native Nav1.7 currents in HEK-293T cells. In the future, we will use a different method to evaluate the expression LNa_v1 sodium channels. A common method used by scientists in the sodium channel field is injection of mRNA generated from runoff transcripts of linearized plasmids and recording of expressed channels in frog oocytes (*Xenopus laevis*).

Table 4.3 Combinations of plasmid vectors used in transfection

Construct (α)	Construct (β)	Reporter construct	Current
LNa_v1 a(+/-)[11].pIRES2-EGFP	-	-	-
LNa_v1a(+/-).pIRES2-EGFP	Tip-E.pIRES DSred	-	-
LNa_v1a(+).pIRES2-EGFP	Rat β1.pcDNA3.1	-	-
LNa_v1a(+).pIRES2-EGFP	LNavβ1.pIRES DSred	-	-
HumanNa_v1.7.pcDNA3	-	EGFP vector	yes
HumanNa_v1.7.pcDNA3	Rat β1.pcDNA3.1	EGFP vector	yes
HumanNa_v1.7.pcDNA3	LNavβ1.pIRES DSred	-	yes

The constructs were expressed in various combinations in an attempt to assess the properties of Lymnaea sodium channel α and β subunits. The same solutions were used in all recordings.

[11] In LNav1a(+/-), the 'a' refers to mutually exclusive exon, novel version, while the '+' refers to optional exon 21present in the sequence and '-' means exon 21 is deleted. (+/-) implies that both versions have been recorded.

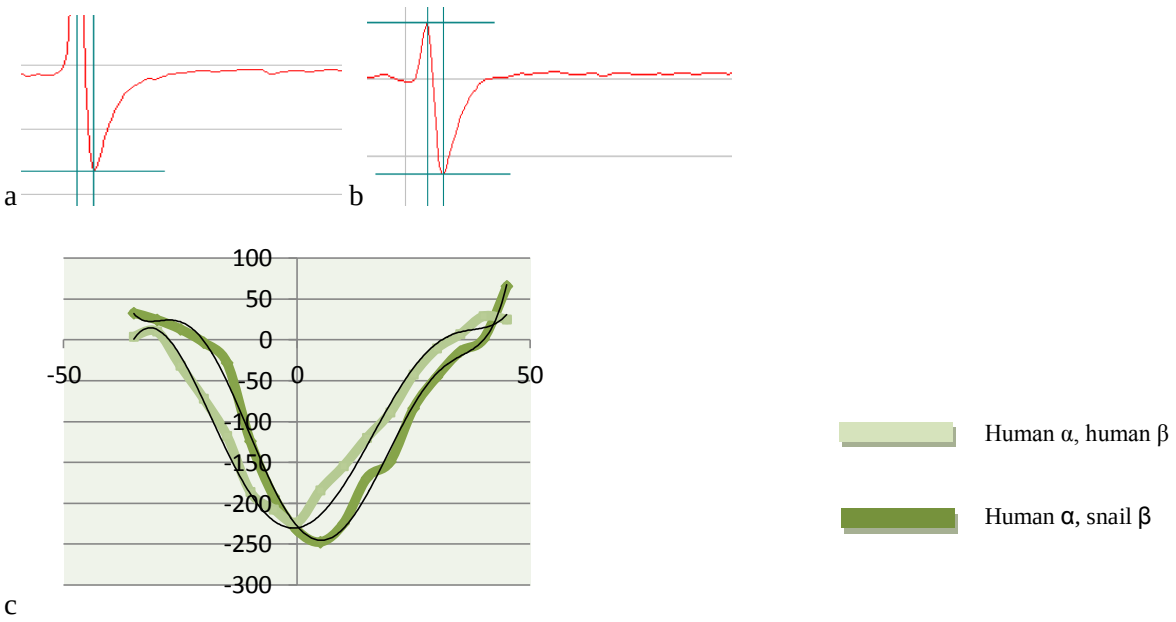

Figure 4.13 Recording of human sodium channel with human and snail β-subunit.

a. Human α human β: peak at 0, tau value 1.0678.
b. Human α, snail β: peak at 5mV, tau value 0.846543. c. IV curve to compare human and snail β-subunits.

The preliminary data indicates that Snail β1 shifts the sodium channel towards depolarization and speeds up the kinetics of the channel. More data needs to be collected before any conclusions can be reached.

4.1.10 The pulldown of the LNa$_v$1 α subunit with the putative β-subunit.

We identified LNa$_v$β1 originally in a pulldown of snail brain homogenate containing the LNa$_v$1 α-subunit. To illustrate their interaction, we attempted the reverse experiment: pulldown of the LNa$_v$1 α-subunit from transfected HEK cell homogenate with His tagged LNa$_v$β1 bound the Ni^{2+} - NTA agarose resin column. The presence of the α subunit would then be detectable with the LNa$_v$1 α-subunit specific antibody. In this single attempt, I was not able to obtain a visible LNa$_v$β1 band in a SDS-PAGE gel, nor was I able to detect a presence of the α-subunit by Western blotting. I did not have time to confirm whether the LNa$_v$β1 with its C-terminal His tag properly bound to the Ni NTA resin in the first place. It is

possible that the tertiary structure of $LNa_v\beta1$ would keep the C-terminal His –tag hidden. Both the cell protein homogenate and the surrounding cell culture medium were loaded onto the Ni NTA resin, as it is expected the $LNa_v\beta1$ is mostly a secreted protein.

4.2 Discussion

4.2.1 Structural identity of snail auxiliary subunit $LNa_v\beta$ homologs.

The small protein that was pulled out of the Lymnaea brain lysate using LNa_v1 specific antibodies in the Co-immunoprecipitation procedure and named $LNa_v\beta1$ has 2 CUB domains and a signal peptide at the N-terminus. Using blast searches of the snail LNavβ1, we found three other LNavβ subunit homologs, LNavβ2, LNavβ3, and LNavβ4. Two out of three of these putative beta subunits were also found in the brain protein complex with LNa_v1 channels, suggesting that snails have four β-subunits, reminiscent of mammalian β-subunits that can differentially modulate Na_v1 sodium channels.

Out of four β-subunits, LNavβ1 and LNavβ3 are predicted to have two CUB domains, unlike LNavβ2 and LNavβ4 that have single CUB domains. While the first CUB domain is highly conserved in all β-subunits, the downstream regions show little homology. The most obvious difference between the Navβ subunits are variable repeat sequences of 2-5 amino acids in length that are C-terminal to the CUB domains. These extracellular repeats, found on LNavβ2 and LNavβ4, form alpha helices that coil together like strands of rope. Coiled coil type proteins have important biological functions such as serving as transcription factors (c-Fos and c-jun) and muscle proteins like tropomyosin (Burkhard, Stetefeld, & Strelkov, 2001).

$LNa_v\beta$ subunits do not appear to possess a transmembrane domain, but contain a signal peptide, so they are likely secreted, and possibly bind to the extracellular side of LNa_v1. As mentioned earlier, $LNa_v\beta1$ has six cysteines, which can form three disulfide links that would stabilize the tertiary structure of the protein (See Figure 4.7). The disulfide bonds are predicted between cysteines 1 -6, 2-5 and 3-4. It is therefore unlikely that LNa_vB1 forms a covalent di-sulfide bond with the α-subunit.

4.2.2 Comparison between LNa$_v$β and other CUB domain proteins

The CUB protein family has over 2000 membrane associated and soluble proteins, involved in multiple functions, among them axonal guidance, angiogenesis, developmental patterning, tissue repair, tumor suppression, and fertilisation (Blanc, et al., 2007). The majority of CUB family proteins have multiple repeats of the CUB domain- up to 27 in cubilin. Some have fewer (2-4) domains and resemble the novel LNa$_v$β1 in their structure. The highly diverse specialised function of the CUB domain proteins depends on the electrostatic interactions between the CUB domains and the target proteins (Gaboriaud, Thielens, Bally, & Arloud, 2011).

Among proteins with similar structure is NETO1 (neuropilin and tolloid like 1) protein which is expressed in mammalian retina and brain (Stohr, Berger, Frohlich, & Weber, 2002). Like LNa$_v$β1, NETO1 has a N-terminal signal peptide, followed by tandem CUB domains, which are then followed by C-terminal LDLa (low density lipoprotein receptor domain class A) and a transmembrane domain. NETO1 is a component of the NMDA receptor multiprotein complex that plays a role in the NMDAR maintenance. NETO1 null mice exhibit spatial learning deficiencies (Ng, et al., 2009). NETO1 CUB domains are highly homologous to those of another CUB family member- neuropilin. Neuropilins participate in neuronal and cardiovascular development. As targets of semaphorin binding, neuropilins are involved in axon steering and formation of new blood vessel branches during embryogenesis (Carmeliet, 2003).

Another example of CUB domain proteins are Sol-1 and Sol-2 found in *C.elegans.* Sol proteins are auxiliary subunits of ionotrophic glutamate receptors (GLR), responsible for glutamate gated current regulation Sol-1 is required for the proper function of the GLR, while Sol-2 helps maintain the stability of GLR/Sol-1 complex on the cell membrane (Zheng, Mellem, Brockie, D., & Maricq, 2003) (Wang, et al., 2012). LEV-10 is another CUB domain containing protein in *C. elegans*, that, like Sol-1 and Sol-2 serves as an auxiliary subunit of ligand gated channels, but in this case is specific for post-synaptic aggregation of acetylcholine receptors. It is interesting that Sol-1/Sol-2 and Lev-10 in invertebrates and Neto-1/Neto-2 in vertebrates are all not homologous to each other, but are auxiliary subunits

of different ligand gated channels. The discovery of gastropod snail Navβ subunits extends the auxiliary subunit function of CUB domain proteins to voltage-gated ion channels.

4.2.3 LNa$_v$β subunits, mammalian Na$_v$1 β-subunits and Drosophila Tip-E/TEH

Although gastropod snail Navβ subunits with their CUB domains are not homologous to the mammalian sodium channels or *Drosophila* Tip-E beta subunits for that matter, there are still some remarkable similarities with both: 1) the CUB domain has remarkable similarity to the immunoglobulin superfamily with their Ig V-fold domain in mammalian beta subunits. The Ig V-fold domain is roughly the same size or smaller (70-110 amino acids) and forms a sandwich-like structure formed by two sheets of antiparallel beta strands. Highly conserved disulphide bonds form between cysteine residues to stabilize the Ig fold. The CUB domain is reminiscent of the Ig fold, forming a compact ellipsoidal structure assembled from ten beta-strands organized in a sandwich of two five-stranded beta sheets, each containing two parallel and four antiparallel strands and conserved cysteines that probably form structure stabilizing di-sulfide bonds. 2) Another similarity with human sodium channel beta subunits is that there are completely soluble versions of human Na$_v$β1, lacking a transmembrane domain and likely secreted as extracellular only proteins. Snail Na$_v$β subunits are completely soluble and extracellular too, and many of the CUB domain containing ligand gated channel auxiliary subunits (Sol/NETO/LEV10) also have soluble spliced isoforms. 3) Different mammalian sodium channel beta subunits will form dimers, and the extracellular repeats in gastropod snail beta subunits indicate that these extracellular repeats possibly could self-associate as well. 4) Sodium channel beta subunits are also not just auxiliary subunits of ion channels, but have very important roles outside of altering the gating and expression of mammalian sodium channels. Sodium channel beta subunits have been shown to function as cell adhesion molecules which can interact with the extracellular matrix and cytoskeleton and serve as regulators of cell migration, and cellular aggregation. The cell adhesion molecule role is ascribed to CUB domain containing proteins as well, with roles in developmental patterning, tissue repair, axon guidance, angiogenesis and cell signaling (Blanc, et al., 2007). 5) Many CUB domain containing proteins have calcium

binding, EGF-like binding domains. This is shared in *Drosophila* beta subunits, where TEH (TipE homologs) resemble TipE but with calcium binding, extracellular EGF like domains.

4.2.4 The significance of LNavβ subunits possessing a cbCUB domain

Many of the CUB domains are endowed with a calcium-binding capacity, which is coordinated by a triad of acidic residues (one glutamic acid and two aspartic acid residues). These, together with a conserved tyrosine associated with the calcium binding site, generate a YEDD signature sequence common in calcium-binding CUB domains. Snail LNavβ subunits also possess the signature YEDD sequence and therefore are likely calcium-binding as well(Gaboriaud, Thielens, Bally, & Arloud, 2011). The ionic interaction with calcium is expected to be a low micromolar affinity calcium interaction similar to members of the LDLR (low density lipoprotein receptor) family. The highly specialized functions in different CUB domain proteins are reported to involve variable electrostatic interactions between the CUB domains and their protein ligands (Gaboriaud, Thielens, Bally, & Arloud, 2011). We will evaluate in the future how the calcium binding capacity of LNavβ subunits of gastropod snails influences the function and regulation of snail Na_v1 channels.

Chapter 5. Conclusions and future directions

This project began with the purpose of exploring the characteristics of expressed Na_v1 and Na_v2 sodium channels of freshwater mollusk *Lymnaea stagnalis*, a protostome invertebrate. Since Nav1 sodium channels are essential to the evolution of nervous systems, our comparative analyses of invertebrate Na_v1 channels should provide insights into the more fundamental and more specialized, adaptive features of nervous systems.

The answers that we have obtained lead to new questions and open doors for further research. Among the experiments we propose are several options designed to obtain recordable sodium currents from the existing full-length constructs I have cloned already of the snail LNa_v1 channels. We plan to do the following: a) clone new variants of LNa_v1 with mutually-exclusive exon 4b instead of exon 4a, since exon 4b more resembles the exon 4 of human Nav1 channels; b) clone in the human $Na_v1.7$ II-III linker containing the ankyrin G binding motif into snail LNa_v1, to see if the mammalian motif responsible for trafficking and clustering expressed neuronal sodium channels will facilitate the expression of snail LNa_v1 to express HEK-93T cells; c) prepare run-off mRNA transcripts of LNa_v1 and accessory subunits to express in *Xenopus* oocytes and evaluate the expression of these subunits in oocytes using two-electrode voltage clamp electrophysiological recordings. We have failed to date to generate LNav1 sodium currents, which may be the result of transfection and expression in human HEK cell lines which is not as efficient as *Xenopus* oocytes and/or that the snail LNa_v1 and its beta subunit is lacking compatible features for expression in human HEK293T cell lines.

If we have recordable Na_v1 channels, we will evaluate whether mutations in Domain IV of Nav1 sodium channel are responsible for the highly TTX insensitive Na_v1 sodium channels in *Lymnaea stagnalis*.

One interesting area of study is to evaluate the mRNA and protein expression patterns of Nav1 sodium channels in snail tissues. We expect that LNa_v1 protein is completely limited to the brain. It will also be interesting to evaluate how snail LNa_v1 channels are distributed along axons in the simpler invertebrate nervous system. No myelinated axons have been found in mollusks, but perhaps there is something equivalent to the axon initial

segment where dense clusters of sodium channels are found to promote action potential generation. We created highly specific LNa$_v$1antibodies for evaluating the expression pattern of LNav1 in different tissues.

We also intend to continue cloning the full length calcium selective Na$_v$2 channel from *Lymnaea stagnalis*. We expect to characterize the electrophysiological features of the calcium selective Na$_v$2 channel and to identify possible, novel splice variants. We also plan to evaluate the expression pattern of the Nav2 channel which we expected to be limited to sensory organs. We also want to make Na$_v$2 specific antibodies raised in rabbits, by immunizing rabbits with His tagged fusion proteins of the I-II and II-III linker, in a manner that what also used generate to generate snail Nav1 antibodies, previously.

I wish to continue the analyses of the putative LNa$_v$β subunits and the consequences of LNa$_v$β1 associating with LNa$_v$1. We are going to collect and compare tissue specific expression data from sodium channel α and β subunits using real-time qPCR. We would like to generate a sodium channel beta subunit specific antibody raised in mice, to evaluate its co-labelling in snail brains with Nav1 sodium channels using immunofluorescence staining.

We also wish to investigate further the binding association of putative LNa$_v$β1 subunit and Nav1 channels. We will reverse our previous co-immuno-precipitation experiment to show that the snail β subunit can be used as a probe to pull out the LNav1 sodium channel in snail brain homogenate. If we succeed in establishing the functional link between LNa$_v$β1 and LNa$_v$1 sodium channels, we will examine the other homologs of LNa$_v$β1 in snails (LNa$_v$β2, LNa$_v$β3 and LNa$_v$β4) and how they differ in their modulation of Nav1 channels, and evaluate their expression patterns in different tissues as measured by real-time qPCR.

5.1 Proposed experiments related to LNa$_v$1 and LNa$_v$2

5.1.1 Substitution of the mutually exclusive exon

The mutually exclusive exons 4a and 4b found in several molluscan species code for the Domain I, segment I of the sodium channel α-subunit. Exon 4b is the only isoform found in one type of snail (*Lottia gigantea*), and exon 4b is more similar in sequence to human

Na_v1 sodium channels. Thus, it is possible that exon 4b is the more expressible exon in snail LNa_v1 channels, than is exon 4a. So far, we have only tested clones of LNa_v1 clones possessing exon 4a. It is possible that exon 4b is more capable of promoting the expression of sodium currents in HEK 293T cells, where exon 4a containing channels generate no obvious expression of sodium currents in HEK 293T cells. Putting the exon 4b splice variant clone LNa_v1 (LNa_v1b+) and expressing it in HEK 293 cells is thus a priority project to establish LNa_v1 sodium channel currents.

5.1.2 Insertion of human II-III linker into snail sodium channels

One of the difficulties of expressing an invertebrate protein in a mammalian cell line is a potential mismatch between the expressed protein and the host cell proteins designated to aid in posttranslational modifications and localization. From work done with α-subunit specific antibodies we know that a full length sodium channel is being expressed, but we cannot be sure whether it reaches the membrane in sufficient quantities to create measurable sodium current. To improve the cell surface expression of LNa_v1 we are going to insert a human $Na_v1.7$ 1175 bp II-III linker region containing the ankyrin G binding fragment into a BlpI restriction enzyme site spanning the II-III linker region of the *Lymnaea* Nav1 sodium channel. The II-III linker of the Na_v1 channel is less likely to affect the channel's biophysical properties. We expect that the chimeric snail channel with the human II-III linker would promote channel surface expression without altering the channel gating properties. A potential side project would be to make an expressible GFP tagged snail channel with the mammalian II-III linker and evaluate how the expression of the mammalian II-III linker effects sodium channel distribution within snail nervous systems.

5.1.3 Using *Xenopus* oocytes as a vehicle for LNa_v1 expression

Unlike mammalian sodium channels which can be expressed and recorded without difficulty in the human HEK293T cell line, invertebrate sodium channels might not be favorable for expression in mammalian cells. Laboratories that work with sodium channels usually use *Xenopus* oocytes as host cells for channel expression of injected run-off mRNA

transcripts(Tan, Liu, Nomura, Goldin, & Dong, 2002). Our lab obtained excellent results recording *Lymnaea* Cav1, Cav2 and Cav3 calcium channels in HEK293 cells; but it is possible that LNav1channel clones just don't generate sodium currents as they would in *Xenopus* oocytes. We want to put the LNa_v1clone into the *Xenopus* oocyte expression vector based on pGH19, a *Xenopus* expression vector. We will do this by putting a customized polylinker into pGH19 that spans the unique MluI-KpnI ends of the full length LNav1 clone in pIRES2-EGFP. We will linearize the plasmid, transcribe the gene into mRNA *in-vitro* and inject the prepared mRNA into oocytes for expression and recording attempts of the LNav1 channel expression using the two electrode voltage clamp technique. We will carry out *Xenopu*s oocyte recording of LNav1 in our lab or in collaboration with Ke Dong, at Michigan State University.

5.1.4 Unique features that we will examine for *in vitro* expressed LNa_v1 channels

We expect that snail $LNa_v\beta$ subunits may alter the expression levels and biophysical properties of LNav1 channels. We want to also pursue whether there is inter-compatibility between human sodium channel beta subunits, snail $Na_v\beta$ subunits and Drosophila Tip-E, in their regulation of LNa_v1 channels. It will address whether these analogous beta subunits in different species perform the same functions, despite their structural dissimilarity with each other.

We know that the I-II linker has conserved PKA and PKC sites that when phosphorylated, dampen human neuronal sodium channel activity. We predict that snail LNa_v1 will respond to PKA and PKC phosphorylation in the same manner.

Snail LNa_v1 channels like other gastropod snail channels are insensitive to TTX. We have seen the changes in Domain IV of pore helix 2 in population of garter snakes of *Thamnophis sirtalis* that allowedthe snakes to adapt to feeding on newts (*Taricha granulosa*) that have toxic levels of TTX in their skins. We will make the appropriate Domain IV, pore helix 2 mutations and address whether this change is responsible for the insensitivity of snail channels to TTX.

5.1.5 We will examine the localization of LNa$_v$1 sodium channels within snail brains.

Based on our qPCR data, LNav1 sodium channels is the most abundant transcript that we have identified, with levels that are 29 fold higher than HPRT control mRNA levels. We will paraffin-embed tissue cross sections of snail brains and label the immune-fluorescent staining with snail LNa$_v$1 antibody using confocal microscopy. We will also attach LNa$_v$1 antibody to a gold conjugate and examine the localization of LNa$_v$1 staining at the transmission electron microscopy level. Our goal is to understand the pattern of localization of sodium channels in invertebrate axons. It has been thought that primitive invertebrates would lack clustering of sodium channels, but it is more likely that there is differential localization to support action potential firing at axon initial segments.

5.1.6 Cloning and expression of snail LNa$_v$2 channel *in vitro* and evaluation of its pattern of expression in snail tissues.

We will try and put together the full length snail Nav2 sequence in PCR products that are generated with cDNA template from *Lymnaea* external sensory organs such as eyes and tentacles. As we did for the LNa$_v$1 channels, we will put in a designer polylinker that has custom restriction sites for cloning LNa$_v$2 PCR products sequentially into pIRES2-EGFP. As we clone LNa$_v$2 we may encounter unique splice variants that we could evaluate further.

Once the LNa$_v$2 channel is sequenced and cloned into the pIRES2-EGFP expression vector, we will record LNav2 and characterize its biophysical properties and unique calcium selectivity. We will identify which exact tissues LNa$_v$2 is expressed in, and whether this includes other sensory organs (lips, pneumostome) and compare the expression levels of these isolated tissues using qPCR analysis.

We will make LNa$_v$2 specific antibodies with antigens grown as 6xHis-tagged bacteria fusion proteins targeting the I-II and the II-III linker of the channel. With a specific LNa$_v$2 antibody, we can address the localization of LNa$_v$2 channels in snail sensory organs.

5.2 Proposed experiments related to putative LNa_vB subunits

5.2.1 Real-time, quantitative PCR to analyze tissue specific expression of LNa_vB1

We will compare the expression patterns of the sodium channel α-subunit and the $LNa_v\beta1$ subunit to understand whether they are co-localized specifically in the same cells of the brain together. We know that $LNa_v\beta1$is expressed abundantly in the brain, since brain lysate was used to isolate the protein and brain mRNA was the source of $LNa_v\beta1$ sequence for PCR amplification. Showing that $LNa_v\beta1$ is expressed only in brain tissue will reinforce the idea of its close functional relationship with the brain specific LNa_v1 channels. However, to determine the protein localization patterns, we will make a $LNa_v\beta$ subunit specific antibody, but not in rabbits. If we generate a mouse specific $LNa_v\beta$ antibody, we can compare the anti-mouse $LNa_v\beta$ localization pattern with the staining of LNa_v1 and LNa_v2 channels, to address whether the $LNa_v\beta$ co-localizes with both channel types, and address whether $LNa_v\beta$ has patterns of expression that also don't overlap with any sodium channel.

5.2.2 Pulling down the α-subunit using β- subunit specific antibodies

We will need to confirm that $LNa_v\beta1$ is a binding partner with LNa_v1 channels in the brain. We first fished out $LNa_v\beta1$ by isolating it from the sodium channel complex bound to LNa_v1 antibody. We will put an N-terminal 3xHA tag on $LNa_v\beta1$ and couple it to HA beads, and fish out whether LNa_v1 from brain homogenate will co-immunoprecipitate with $LNa_v\beta1$ bound to beads. The presence of α- subunit in the alpha-beta complex of sodium channels bound to beads will be confirmed using Western blotting and the LNav1 α-subunit specific antibody. Using the $LNa_v\beta1$ bound to beads and to pull out the α-subunits from the brain homogenate will provide adequate proof that $LNa_v\beta1$ is a sodium channel auxiliary subunit.

5.2.3 Calcium binding properties of $LNa_v\beta1$

While analyzing the sequence of the putative sodium channel β-subunit we discovered that the first CUB domain of each LNa_vB homolog contains a calcium binding CUB domain signature motif YEDD. We intend to evaluate the calcium binding properties of $LNa_v\beta1$ by loading HEK cells expressing the $LNa_v\beta1$/pIRES DSred clones with free Ca^{2+} ion

and to use the Ca^{2+}-sensing fluorescent indicator dye, to analyze the rate of calcium binding under the confocal microscope. Mutations in any of the YEDD signature sequence should eliminate the calcium binding capacity of $LNa_v\beta1$ subunits. We can address whether the mutation of the YEDD signature sequence is vital to the modulation of snail LNav1 sodium channels.

5.2.4 Investigating of the LNa_vB homologs

Like other members of the large CUB domain family, LNa_vB proteins could play multiple roles in neural system development and maintenance. There are variable repeat sequences in the C-terminal tail of LNa_vB3 and LNa_vB4 that hint at their potential role as possible transcription factors. We will test whether these novel sodium channel beta subunits have different effects on LNa_v1 channels expressed in vitro. We may expect a nuclear targeting of a subset of $LNa_v\beta1$ subunits if they are capable of serving as transcription factors. We could carry out a co-immunoprecipitation or yeast-2-hybrid assay, to evaluate what binding partners are associated with $LNa_v\beta1$, outside of LNa_v1 sodium channels. The study of $LNa_v\beta$ homologs could open exciting new research directions in understanding how the invertebrate nervous system operates.

Appendix A. Primer sequences

Table 5.1.Primers for LNa$_v$1 α-subunit sequencing

	Name	Sequence 5'→3'
1	Nav1FIGVIIf	TTYATHTTYGCNGTNATGGNCARCA
3.	Nav1FIGVIIb1	AAGACCAATGCTGCCAGTTT
4.	Nav1FIGVIIb2	TCATTCGTTTCATGGCATTG
5.	Nav1AKHAEKf	GARGARGCNGCNAARCAYGCNGARAA
6.	Nav1PWNWLDb	ACRAARAARTCNARCCARTTCCANGG
7.	5' raceb2	TTTCTGCCAGCCTCAAGTTT
8.	5' raceb1	TGATGGAGGGAGTTTTCTGC
9.	3' RACE F1	CTGGTTGGAGCGATGTTCTA
10.	3' RACE F2	TGGAGCGATGTTCTAAATGC
11.	2.2kbF1	GCCATAACTTCGTGGACACC
12.	2.2kbF2	AACCCTCTCAAGGGGCTTTA
13.	2.2kbB1	CACACAGCACACGAAACACA
14.	2.2kbB2	GTTCCACCTGGGCATGTTAT
15.	LNav1_TVELGPDSb2	CTGTYNGGNCCNAGYTCNACNGT
16.	LNav1_GPDSGVVAb1	GCCACYAYNCCNCTGTYNGGNCC
17.	LNav1-ex16f1	TCCTTCAAAGCTGCCAGAAT
18.	LNav1-ex16b1	AACACCTTAGAGCCCACCAA
19.	LNav1-ex16f2	AAGCTGCCAGAATTGAATGG
20.	LNav1-ex16b2	GGGAGGTTTTTCAATGACCA

Degenerate primers are based on molluscan consensus sequences, derived from sodium channel sequences of Lottei, Aplysia and Biomphalaria.

Table 5.2. Primers for full length α-subunit contig construction in pIRES vector

	Name	Sequence 5'→3'
21.	Nav1PolylinkerA	TCGACCCAAACGCGTCCAAACTAGTCCAAAAGCTTCCAAGAATTCCCAAC
22.	Nav1PolylinkerB	GGCCGTTGGGAATTCTTGGAAGCTTTTGGACTAGTTTGGACGCGTTTGGG
23.	Nav1ATGff	TCGCGAGCACTACTCATAGC
24.	Nav1SpeIbb	GGATCCTGGCAAACTGAGAC
25.	Nav1ATGf	GGCCGTCGACACGCGTGCCGCCACCATGGAAGAGGAAACTGTAGAACG
26.	Nav1SpeIb	GTTTAAGGTGAGCGCTGGTC
27.	Nav1SpeIff	ATGCTGGCGAGAAGGATTTA

28.	Nav1HIIIbb	ATTCTGGCAGCTTTGAAGGA
29.	Nav1SpeIf	CCTAACTAGTGACCAGTCGATGACCAG
30.	Nav1HIIIb	AGTTTTTCTGGCGTTGAAGcTTGACTT
31.	Nav1HIIIff	CGCTCAGAGTCTGCTGATGA
32.	Nav1EcoRIbb	AGAACTCGACCCACTCGAAA
33.	Nav1HIIIf	GTCAAgCTTCAACGCCAGAAAAACT
34.	Nav1EcoRIb	TGAGCAGGGTTGGTGATATG
35.	Nav1EcoRIff	GTTTGGTCTGCGCTGGTATT
36.	Nav1Xma1bb	TGGATTGATTCCAAAGCTGA
37.	Nav1EcoRIf	GGTTCCCTGGAATGTCTTTG
38.	Nav1Xma1b	TCCATGCCCGGGTCACGCCACAATGCCACTGTTAG

The primers named polylinker A and B were designed to form an adaptor which would equip the pIRES vector with the necessary restriction sites. The polylinker contains in the following order: XhoI, MluI, SpeI, HindIII, EcoRI and XmaI.

Table 5.3. A list of primers used in the construction of two expression vectors (antigen production)

	Primer	Restriction site	Direction	Sequence (5' – 3')
39.	1,2-Linker	NdeI	F	GACACATATGGAGTTTGATGCTGGCGAGAAGG
40.	1,2-Linker	XhoI	B	GCTGCTCGAGAAGGAAAGGGTTGCTCTCAGAAG
41.	2,3-Linker	NdeI	F	GACGCATATGGTCTCAAGAGCAGGCAGCATATATTC
42.	2,3-Linker	BglI	F	GACGAGATCTGTCTCAAGAGCAGGCAGCATATATTC
43.	2,3-Linker	BamHI	B	CAGTGGATCCGATCTCATGATCACCTTCCAGGTCAAT
44.	2,3-Linker	XhoI	B	GAGTCTCGAGGATCTCATGATCACCTTCCAGGTCAA

These primers were designed by Dr Spafford for the undergraduate project of Neil Hsueh.

Table 5.4. Primers used for LNav B1 sequencing, amplification and cloning

	Name	Sequence 5'→3'
45. 1	LNavbeta1fff	TGGAGCATCCTTCAATTTGC
46. 2	LNavbeta1bbb	CGTAGCCTGCCATTTGTTCT
47. 3	LNavbeta1ff	GCGGCTGCGTAAACATAAAG
48. 4	LNavbeta1bb	CGAACAACCTGTCGTCAAAA
49. 5	LNavbeta1f	GCATTTGGTGGACATGATGA
50. 6	LNavbeta1b	CAGAACGACGATTTGATTTTG

51. 7	LB1.Histag.Xmal	CCCGGGTTAATGGTGATGGTGATGGTGTTTTTTGTAATTAATGGCCCTGCC
52. 8	LNavB1f.Sall	TCAGATGTCGACTACCACC ATGATGAGATGTGGTGCCCT
53. 9	LymbetaBBamHI	GGTTGGATCCCGACTAATCTTTTACATTATTTTTTGT

Primers 33-38 were used for amplification and sequencing of Sodium channel auxiliary subunit LNavB1. Juvenile brain cDNA was used as a source of mRNA. Primers 39-41contain restriction sites that enable to clone the sequence into pIRES2DSred vector.

Table 5.5. Primers for cloning LNav2

	Name	**Sequence 5'→3'**
1.	Nav2Cff	GTGGTNAATGCNCTNATGAATGC
2.	Nav2Cbb	TCATTTGGCTTTGGGATTTG
3.	Nav2CF	TTYTGGCTCATNTTCAGCATCAT
4.	Nav2Cb	CAAATCCCCAACAAAATTGG
5.	Nav23'RACEff	AATCCCAAAGCCAAATGAAA
6.	Nav23'RACEf	CCCCATAATGGAAGGTGAGA
7.	Nav2-A1f	AGCTGAGAACATTGAGTACTTGTTTT
8.	Nav2-A1b	GCAACGCCAAGAAAAGATTG
9.	Nav2-B1f	GCCATCTACACATTGGAGTGC
10.	Nav2-B1b	TCCAAAGACCAATGCTGGTA
11.	Nav2-C1f	AGGCCTCAAGTGAACTTTGC
12.	Nav2-C1b	TGTCATTCCATCCAGCAGAT
13.	Nav2-D1f	TACCAGCATTGGTCTTTGGA
14.	Nav2-D1b	TTTCAGTCATGACGCCATTC
15.	Nav2-E1f	TGTTCACCGCTGTGTTTACG
16.	Nav2-E1b	GGTCAGGTTGGTGTCAAGGT
17.	Nav2-F1f	CGCTGTGTTTACGTTGGAAG
18.	Nav2-F1b	CTACGCCAAGCCCTTTGTAG
19.	Nav2topf1	CAAGAYGCNCATYTNGTTGATGG
20.	Nav2topf2	GGNATACCTATTGARGAAATTGA

21.	Nav2topb2	GACDATRAAATCCAACCAATTCCA
22.	Nav2topb1	AAACACCATNARACARAARAATGT
23.	Nav2midf1	ATTCGAGCNACAGGNCCNTGGAATGT
24.	Nav2midf2	GTTTCAATGTCNTATGARGARGARGC
25.	Nav2midb2	NACTCNAAATATCATCAGCATNGA
26.	Nav2midb1	NGCTGGCAAGAANACNACCATNCA

Table 5.6. Vectors used for cloning

Name	Size(Kb)	Resistance	Target cell	Reporter
1. pGEMt Easy	3.0	Amp	E coli	LacZ
2. pIRES2 EGFP	5.3	Kan/Neo	E coli/HEK	EGFP
3. pIRES DSred	5.3	Kan/Neo	E coli/HEK	DSred
4. pGH19	5.6	Amp	X.oocyte	--
5. Blunt-II-TOPO	3.5	Kan/Zeo	E.coli	LacZ
6. pET22b	5.5	Amp	E.coli	--
7. pcDNA3	5.4	Amp/Neo	E coli/HEK	--

Appendix B. Vector maps

1. LNav1α a+ in pIRESII-EGFP, inserted between MluI and AclI

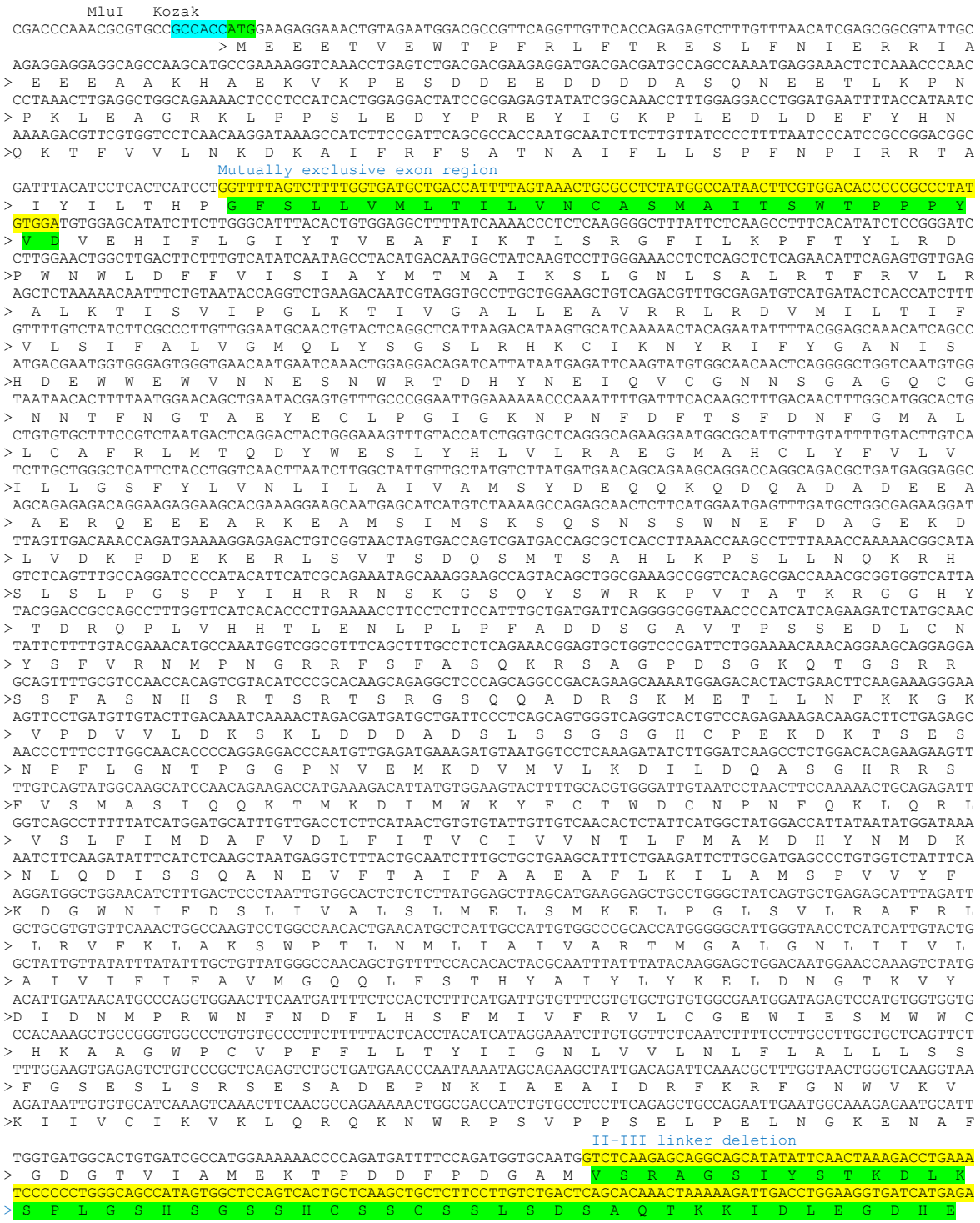

TCAATGAAGTAGAGATTGTCTATGCCAAGGAACCAGATGATTGCTTCTGCTATTCCCTCACAAAGCGCTGTACTTGGTGTTTGGTCATTGAAAAATCTCCCAT
>I N E V E I V Y A K E P D D C F C Y S L T K R C T W C L V I E K S P I
CGGTCGAGCTTGGTGGGCTCTAAGGTGTTTTATGTATCGGCTAGCAGAGCATCGATACTTTGACACTTTCATTATAGTGATGATCTTGCTCAGCAGTTGTGCA
> G R A W W A L R C F M Y R L A E H R Y F D T F I I V M I L L S S C A
TTGGCTTTAGAAGATGCCTACCTTCATGAGAAGCCACTGCTGAAGGAGATTCTGGAGTACATGGACAAAGTGTTTACTGTCATCTTCATTGTAGAGATGTTGG
> L A L E D A Y L H E K P L L K E I L E Y M D K V F T V I F I V E M L
TCAAGTGGTTTGCCTTTGGCTTCAAAACTTACTTCACTGACGCCTGGTGCTGGCTGGACTTTTGTATTGTCATGTTATCTATTATGATGCTTATGGCTGACAT
>V K W F A F G F K T Y F T D A W C W L D F C I V M L S I M M L M A D M
GATGGCATCTGCTGATGGACATGGTGGAGGCAAAATGGGGGCAATGAGATCCATTAGGACATTGAGAGCCTTACGTCCACTCCGAGCGGTCAGTCGTTGGGAG
> M A S A D G H G G G K M G A M R S I R T L R A L R P L R A V S R W E
GGAATGAGGGTTGTAGTGAATGCCCTATTCAAAGCTATCCCATCCATCTGTAATGTGCTGCTAGTGTGTCTAGTTTTCTGGCTCATATTCGGAATTATGGGAG
> G M R V V V N A L F K A I P S I C N V L L V C L V F W L I F G I M G
TACAGCTCTTCAATGGGAAATTTCACGCTTGCGTCTGTGAAAATGGCACAAGATGTGAACCAGATGTGATACCTAATCGGACTGTTTGTGAGTTACAAGGCTA
>V Q L F N G K F H A C V C E N G T R C E P D V I P N R T V C E L Q G Y
CAACTGGACCAACGCTCAGATCAACTTTGATAATGTTATTGCTGCATACTTGGCTCTCTTTCAAGTGGCCACCTACAAGGGATGGGTGGACATAATGAACAAT
> N W T N A Q I N F D N V I A A Y L A L F Q V A A T Y K G W V D I M N N
GCCATTGATGCAAGAGAGATTGGTATCCAACCAAAGAGAGAGGAAAATATCTACTCATACCTATTTTTTGTACTTTTCATCATATTTGGTTCTTTCTTCACCC
> A I D A R E I G I Q P K R E E N I Y S Y L F F V L F I I F G S F F T
TCAACTTATTCATTGGTGTCATCATTGATAACTTCAATTCCCAGAAAAAGAAGGCTGGTGGCTCTCTAGAAATGTTCATGACAGACGATCAAAAGAAATACTA
>L N L F I G V I I D N F N S Q K K A G G S L E M F M T D D Q K K Y Y
CAATGCCATGAAACGAATGAAGTCTAAATCCCCACAAAAATCAATTCCCAGGCCTAAGTACAAACTGGCAGCATTGGTCTTTGACATCACCACTGACCAGAAG
> N A M K R M K S K S P Q K S I P R P K Y K L A A L V F D I T T D Q K
TTTGATATTGTCATCATGATAATTATCATCCTCAACATGCTGACCATGATGTTTGAGTATGAAGACATGTCCAAACAGATGAAAGATATTCTGGGAATTTTCA
> F D I V I M I I I I L N M L T M M F E Y E D M S K Q M K D I L G I F
ATCTTGTCTTTATCACCATATTCACTGCAGAATGTGTTCTCAAACTGTTTGGTCTGCGCTGGTATTACTTCAAGGTTCCCTGGAATGTCTTTGATTTCATTGT
>N L V F I T I F T A E C V L K L F G L R W Y Y F K V P W N V F D F I V
CGTCGTCTTATCAATCATGGCATCATCTTTGGATGAATTCGAAGACAGCTTCTTCATATCACCAACCCTGCTCAGGGTCATTCGAGTATTTCGAGTGGGTCGA
> V V L S I M A S S L D E F E D S F F I S P T L L R V I R V F R V G R
GTTCTACGTCTGGTCAAATCTGCAAAAGGAATACGCACACTTCTCTTCTCCCTTGCTGTATCACTTCCTGCCCTATTCAACATCGGCCTTCTCCTGGGCTTAG
> V L R L V K S A K G I R T L L F S L A V S L P A L F N I G L L L G L
TCATGTTCATCTATGCCATCATGGGCATGAATTTCTTCCAAGGTTATCCTCAGACGTTTGGGATGGATGATGCTTTTAATTTTGACACCTTCTTGAGTAGCTT
>V M F I Y A I M G M N F F Q G Y P Q T F G M D D A F N F D T F L S S F
CATTCTTCTTTTCCAAATGTGCACCAGTGCTGGTTGGAGCGATGTTCTAAATGCCCTTATCTCCCCTTGCCCACCTACAGGTAGTTGCTCTCATTATAACAAG
> I L L F Q M C T S A G W S D V L N A L I S P C P P T G S C S H Y N K
GCCACTCTGTACCTGGCCACTTACCTGATCATCTCATTCCTTGTGGTCGTGAACATGTACATTGCTGTAATACTGGAGAATTTCAGTCAGGCCACTGAGGATG
> A T L Y L A T Y L I I S F L V V V N M Y I A V I L E N F S Q A T E D
TACAACAGGGTCTGACTCCAGATGACTTTGATATGTACTACGAAAAATGGGAGAAATATGATCCCAAGGCTACTAAATACATCCCACTGGACCAGCTGTCCGA
>V Q Q G L T P D D F D M Y Y E K W E K Y D P K A T K Y I P L D Q L S D
CTTTGTGGATTACCTCGAGGAGCCCTCTCAGGCTCCCAAAACCCAACCACTTTATCCTGGTCAAACTGGACATACCCATTTGTGAAGGGGATAAGTGCTACTGT
> F V D Y L E E P L R L P K P N H F I L V K L D I P I C E G D K C Y C
AGGGATATCCTTGATGCACTTACCAAGAATTTTCTAGGGACATCGGAGACAGCAGATATTCCCATCAAGGAGACTGACAAGGAGAAAGAGGAATACACGCCCA
> R D I L D A L T K N F L G T S E T A D I P I K E T D K E K E E Y T P
TCAGTAGCACCTTGAGGAGGCAGAAGGAGCACTACGCAGCTAGGATAATACAGAAGGCCTACAGAAACTACAAAGGGCTGACCATATCCGAGGTCAGCTATGG
>I S S T L R R Q K E H Y A A R I I Q K A Y R N Y K G L T I S E V S Y G
CCATGAAGATGTGATGGATAGTTATAGTCAGGATAATGATGACAGGGACAGCGGTGGCAGCAGTGGAAGGAACTTGGATAAATCCTTCCCCAGTCCACCC
> H E D V M D S Y S Q D N D D D R D S G G S S G R N L D K S F P S P P
TCCAGCTACAAAAGTGACAAAAAGCCACCAGAAAACGGGACAAAGGAGAAAAAATCTGAGGACAGCTCCAAGAAGGCAAAGGATAAGAAAGACAAGGGAAAAG
> S S Y K S D K K P P E N G T K E K K S E D S S K K A K D K K D K G K
ATAAGAAAGCCAAGTCTGATAAGAAAGATGATGGTAAAAAAAAAAAGGATGCTAGCAAACCGCCCAATGGCTTATCAAAAACAACGCGGTCAAAAGAAAGTGC
>D K K A K S D K K D D G K K K D A S K P P N G L S K T T R S K E S A
TGCGATAACTTTGATCAATGAAACGGAAGGAGAAAATAAAACGGTGGAATTGGGCCCTAACAGTGGCATTGTGGCGTGACATGGAAGGAAATCGGTATCAGAT
> A I T L I N E T E G E N K T V E L G P N S G I V A
TTATGTTCTTAATAAGGATCTTTCATTTTGTCTTATGCTTGAGCAGTGCTATGATATCAACTCAGCTATGGAATGATATCTCACTCAGCTATGCAATGATATC
AclI
AAATCAGCTTTGGAATCAATCCAAAGGGCGAATTCCCAACGGGATCCGCCCCTCTCCCTCCCCCCCCCCCTAACGTTACTGGCCGAAGCCGCTTGGAATAAGGC

CGGTGTGCGTTTGTCTATATGTTATTTTCCACCATATTGCCGTCTTTTGGCAATGTGAGGGCCCGGAAACCTGGCCCTGTCTTCTTGACGAGCATTCCTAGGGGTCTTTCCCCTCTGCCCAAAGGAATGCAAGGTCTGTTGAATGTCGTGAAGGAAGCAGTTCCTCTGGAAGCTTCTTG
AAGACAAACAACGTCTGTAGCGACCCTTTGCAGGCAGCGGAACCCCCCACCTGGCGACAGGTGCCTCTGCGGCCAAAAGCCACGTGTATAAGATACACCTGCAAAGGCGGCACAACCCCAGTGCCACGTTGTGAGTTGGATAGTTGTGGAAAGAGTCAAATGGCTCTCCTCAAGCGTAT
TCAACAAGGGGCTGAAGGATGCCCAGAAGGTACCCCATTGTATGGGATCTGATCTGGGGCCTCGGTGCACATGCTTTACATGTGTTTAGTCGAGGTTAAAAAACGTCTAGGCCCCCCGAACCACGGGGACGTGGTTTTCCTTTGAAAACACGATGATAATATGGCCACAACCATGGT
GAGCAAGGGCGAGGAGCTGTTCACCGGGGTGGTGCCCATCCTGGTCGAGCTGGACGGCGACGTAAACGGCCACAAGTTCAGCGTGTCCGGCGAGGGCGAGGGCGATGCCACCTACGGCAAGCTGACCCTGAAGTTCATCTGCACCACCGGCAAGCTGCCCGTGCCCTGGCCCACCCTCGT
TGACCACCCTGACCTACGGCGTGCAGTGCTTCAGCCGCTACCCCGACCACATGAAGCAGCACGACTTCTTCAAGTCCGCCATGCCCGAAGGCTACGTCCAGGAGCGCACCATCTTCTTCAAGGACGACGGCAACTACAAGACCCGCGCCGAGGTGAAGTTCGAGGGCGACACCCTGGTG
AACCGCATCGAGCTGAAGGGCATCGACTTCAAGGAGGACGGCAACATCCTGGGGCACAAGCTGGAGTACAACTACAACAGCCACAACGTCTATATCATGGCCGACAAGCAGAAGAACGGCATCAAGGTGAACTTCAAGATCCGCCACAACATCGAGGACGGCAGCGTGCAGCTCGCCGA
CCACTACCAGCAGAACACCCCCATCGGCGACGGCCCCGTGCTGCTGCCCGACAACCACTACCTGAGCACCCAGTCCGCCCTGAGCAAAGACCCCAACGAGAAGCGCGATCACATGGTCCTGCTGGAGTTCGTGACCGCCGCCGGGATCACTCTCGGCATGGCGAGCTGTACAAGTAAAG
CGGCCGGCACTCTAGATCATAATCAGCCATACCACATTTGTAGAGGTTTTACTTGCTTTAAAAAACCTCCCACACCTCCCCCTGAACCTGAAACATAAAATGAATGCAATTGTTGTTGTTAACTTGTTTATTGCAGCTTATAATGGTTACAAATAAAGCAATAGCATCACAAATTTCAC
AAATAAAGCATTTTTTTCACTGCATTCTAGTTGTGGTTTGTCCAAACTCATCAATGTATCTTAAGGCGTAAATTGTAAGCGTTAATATTTTGTTAAAATTCGCGTTAAATTTTTGTTAAATCAGCTCATTTTTTAACCAATAGGCCGAAATCGGCAAAATCCCTTATAAATCAAAAGAA
TAGACCGAGATAGGGTTGAGTGTTGTTCCAGTTTGGAACAAGAGTCCACTATTAAAGAACGTGGACTCCAACGTCAAAGGGCGAAAAACCGTCTATCAGGGCGATGGCCCACTACGTGAACCATCACCCTAATCAAGTTTTTTGGGGTCGAGGTGCCGTAAAGCACTAAATCGGAACCC
TAAAGGGAGCCCCCGATTTAGAGCTTGACGGGGAAAGCCGGCGAACGTGGCGAGAAAGGAAGGGAAGAAAGCGAAAGGAGCGGGCGCTAGGGCGCTGGCAAGTGTAGCGGTCACGCTGCGCGTAACCACCACACCCGCCGCGCTTAATGCGCCGCTACAGGGCGCGTCAGGTGGCACTT
TTCGGGGAAATGTGCGCGGAACCCTATTTGTTTATTTTCTAAATACATTCAAATATGTATCCGCTCATGAGACAATAACCCTGATAAATGCTTCAATAATATTGAAAAAGGAAGAGTCCTGAGGCGGAAAGAACCAGCTGTGGAATGTGTGTCAGTTAGGGTGTGGAAAGTCCCCAG
GCTCCCCAGCAGGCAGAAGTATGC
AAAGCATGCATCTCAATTAGTCAGCAACCAGGTGTGGAAAGTCCCCAGGCTCCCCAGCAGGCAGAAGTATGCAAAGCATGCATCTCAATTAGTCAGCAACCATAGTCCCGCCCCTAACTCCGCCCATCCCGCCCCTAACTCCGCCCAGTTCCGCCCATTCTCCGCCCCATGGCTGACTA
ATTTTTTTTATTTATGCAGAGGCCGAGGCCGCCTCGGCCTCTGAGCTATTCCAGAAGTAGTGAGGAGGCTTTTTTGGAGGCCTAGGCTTTTGCAAAGATCGATCAAGAGACAGGATGAGGATCGTTTCGCATGATTGAACAAGATGGATTGCACGCAGGTTCTCCGGCCGCTTGGGTGG
AGAGGCTATTCGGCTATGACTGGGCACAACAGACAATCGGCTGCTCTGATGCCGCCGTGTTCCGGCTGTCAGCGCAGGGGCGCCCGGTTCTTTTTGTCAAGACCGACCTGTCCGGTGCCCTGAATGAACTGCAAGACGAGGCAGCGCGGCTATCGTGGCTGGCCACGACGGGCGTTCCT
TGCGCAGCTGTGCTCGACGTTGTCACTGAAGCGGGAAGGGACTGGCTGCTATTGGGCGAAGTGCCGGGGCAGGATCTCCTGTCATCTCACCTTGCTCCTGCCGAGAAAGTATCCATCATGGCTGATGCAATGCGGCGGCTGCATACGCTTGATCCGGCTACCTGCCCATTCGACCACCA
AGCGAAACATCGCATCGAGCGAGCACGTACTCGGATGGAAGCCGGTCTTGTCGATCAGGATGATCTGGACGAAGAGCATCAGGGGCTCGCGCCAGCCGAACTGTTCGCCAGGCTCAAGGCGAGCATGCCCGACGGCGAGGATCTCGTCGTGACCCATGGCGATGCCTGCTTGCCGAATA
TCATGGTCGGAAATGGCGCGCTTTCTGGATTCATCGACTGTGGCCGGCTGGGTGTGGCGGACCGCTATCAGGACATAGCGTTGGCTACCCGTGATATTGCTGAAGAGCTTGGCGGCGAATGGGCTGACCGCTTCCTCGTGCTTTACGGTATCGCCGCTCCCGATTCGCAGCGCATCGCC
TTCTATCGCCTTCTTGACGAGTTCTTCTGAGCGGGACTCTGGGGTTCGAAATGACCGACCAAGCGACGCCCAACCTGCCATCACGAGATTTCGATTCCACCGCCGCCTTCTATGAAAGGTTGGGCTTCGGAATCGTTTTCCGGGACGCCGGCTGGATGATCCTCCAGCGCGGGGATCTC
ATGCTGGAGTTCTTCGCCCACCCTAGGGGGAGGCTAACTGAAACACGGAAGGAGACAATACCGGAAGGAACCCGCGCTATGACGGCAATAAAAAGACAGAATAAAACGCACGGTGTTGGGTCGTTTGTTCATAAACGCGGGGTTCGGTCCCAGGGCTGGCACTCTGTCGATACCCCACC
GAGACCCATTGGGCCAATACGCCCGGTTTCTTCCTTTTCCCACCCACCCCCAAGTTCGGGTGAAGGCCCAGGGCTCGCAGCCAACGTCGGGGCGGCAGGCCCTGCCATAGCCTCAGGTTACTCATATATACTTTAGATTGATTTAAAACTTCATTTTTAATTTAAAAGGATCTC
AGGTGAAGATCCTTTTTGATAATCTCATGACCAAAATCCCTTAACGTGAGTTTTCGTTCCACTGAGCGTCAGACCCCGTAGAAAAGATCAAAGGATCTTCTTGAGATCCTTTTTTTCTGCGCGTAATCTGCTGCTTGCAAACAAAAAAACCACCGCTACCAGCGGTGGTTTGTTTGCCG
GATCAAGAGCTACCAACTCTTTTTCCGAAGGTAACTGGCTTCAGCAGAGCGCAGATACCAAATACTGTCCTTCTAGTGTAGCCGTAGTTAGGCCACCACTTCAAGAACTCTGTAGCACCGCCTACATACCTCGCTCTGCTAATCCTGTTACCAGTGGCTGCTGCCAGTGGCGATAAGTC
GTGTCTTACCGGGTTGGACTCAAGACGATAGTTACCGGATAAGGCGCAGCGGTCGGGCTGAACGGGGGGTTCGTGCACACAGCCCAGCTTGGAGCGAACGACCTACACCGAACTGAGATACCTACAGCGTGAGCTATGAGAAAGCGCCACGCTTCCCGAAGGGAGAAAGGCGGACAGGT
ATCCGGTAAGCGGCAGGGTCGGAACAGGAGAGCGCACGAGGGAGCTTCCAGGGGGAAACGCCTGGTATCTTTATAGTCCTGTCGGGTTTCGCCACCTCTGACTTGAGCGTCGATTTTTGTGATGCTCGTCAGGGGGGCGGAGCCTATGGAAAAACGCCAGCAACGCGGCCTTTTTACGG
TTCCTGGCCTTTTGCTGGCCTTTTGCTCACATGTTCTTTCCTGCGTTATCCCCTGATTCTGTGGATAACCGTATTACCGCCATGCATTAGTTATTAATAGTAATCAATTACGGGGTCATTAGTTCATAGCCCATATATGGAGTTCCGCGTTACATAACTTACGGTAAATGGCCCGCCTG
GCTGACCGCCCAACGACCCCCGCCCATTGACGTCAATAATGACGTATGTTCCCATAGTAACGCCAATAGGGACTTTCCATTGACGTCAATGGGTGGAGTATTTACGGTAAACTGCCCACTTGGCAGTACATCAAGTGTATCATATGCCAAGTACGCCCCCTATTGACGTCAATGACGGT
AAATGGCCCGCCTGGCATTATGCCCAGTACATGACCTTATGGGACTTTCCTACTTGGCAGTACATCTACGTATTAGTCATCGCTATTACCATGGTGATGCGGTTTTGGCAGTACATCAATGGGCGTGGATAGCGGTTTGACTCACGGGGATTTCCAAGTCTCCACCCCATTGACGTCAA
TGGGAGTTTGTTTTGGCACCAAAATCAACGGGACTTTCCAAAATGTCGTAACAACTCCGCCCCATTGACGCAAATGGGCGGTAGGCGTGTACGGTGGGAGGTCTATATAAGCAGAGCTGGTTTAGTGAACCGTCAGATCCGCTAGCGCTACCGGACTCAGATCT

2. LNavB1/pIRES DS red

LNavB1 inserted between XhoL and BamHI sites of pIRES DSred vector.

XhoI/SalI combination created a scar.

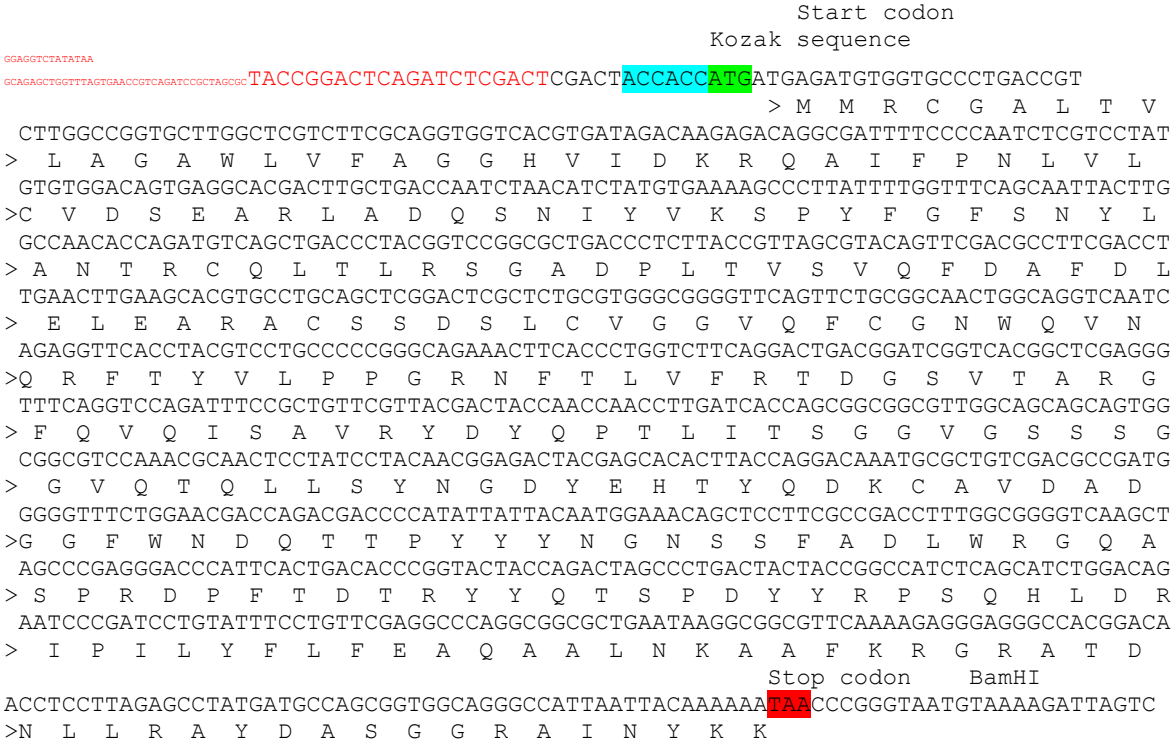

3. LNavB1xHis/pIRES DS red

LNavB1xHis inserted between XhoL and BamHI sites of pIRES DSred vector.

XhoI/SalI combination created a scar.

4. I-II linker construct in pET22b

5. II-III linker in pET22b

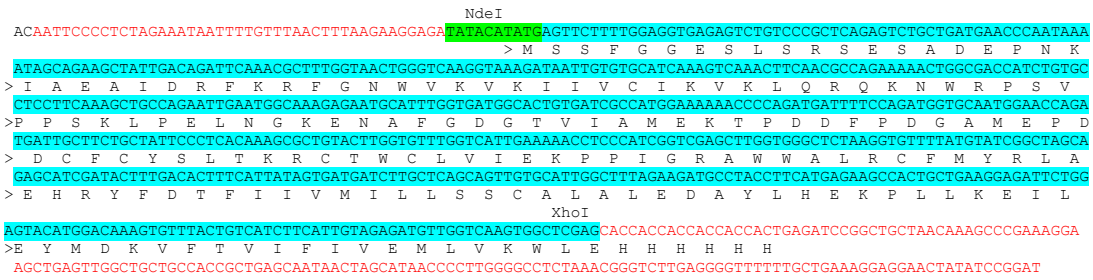

Appendix C. Sequence alignments

Alignment 1. LNa$_v$1 α-subunit aligned with other molluscan sodium channel *α*-subunits

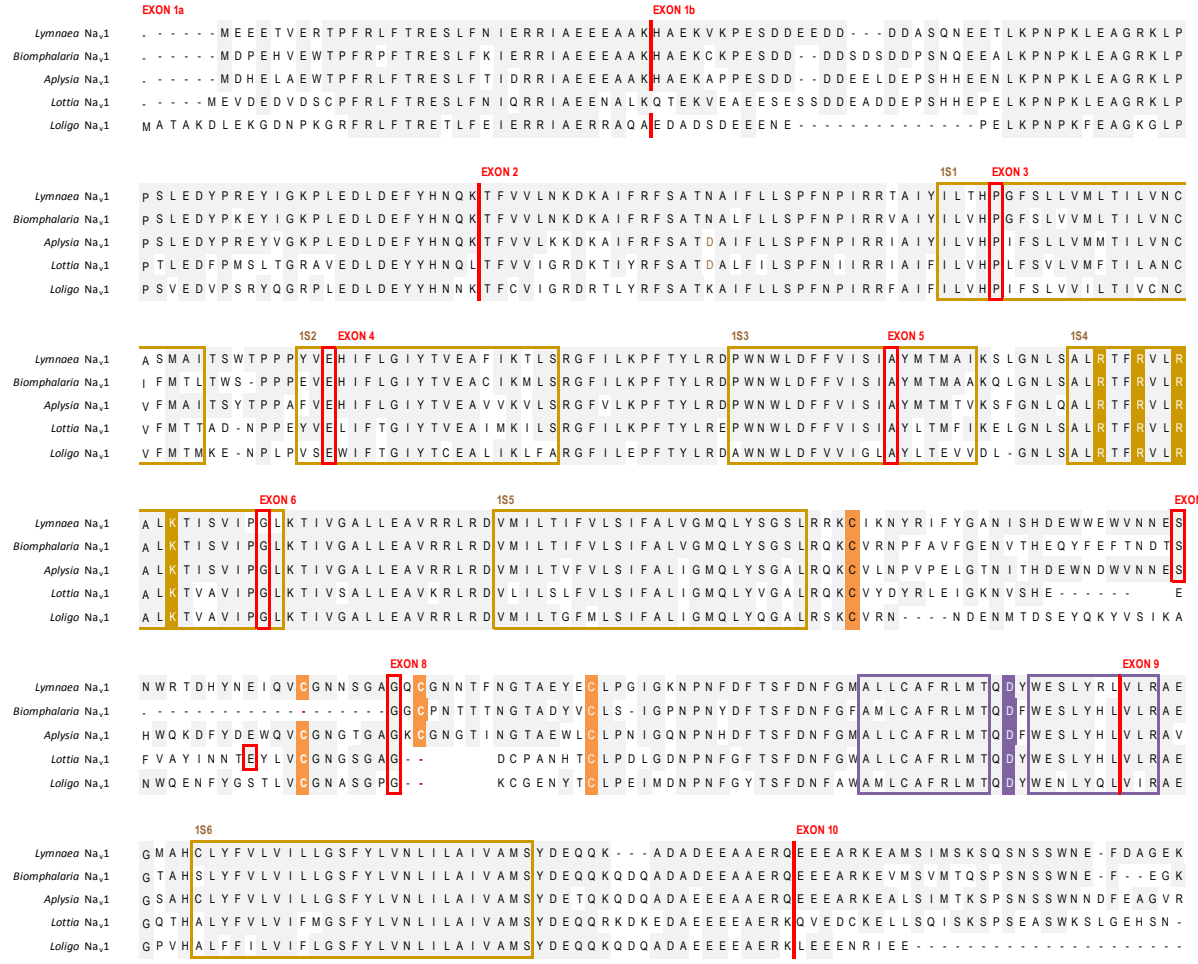

Domain I of molluscan sodium channel Na$_v$1 α subunit.

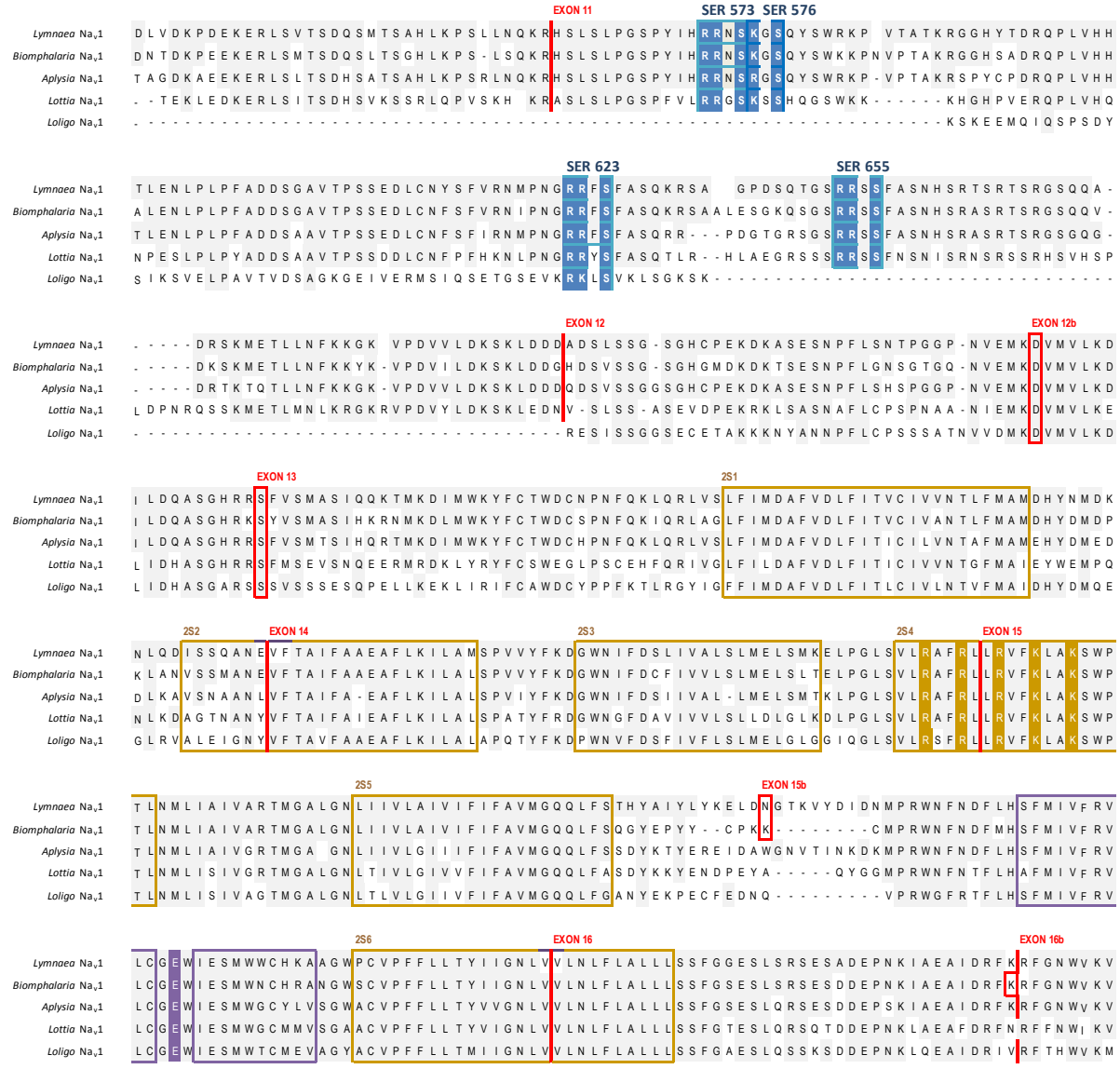

Domain II of molluscan sodium channel Na_v1 α subunit.

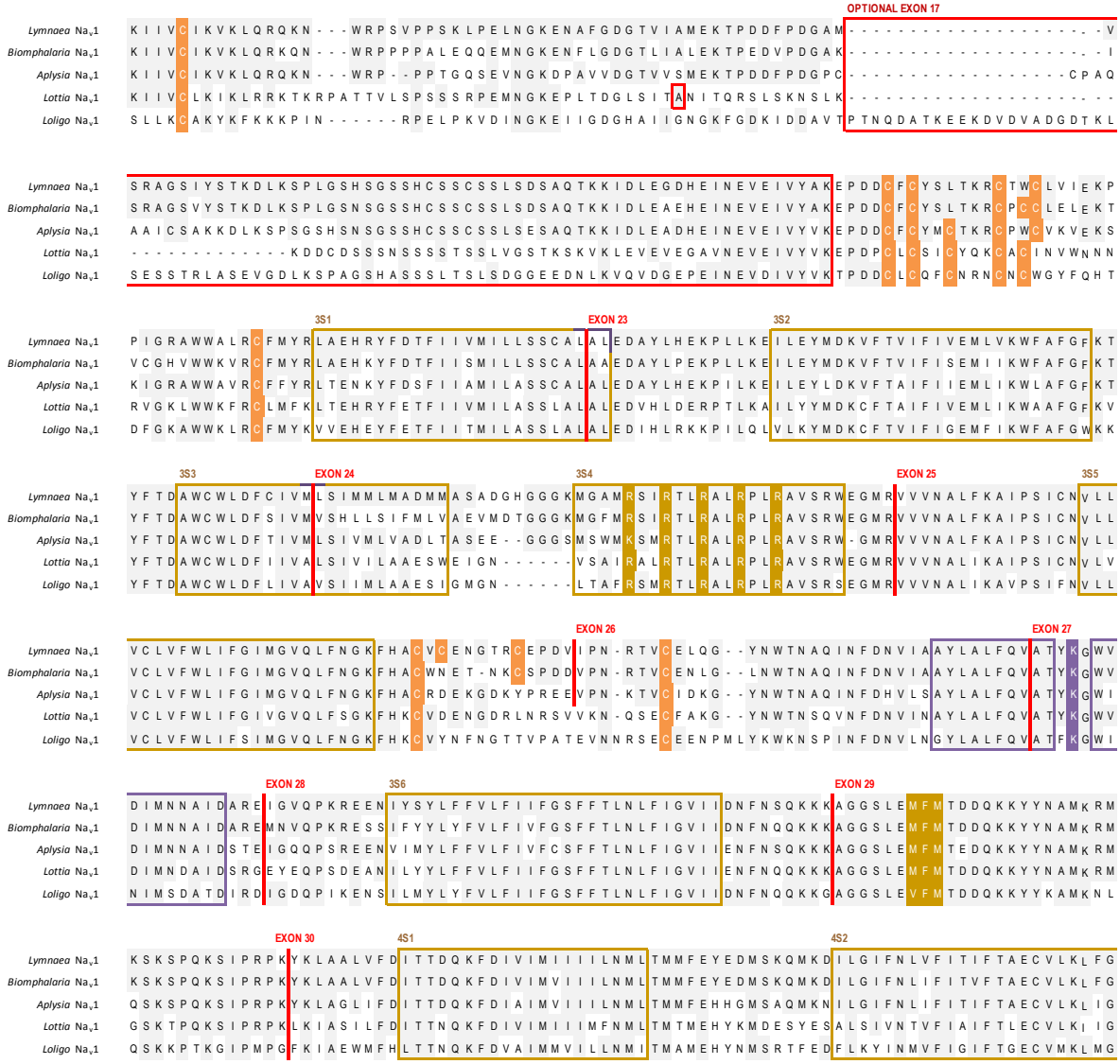

Domain III of molluscan sodium channel Na_v1 α subunit.

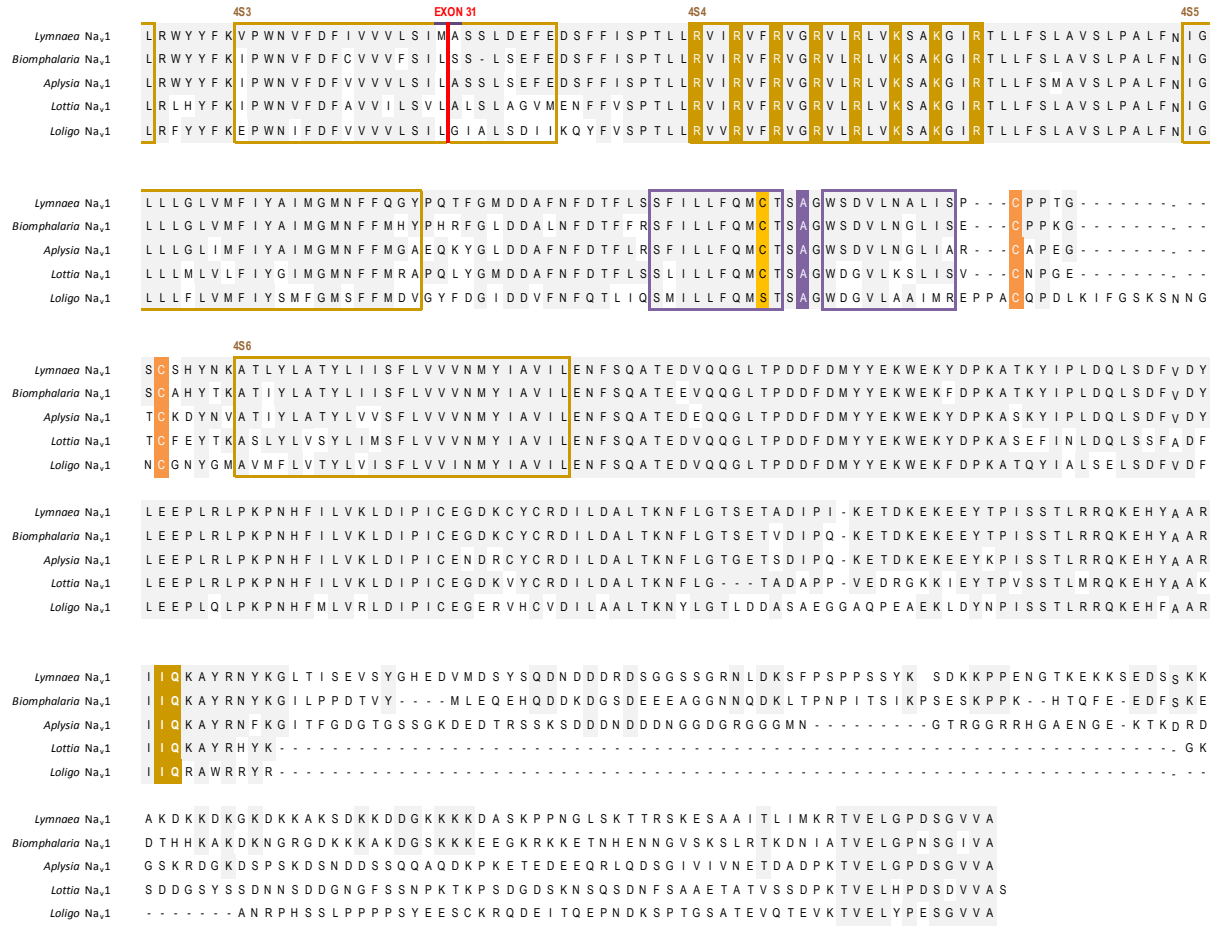

Domain IV of molluscan sodium channel Na$_v$1 α subunit.
Lymnaea sequence is most homologous to *Biomphalaria glabrata*, another pulmonate freshwater snail with Loligo sodium channel being the least homologous. The conserved serine residues in DI-II linker (blue) are PKA phosphorylation sites. Selectivity filter DEKA is shown in purple color and S4 voltage sensors are shown in tan color.

Alignment 2 Full amino acid sequences of snail LNa$_v$1 and human Na$_v$1.1 and Na$_v$1.7

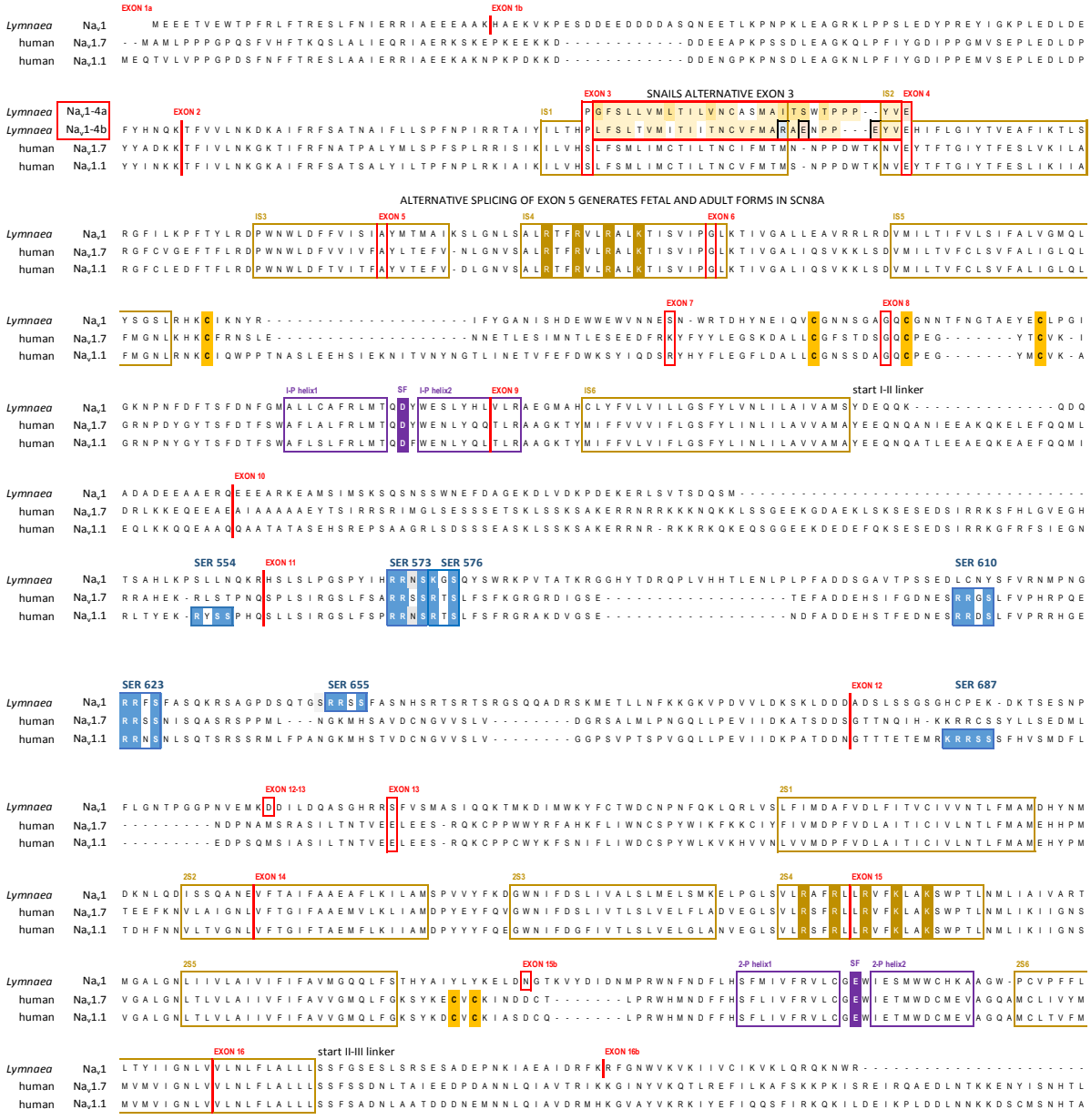

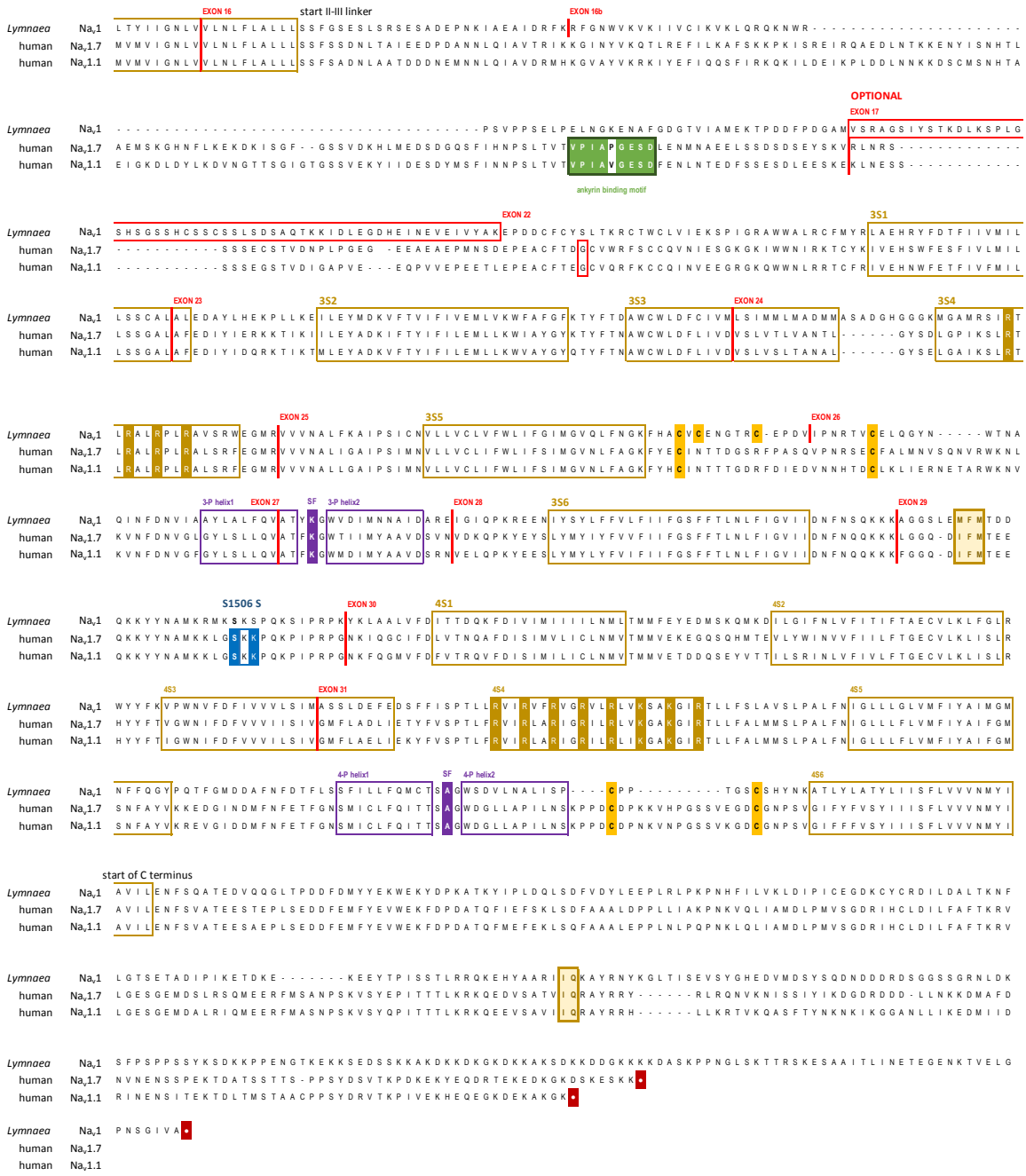

Exon arrangement shown with numbering system from human Nav1 channels.
Positively-charged residues (R/K) in voltage-sensor S4 segments are shown in brown color.
Calmodulin binding IQ motif conserved in C-terminus and the key “IFM” residues for rapid N-type inactivation are shown in the III-IV linker (tan color)
Conserved putative phosphorylation sites in the I-II linker are shown in blue color.
Conserved ankyrin binding site in II-III linker of vertebrate Nav1 channels are shown in green color.

Alignment 3. Alignment of the I-II linker between snail and human Na_v1 channels.

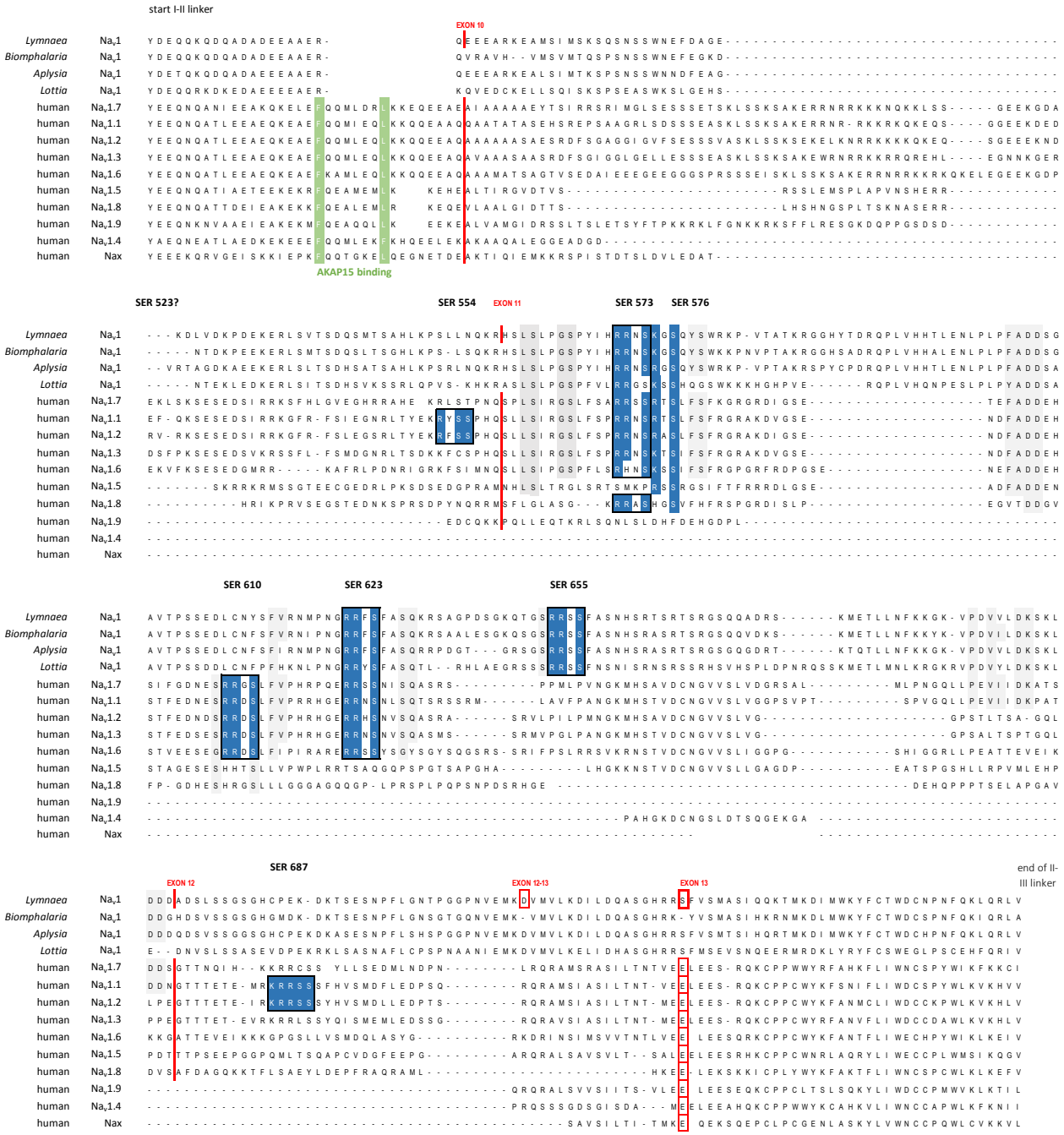

Conserved serines that are targeted by PKA are shown in blue. Three consensus phosphorylation sites that are conserved both in snail and in most human sodium channels include serine 573, 576 and 623, all harbored in exon 11. Serine 655 appears to be a PKA site that is uniquely conserved in invertebrate (molluscan) Na_v1 channels while conserved Serine 610 is seen in humans but not in snails. Shown in green is cAMP-dependent protein kinase-anchoring protein (AKAP) binding site(Cantrell, et al., 2002).

Alignment 4. Alignment of the II-III linker between snail and human Na_v1 channels.

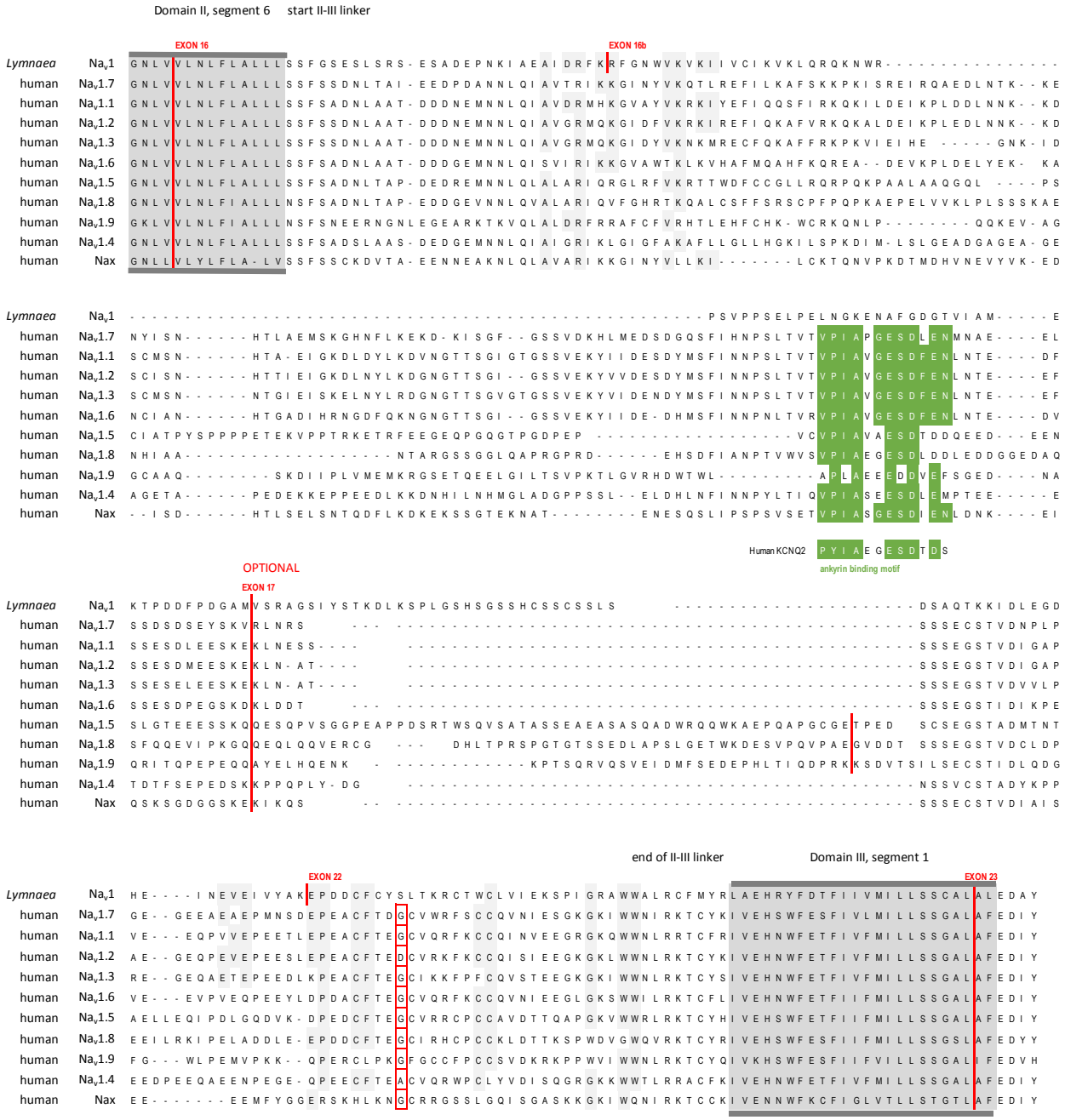

Ankyrin binding motif conserved in exon 16 of vertebrate but not invertebrate Na_v1 channels. Ion channel clustering ankyrin motif is shared by KCNQ2/3 channels also localized at vertebrate Nodes of Ranvier. An optional exon 17 lies downstream of exon 16 in snail LNa_v1 channel

Alignment 5. Auxiliary subunits of snail sodium channels (*Lymnaea* and *Biomphalaria*)

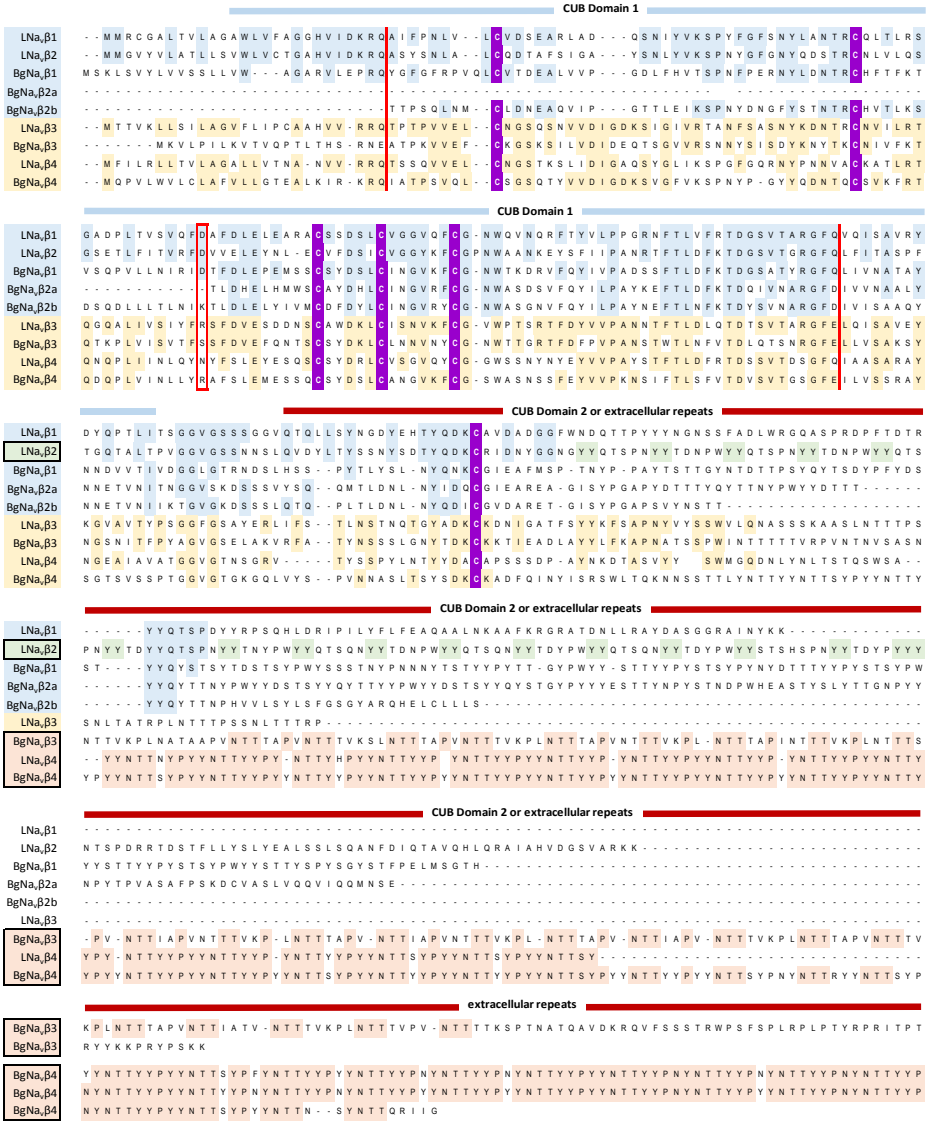

Alignment of *Lymnaea* and *Biomphalaria* sodium channel beta subunits, LNa$_v$β1, β2, β3 and β4. *Biomphalaria*, like *Lymnaea* is a pulmonate, freshwater snail, and has homologs of the LNa$_v$β subunits. LNa$_v$β1 and LNa$_v$β3 have two CUB domains, compared to one in LNa$_v$β2 and LNa$_v$β4, according to Phyr2 protein homology modelling. There appear to be two distinct isoforms based on structural similarity. Na$_v$β1 and Na$_v$β2 are more similar to each other, and Na$_v$β3 and Na$_v$β4 are more similar to each other. Instead of a second CUB domain, LNa$_v$β2, LNa$_v$β4, BgNa$_v$β3, and BgNa$_v$β4 have extensive extracellular repeats. While CUB domain containing proteins are widespread in invertebrates, the presence of direct homologs of these sodium channel beta subunits don't appear to be in more distant gastropods like *Lottia* or *Aplysia* or mollusks**.** Conserved cysteines are shown in purple. Black frames show the Ca^{2+} binding motif YEDD in CUB 1.

Alignment 6. Complete alignment of molluscan Na_v2 channels (3 pages)

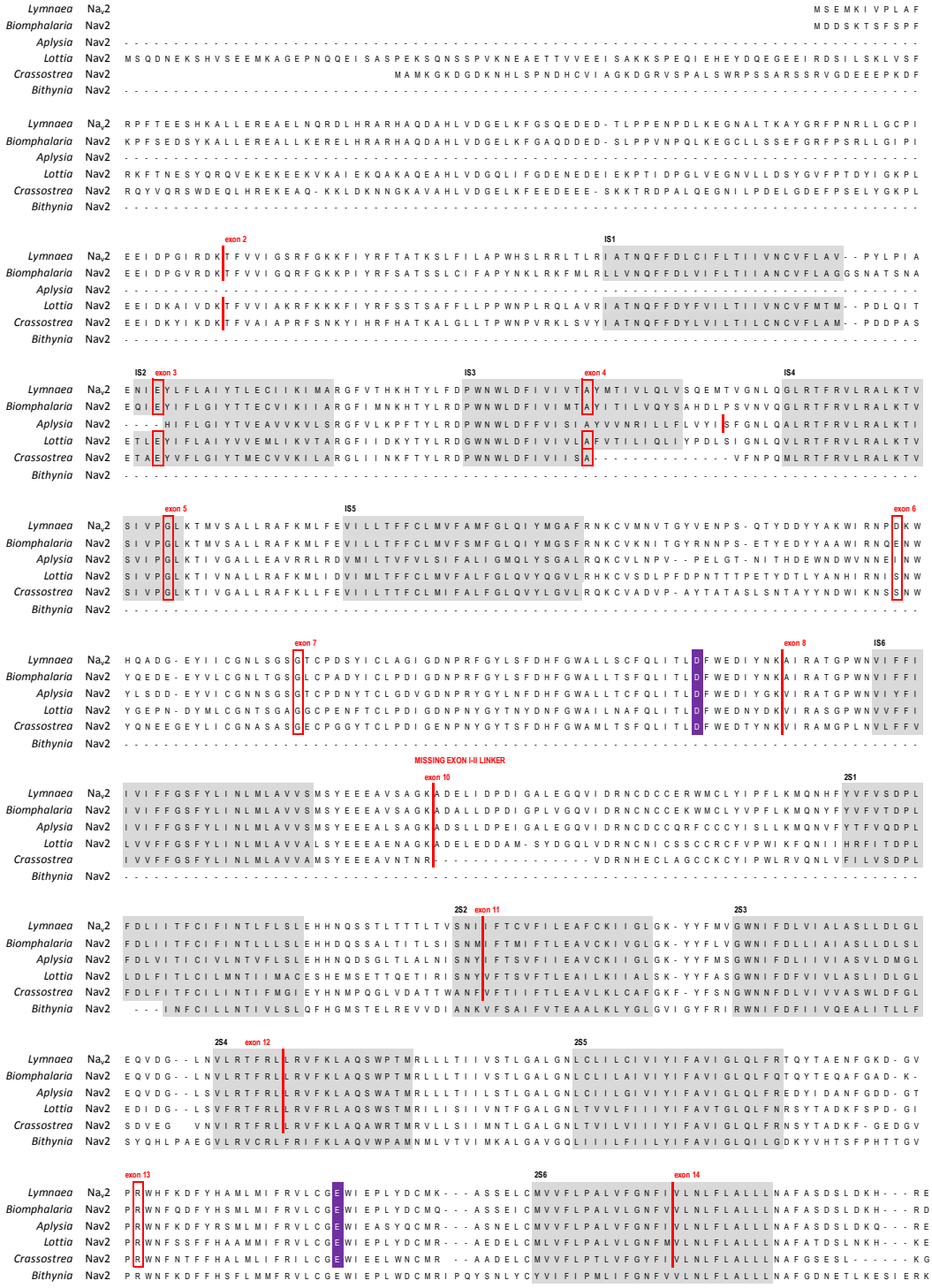

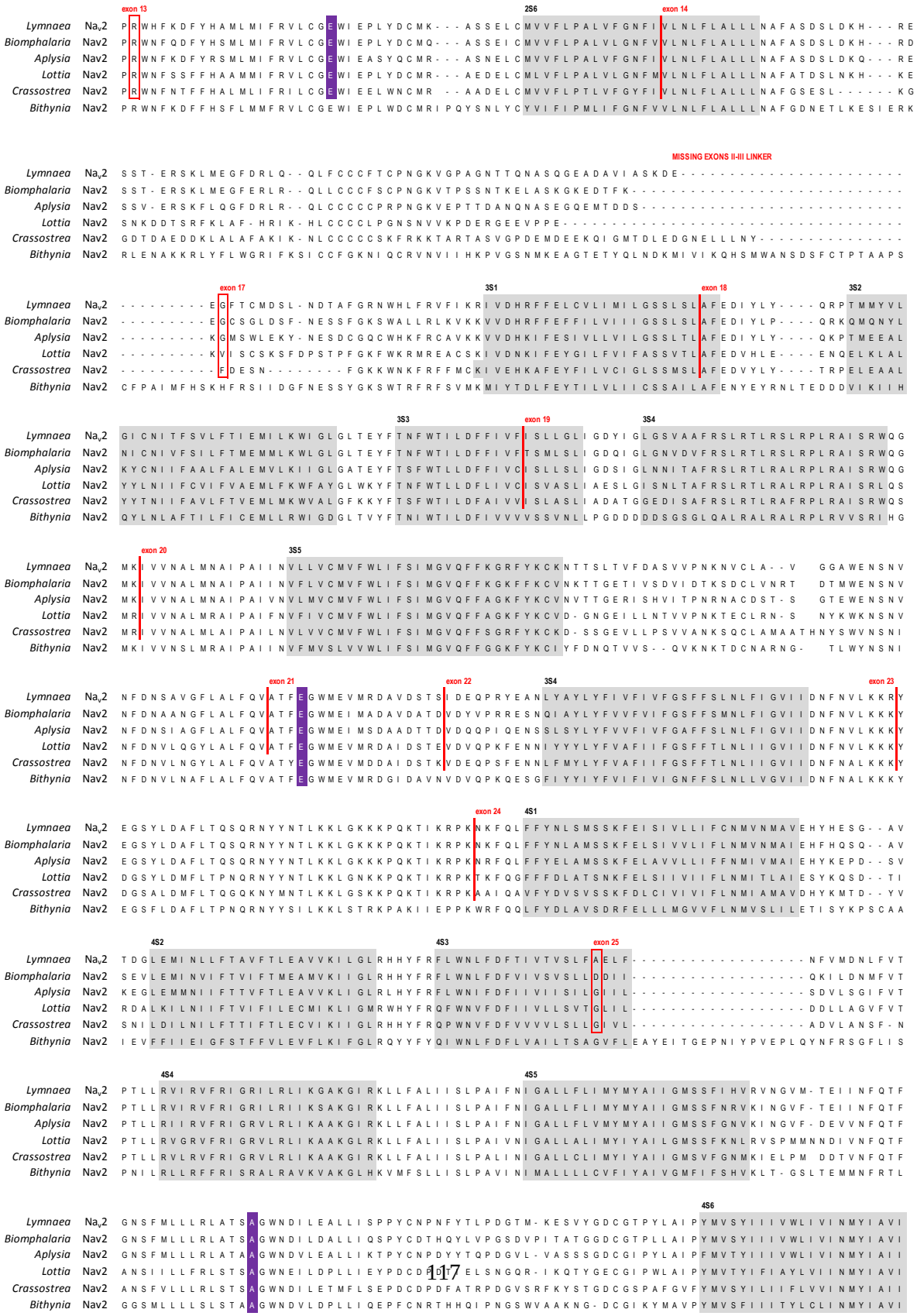
exon 13
2S6
exon 14
MISSING EXONS II-III LINKER
exon 17
3S1
exon 18
3S2
3S3
exon 19
3S4
exon 20
3S5
exon 21
exon 22
3S4
exon 23
exon 24
4S1
4S2
4S3
exon 25
4S4
4S5
4S6
Lymnaea Nav2
Biomphalaria Nav2
Aplysia Nav2
Lottia Nav2
Crassostrea Nav2
Bithynia Nav2

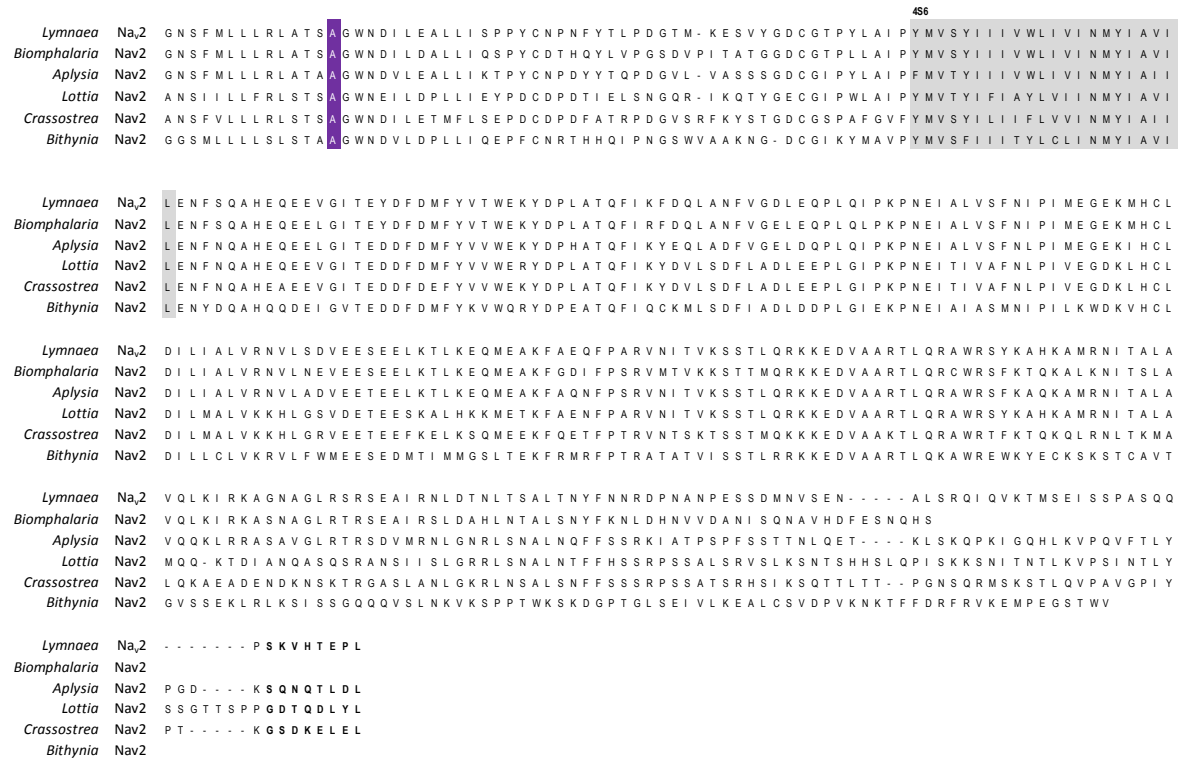

The likely transmembrane regions are shown as gray boxes, Selectivity filter components are shown in purple color.

Appendix D. Genomic regions of sodium channels

Genomic region 1. Exons 4a and 4b of α-subunit

```
ATTTTCTGTATGTAAATATTCTTTAAAAAATAAGCAAAGTCGAATGGTTTAAAATATTTTAAACATTTTTTTTTTTAATATGATAAAA
TTTGTTATAGTGAAACATTTTTTTTTTTAAATAACAGAAGAGTTATGACAATTGAAATTATCAGTTATGTTAATTATTTTGTATCTCA
TTTACCTAGTTTCAGTTTTAACGTAATGTTCACCTTTATCTTGAGTGGAATAATTTCATGTTTTGTTTTTCTCTTAACAACTCTTCA
 exon 4a Novel
CTGGTTTTAGTCTTTTGGTGATGCTGACCATTTTAGTAAACTGCGCCTCTATGGCCATAACTTCGTGGACACCCCCGCCCTATGTGG
 > G  F  S  L  L  V  M  L  T  I  L  V  N  C  A  S  M  A  I  T  S  W  T  P  P  P  Y  V
AGTAAGTAGGCCAGCTGCCACATTGGCTTTCTCTCCATTTCTATAGCAATAATACTCGAGCGTGCATTTTTTTTTTAACTCGTCAGCT
TATAAATTAGCTTTATATCTTTCTATTTATCCGATATTTTGTTTTTTATAAATACAAATCAATTCTATAGATGAGGTATCATTTATT
AAACATATATACCGGTAAATATGTTTTCATTATTTTCAAAGGACGCTATCAGAGGGGGTGGGGTGTGTTAGTTTCTTTTTTAGATTT
TACATATTCCAATTCCGGTTTTAAATAACATTTTAGGACACATATAATATAATTTTTTGAGAGATAATGTGTATCATTATTCAAGTA
ACTATTGTTCTGGCAAAGTTAAAAGAAATATCCTGAATATTTCTTCTTCAATAACATCATATTTTCTCTACAAATCTTACCTCTACA
TATCTCTTCTGTGTACCGCTAGACCTATATCTCTTCTCATTTCTCCATGCATCTTTTATCCTATAAATCTCTTCTCTACGCATCTTT
ATCCTATAACCCTCTTTCTGTGCATCTTTTCTCTTTACATATTTATATTTCCTCCTATACATCTTTTCTCCAATACTGCTTTGTTCT
ATACATTTTTGTTCTATACAAATACAACAATTTCAAATTAAAATTGATTTAAGGTTAAGCACTTGGCGGGGAAAATGTATTTCTTTT
AACAGTCAAAATGAGGCGCCCCTCCCCCCTTTTTTCTGTTGTATCAAGAAAGTAGTTCACGCCAGCTCTCTGTGTCCATGCGTTAGC
TGCCGAGAAATGATTTGATCTCCTTGTTAACTTGAAAATGACTCAACAAAAGACATGGTGATATGGTGGCGTATACTCGTTTACAGT
GATGTTGCGTTGCACTGTCACTCAGTGTCTGGATTCCTTTGATATTTCAAACCATAATTGAAGCTCATGACATTAGATGCTAGGCAA
TATTTGAATCGCCCGAGATCTAAGCAATATTTTGACCATCTGTCATCGAGTCCTTTCAAATGGAAGCGCCTGAAATCTTAAACAATG
TTTATTTAGAGCTACTGATATCGAATCCCTGATTTTGAAACGACTGAAATCCTAGACAATATTTGAAGCACCTGATATCAGAATCTA
AATTCTAGACAATATTTGAAGCACCTGATATCAGAATCTAAATTCTAGACAATATTTGGAGCACCTGATATCAGAATCCAAATCCTA
GACAATATTCGGAGCACCTGATATCAGAATCTAAATTCTAGACAATATTTGGATCACCTGATATCAGAATGCAAGTCCTTGACAATA
TTCGGAGCACCTGATATCAGAATCTAAATTCTAGACAATATTTAATTCGGATCATCTGATAACAAAATTCAAATCCTAGACAATATT
TGCACCTGATAACAGAATTCAAATCCTAGACAATATTTGGAGTACCTGATATCAGAATCCAAATTCTAGACAATATTTTGAGCACCT
GACATCAGTTGAAATGCCCAACACAGATCACCAGATAAAAATCGAAGATCCCAACACAAATCTCCAGATAAAATTTGAAGAGCCCAA
CAGAAATCACCAGAGATTAAAAACTTAGAACACAAGTTTTCATAATTAAATCTTTTGTGTCATTTTGACAACCTTCCCATCATCTTT
CCTCGTTATTTTGTGTCTTTTAGGTTTGCCGGAACAATAGATACAATTTAAAAAGAATTTTAAAAAATAAAAAATGGTTTTAAAGAT
TGTTCTCTTGTATTTTTACCAACCCTTTTTTTAAAGCAATAAAACAAAACAAAAATTGCTTTTCGTTTATTCTAATTTCATCAATGT
TCAATTCTGGAAACATTTATTCTCATTTTTTTCCTTGTTACTTCCAATGTTGTAAATTGCTTCCAGCTATAAAAAAAAGTTGCTTTA
CAATACTCATCCATGTCGTCTTGTCTTGATACTACTCATCCATGTTGTATTGTAATTTCAATTACAGCTTCTATTATATTTTTTTCA
ACATTGTATTTTTCAGCTAAAGTCATTTTGTCCCACGTACCTCTGTATTGTACTTTTTCTTTATTTTAGTTCGAAGTTTTATTTTCA
AATTTTATTTCAAAATAATTAAAGAGAAACCATATGGCATCCAAGATTGTAAAAATATAATATGTATTTAAACTAAAAGACAGCATT
ATATGCTCGTAAGCAAATTGTACAAAGTCTCTGCTTCTAGGACTGTTTGCTATTTGCTAGTGGTAATTTTAAAGTTCTTCTTGAAAC
TGAAATAACTGTTTAGTTGTAACGAGCAAGCTATTGCTCAAATCAGCCCCCTATTTCTTCCAAACATTGCTGCTAAAATTTATATTC
ATTTGTTTTTGTTTTACCATAAATACCGGTATAACAATAAGCCTTAGTCTTTGGAGCATTTTGGTTCAATGGTTTCTTAATTTAGCT
TTTTGTTTCTTAAATAATGTGAAAGTGCAATATTTTGTATGCATAATCACTATAAATATAATCGCTTATCGTTCATACTCCATTATT
TACCCTGAACTTTTACATGCATAGATTTATGGGGGTTTTTTTACTTTCGTTTACAGAGGAAACATATTAGTAATTGACTTTTTTTTA
AATTAAGGAAATCAAAATCTCTCCAAAGATCAAATTGCACTTTTAATTACCGGTATTCCATTCCATTTGTAATCATTCAGTACCCTC
TCCTGCTGCCTTCTCTCCCTTAGCCTGAGTACATTGATGAATTTTGCACAGTTTATTAATAATATTGACAATGTAATCTTATTTATT
TTAAATATTTTTATTTCACCAGCCATTATCATAAAAGTAATTTATACCCCTATTGATTGTAACATGTCATTTAGACTTATTTAAGTA
AATCATCATTCTCAGAGTGTTATAAAAAAGAGAATTTGTTAAAAGATTTATGCTGAACCCTAATAGTAATCGTTTCTTTAAAAATAA
TCAATTATCTTACCATATGCATAGCGTGTCACAGGCAATATTAGCCAATTATAAAGTAACTTTAAATATAAGGAATATATATTTAAC
TCTTTGCTTCCATCAACTCCCAATGATCACCATGTTCGACAGAGGTCTCTGTGTTTCAGTTCTCAGTCAGCAGTTGTCATTTAACAT
GCACCGACGCAAATAACTATTCTTTGCATAAACAAAAAATTAGCTTCATCAGTTCATAAGCCACTAAACTAAAATATTCACTGAAAA
GCAATAAGAAGTTGATTGTGGTCTCCATAACAAATCATTTAGACATAGAAGTCTCTACACTTCAAATCCCACAATTTCTATGACCAG
GTTGTGTCTATTTAGTCATGAGAAATAATGATGTTCTTAAAATCAAGCACAAACATCGGATCAGACTCTTCTGGTCATGGGTTAACC
CTCGTGTGAAGCACGCAATATAAGTCTGGGCCTACTTTTCACTGGAACTTACTTAAGTTACAGGCGTAGGGATGCGAAATCCCATCA
TCTTCCTGATCACAAAGCCATTGGGGATTTAAACCTTCGGCCTATTCAATTGGGATGAAAATTTCAAACTCTAAATTTTCAAATACA
TTATATATGTATTTATTGTTTGTTTGATTTGTTTTATGTGTGACTTTTGTTTTAAATAATCACATGATTATAGATTTTTCTCCCTTG
AAAAATATTTGTTGAATTGTGGCTTTAATAATATATTCTTATTGTGATTCAACTAACCCGCCTCCCCCCCCCTTCTCCCCAAACCT
TACAGTTAGTTGCTGTTAATTATTTGTCATTTGAAAGTTTGCCTGAGCTCCGTCTGAAAAGCATCGTGTGTCTGGCTGTACCGTTTT
TGAAAATCCTTGTTTAATTATTTATGGTTTTAAACATGAAGCATTTTTAAAACCCTGAACTAATGCCTTTTTAAAGATGGTGACATC
TCCCCNNTTTAATATAATGGCTCGTTTGGCTTGACCGATTCTGTGGTTGCAGTAGTAAGTCTACAATGCCATATTTTTGTTTTTATT
TTTTTTGCCCTTGGTTTTATTTCTACGGATATCCTGCTGCCATACATAAGGCTGAACATATTTGAATGAAGGATGATGTGTTTGGCC
                    exon 3b Transcriptome clone
AAATCTTCCTTAACTGGCCCACTTTGTTTAGTTTGACTGTTATGATCACCATCATCACCAACTGTGTCTTTATGGCTCGCGCTGAAA
                    > L  F  S  L  T  V  M  I  T  T  I  I  T  N  C  V  F  M  A  R  A  E
ATCCGCCAGAATATGTGGAGTAAGTACGGCATCACGTCCTCACGTTTGTTTGTTTGTTGACGGCGACGCCCACTAACAGCAATCACT
>N  P  P  E  Y  V
ATCCAAGAAACCCCGCATAATGGAATACTTACAAAATATTTAAAAGTTCATGTATTGTTAAATAACAATAGAAAGTAGTTTCAAATA
TTTTGCTTAAATTACGATGAAGCAGTATTTATTTTTTTTTAAAGTAGTTTCAAAGATTTTGCTTAAATTACAATAAGCAGTATTTA
```

Genomic region 2. Genomic region of Nav2 with exon 1 and 2

Bibliography

Anderson, P., Holman, M., & Greenberg, R. (1993). Deduced Amino Acid Sequence of a Putative Sodium Channel from the Scyphozoan Jellyfish Cyanea Capillata. *Proc. Natl. Acad. Sci. USA. (90)*, 7419–7423.

Arikkath, J., & Campbell, K. (2003). Auxiliary subunits: essential components of the voltage-gated calcium channel complex. *Current Opinion in Neurobiology (13)*, 298–307.

Benjamin, P. (2008). *Lymnaea.* Scholarpedia, 3(1):4124.

Ben-Johny, M., Yang, P., Niu, J., Yang, W., Joshi-Mukherjee, J., & Yue, D. (2014). Conservation of Ca2+ /Calmodulin Regulation across Na and Ca2+ Channels. *Cell (157)*, 1657–1670.

Bennett, V., & Lorenzo, D. (2013). Spectrin- and Ankyrin-based Membrane Domains and the Evolution of Vertebrates. *Current topics in membranes (27)*, 1-37.

Birnboim, H., & Doly, J. (1979). A rapid alkaline extraction procedure for screening recombinant plasmid DNA. *Nucleic Acid Residues 7(6)*, 1513-1523. doi:10.1093/nar/7.6.1513

Blanc, G., Font, B., Eichenberger, D., Moreau, C., Ricard-Blum, S., Hulmes, J. S., & Moali, C. (2007). Insights into How CUB Domains Can Exert Specific Functions while Sharing a Common Fold. *JBC(282)*, 16924-16933.

Brackenbury, W., & Isom, L. (2011). Na+channel βsubunits: Overachievers of the Ion Channel Family. *Frontiers in Pharmacology*, 1-11.

Bullock, T., Moore, J., & Fields, R. (1984). Evolution of Myelin Sheaths: Both Lamprey and Hagfish Lack Myelin. *Neuroscience Letters 48(2)*, 145-148. doi:10.1016/0304-3940(84)90010-7

Burkhard, P., Stetefeld, J., & Strelkov, S. (2001). Coiled Coils: a Highly Versatile Protein Folding Motif. *Trends in Cell Biology (11)*, 82-88.

Cantrell, A., Tibbs, V., Yu, F., Murphy, B., Sharp, E., Qu, Y., . . . Scheuer, T. (2002). Molecular Mechanism of Convergent Regulation of Brain Na+ Channels by Protein Kinase C and Protein Kinase A Anchored to AKAP-15. *Molecular and Cellular Neuroscience (21)*, 63-80.

Carmeliet, P. (2003). Blood Vessels and Nerves: Common Signals, Pathways and Diseases. *Nature Reviews Genetics (4)*, 710-720.

Catterall, W.A. (1993). Structure and Modulation of Na+ and Ca+ Channels. *Annals of New York Academy of Sciences (707)*, 1-19.

Catterall, W.A. (2000). From Ionic Currents to Molecular Mechanisms: The Structure and Function of Voltage-Gated Sodium Channels. *Neuron (26)*, 13-25.

Catterall, W.A. (2014). Sodium Channels, Inherited Epilepsy, and Antiepileptic Drugs. *The Annual Review of Pharmacology and Toxicology (54)*, 317–338.

Catterall, W. A. (2005). International Union of Pharmacology. XLVII. Nomenclature and structure-function relationships of voltage-gated sodium channels. *Pharmacol. Rev*, 397-409.

Catterall, W. A., Goldin, A. L., & Waxman, S. G. (2005). International Union of Pharmacology. XLVII. Nomenclature and structure-function relationships of voltage-gated sodium channels. *Pharmacol. Rev*, 397-409.

Catterall, W.A., Hulme, J., Xin, J., Preston, J., & Few, W. (2006). Regulation of Sodium and Calcium Channels by Signaling Complexes. *Journal of Receptors and Signal Transduction (26)*, 577-598.

Cestele, S., & Catteral, W.A. (2000). Molecular Mechanisms of Neurotoxin Action on Voltage-Gated Sodium Channels. *Biochimie*, 883-892.

Croll, R. (2000). Insights Into Early Molluscan Neuronal Development Through Studies of Tramsmitter Phenotypes in Embrionic Pond Snails. *Microscopy research and technique (49)*, 570-578.

Cusick, K., & Sayler, G. (2013). An Overview on the Marine Neurotoxin Genetics, Molecular Targets, Methods of Detection and Ecological Functions. *Mar. Drugs*, 991-1018.

Davis, T., Chen, C., & Isom, L. (2004). Sodium Channel β1 Subunits Promote Neurite Outgrowth in Cerebellar Granule Neurons. *The Journal of Biological Chemistry (279)*, 51424–51432,.

Dawson, T. F., Boone, A. N., Senatore, A., Piticaru, J., Thiyagalingam, S., Jackson, D., . . . Spafford, J. (2014). Gene Splicing of an Invertebrate Beta Subunit (LCavβ) in the N-Terminal and HOOK Domains and Its Regulation of LCav1 and LCav2 Calcium Channels. *PLOSone (9)*, 1-17. doi:10.1371/journal.pone.0092941

Dereeper, A., Guignon, V., Blanc, G., Audic, S., Buffet, S., Chevenet, F., . . . Gascuel, O. (2008). Phylogeny.fr: robust phylogenetic analysis for the non-specialist. *Nucleic Acids Research*, 465-469. doi:10.1093/nar/gkn180

Derst, C., Walther, C., Veh, R., Wicher, D., & Heinemann, S. (2006). Four Novel Sequences in Drosophila Melanogaster Homologous to the Auxiliary Para Sodium Channel Subunit TipE. *Biochemical and Biophysical Research Communications, Vol. 339*, 939-948.

Dong, K. (2007). Insect Sodium Channels and Insecticide Resistance. *Invertebrate Neuroscience*, 17-30.

Ekberg, J., Jayamanne, A., Vaughan, C. W., Aslan, S., Thomas, L., Mould, J., . . . Lewis, R. J. (2006). μO-Conotoxin MrVIB Selectively Blocks Nav1.8 Sensory Neuron Specific Sodium Channels and Chronic Pain Behavior Without Motor Deficits. *PNAS*, 17030–17035.

Fache, M. P., Moussif, A., Fernandes, F., Giraud, P., Garrido, J. J., & Dargent, B. (2004). Endocytotic Elimination and Domain-Selective Tethering Constitute a Potential

Mechanism of Protein Segregation at the Axonal Initial Segment. *The Journal of Cell Biology (166)*, 571-578.

Feldkamp, M., Yu, L., & Shea, M. (2011). Structural and Energetic Determinants of Apo Calmodulin Binding to the IQ Motif of The Na(V)1.2 Voltage-Dependent Sodium Channel. *PMC 19(5)*, 733-47.

Feng, Z., Zhang, Z., Van Kesteren, R., Straub, V., Van Nierop, P., Jin, K., . . . Smit, A. (2009). Transcriptome analysis of the central nervous system of the mollusc Lymnaea stagnalis. *BMC genomics*, 1-15.

Gaboriaud, C. G.-P., Thielens, N., Bally, I., & Arloud, G. (2011). Structure and properties of the Ca2+ -binding CUB domain, a widespread ligand -recognitionunit involved in major biological functions. *Biochemical Journal*, 185-193.

Gally, C., Eimer, S., RichmondJ.E., & Bessereau, J.-L. (2004). A Transmembrane Protein Required for Acetylcholine Receptor Clustering in Caenorhabditis Elegans. *Nature (431)*, 578-582.

Garrido, J. J., Fernandes, F., Moussif, A., Fache, M., Giraud, P., & Dargent, B. (2003). Dynamic Compartmentalisation of the Voltage Gated Sodium Channels in Axons. *Biology of the Cell (95)*, 437–445.

Geffeney, S., & Ruben, P. (2006). The Structural Basis and Functional Consequences of Interactions Between Tetrodotoxin and Voltage-Gated Sodium Channels. *Marine drugs 4(3)*, 1-34.

Geffeney, S., Brodie, E., Ruben, P., & Brodie, E. (2002). Mechanisms of adaptation in a predator-prey arms race: TTX-resistant sodium channels. *Science 297*, 1336-1339.

Goldin, A. (2002). Evolution of Voltage Gated Na+ Channels. *The Journal of Experimental Biology, Vol 205*, 75-584.

Gur Barzilai, M., Reitzel, A., Kraus, E., Gordon, D., Technau, U., & Gurevitz, M. (2012). Convergent Evolution of Sodium Ion Selectivity in Metazoan Neuronal Signaling. *Cell reports*, http://dx.doi.org/10.1016/j.celrep.2012.06.016.

Hakim, P., Gurung, I., Pedersen, T., Thresher, R., Brice, N., Lawrence, J., . . . Huang, C. (2008). Scn3b Knockout Mice Exhibit Abnormal Ventricular Electrophysiological Properties. *Progress in Biophysics and Molecular Biology*, 251-266.

Harlow, E., & Lane, D. (1999). *Using Antibodies: A Laboratory Manual.* NY: CSHL Press.

Harlow, E., & Lane, D. (1999). *Using Antibodies: A Laboratory Manual.* NY: CSHL Press.

Hartline, D., & Colman, D. (2007). Rapid Conduction and the Evolution of Giant Axons and Myelinated Fibers. *Current Biology*, 29-35.

He, B., & Soderlund, D. (2010). Human Embrionic Kidney (HEK293) Cells Express Endogenous Voltage Gated Sodium Currents and Nav1.7 Sodium Channels. *Neuroscience letters*, 1-11.

He, Z., & Tessier-Lavigne, M. (1997). Neuropilin Is a Receptor for the Axonal Chemorepellent Semaphorin III. *Cell (90)*, 39–751.

Hedstrom, K., Ogawa, Y., & Rasband, M. (2008). AnkyrinG is required for maintenance of the axon initial segment and neuronal polarity. *The Journal of Cell Biology*, 635-640.

Heinemann, S. H., Terlau, H., Stühmer, W., Imoto, K., & Numa, S. (1992). Calcium Channel Characteristics Conferred on the Sodium Channel by Single Mutations. *Nature*, 441-443.

Hill, A., Nishino, A., Nakajo, K., Zhang, G., Fineman, J., Selzer, M., . . . Cooper, E. (2008). Ion channel Clustering at the Axon Initial Segment and Node of Ranvier Evolved Sequentially in Early Chordates. *PloS Genetics*, 1-15.

Hille, B. (1975). Ionic Selectivity, Saturation and Block in Sodium Cannels. *The Jouurnal of Genearal Physiology (66)*, 535-560.

Hodgkin, A. L., & Huxley, A. F. (1945). Resting and Action Potentias in Single Nerve Fibers. *Journal of physiology (104)*, 176-195.

Hodgkin, A., & Haxley, A. (1952). The Components of Membrane Conductance in the Giant Axon of Loligo. *Journal of Physiology*, 473-496.

Hofmann, K., & Stoffel, W. (1993). TMbase - A database of membrane spanning proteins segments. *Biol. Chem.*, 166.

Hui, S., Xing, X., & Bader, G. D. (2013). Predicting PDZ Domain Mediated Protein Interactions from Structure. *BMC Bioinformatics*, 1-17.

Hwang, D., Tai, K., Chueh, C., Lin, L., & Jeng, S. (1991). Tetrodotoxin and Derivatives in Several Species of the Gastropod Naticidae. *Toxicon. 29(8)*, 1019-1024.

Isom, L., Ragsdale, D., De Jongh, K., Westenbroek, R., Reber, B., Scheuer, T., & Catterall, W. (1995). Structure and Function of the p2 Subunit of Brain Sodium Channels, a Transmembrane Glycoprotein with a CAM Motif. *Cell (83)*, 433–442.

Kazen-Gillespie, K., Ragsdale, D., D'Andrea, M., Mattei, L. N., Rogers, K., & Isom, L. (2000). Cloning, Localization, and Functional Expression of Sodium Channel Beta1A subunits. *The Journal of Biological Chemistry (275)*, 1079-88.

Kelley, L., & Sternberg, M. (2009). Protein Structure Prediction on the Web: a Case Study Using the Phyre Server . *Nature Protocols (4)* , 363 - 371 .

Kemenes, G., & Benamin, P. (2009). Limnaea. *Current Biology (19)*, 9-11.

Kung, C., Preston, R., Maley, M., Ling, K.-Y., Kanabrocki, J., Seavey, B., & Saimi, Y. (1992). In Vivo Paramecium Mutants Show That Calmodulin Orchestrates Membrane Responses to Stimuli. *Cell calcium (13)*, 413-425.

Kuo, C.-C. (1998). A Common Anticonvulsant Binding Site for Phenytoin, Carbamazepine, and Lamotrigine in Neuronal Na+ Channels. *Molecular Pharmacology 54(4)*, 712-721.

Laedermann, C., Syam, N., Petrin, M., Decosterd, I., & Abriel, H. (2013). B1- and B3-voltage -gated sodium channel subunits modulate cell surface expression and glycosylation of Nav1.7 in HEK293 cells. *Frontiers in Cellular Neurosciense*, 1-7.

Lai, H., & Jan, N. (2006). The Distribution and Targeting of Neuronal Voltage-Gated Ion Channels. *Nature*, 546-562.

Lee, H. J., & Zheng, J. J. (2010). PDZ Domains and Their Binding Partners: Structure, Specificity, and Modification. *Cell Communication and Signalling*, 1-18.

Leterrier, C., Brachet, A., Fache, M., & Dargent, B. (2010). Voltage -gated sodium channel organisation in neurons: Protein interactions and trafficing pathways. *Neurosciense Letters*, 92-100.

Li, J., Waterhouse, R., & Zdobnov, E. (2011). A Remarkably Stable TipE Gene Cluster: Evolution of Insect Para Sodium Channel Auxiliary Subunits. *Evolutionary Biology, Vol.337*, 1-11.

Liebeskind, B., Hillis, D., & Zakon, H. (2011). Evolution of Sodium Channels Predates the Origin of Nervous System in Animals. *PNAS*, 9154-9159.

Lin, W., Right, D., Muraro, N., & Bains, R. (2009). Alternative Splicing in the Voltage-Gated Sodium Channel DmNav Regulates Activation, Inactivation and Persistent Current. *Journal of Neurophysiology*, 1-45.

Littleton, J., & Ganetzky, B. (2000). Ion Channels and Synaptic Organization: Analysis of the Drosophila Genome. *Neuron 26*, 35-43.

Liu, M., Davey, J., Banerjee, R., Han, J., Yang, F., Aboobaker, A., . . . Davidson, A. (2013). Fine Mapping of the Pond Snail Left-Right Asymmetry (Chirality) Locus Using RAD-Seq and Fibre-FISH . *PLOS one (8)*, 1-7.

Lopreato, G., Lu, Y., Southwell, A., Atkinson, N., Hillis.D., Wilcox, T., & Zakon, H. (2001). Evolution and Divergence of Sodium Channel Genes in Vertebrates. *PNAS*, 7588 – 7592.

McCusker, E., Bagne, C., Naylor, C., Cole, A., & D'Avanzo, N. (2012). Structure of a Bacterial Voltage-Gated Sodium Channel Pore Reveals Mechanisms of Opening and Closing. *Nature Communications*, 1-8.

Messner, D., & Catterall, W. (1986). The Sodium Channel from Rat Brain; Role of the B1 ans B2 Subunits in Saxitoxin Binding. *The Journal of Biological Chemistry (261)*, 211-215.

Moldovan, M., Alvarez, S., Rosberg, M., & Krarup, C. (2013). Axonal Voltage-Gated Ion Channels as Pharmacological Targets for Pain. *European Journal of Pharmacology (708)*, 105-112.

Nakamura, H., Kojima, S., Kobayashi, S., Ito, I., Fujito, Y., Suzuki, H., & Ito, E. (1999). Physiological Cracterization of Lip and Tentacle Nerves in Lymnaea Stagnalis. *Neuroscience Research (33)*, 291-298.

Neher, E. (1988). The Use of the Patch Clamp Technique to Study Second Messenger-Mediated Cellular Events. *Neuroscience (26)*, 327-334.

Ng, D., Pitcher, G., Szilard, R. K., Sertie, A., Kanisek, M., Clapcote, S. J., . . . McInnes, R. R. (2009). Neto1 Is a Novel CUB-Domain NMDA Receptor–Interacting Protein Required for Synaptic Plasticity and Learning. *PLoS biology*, 278-300.

Oyama, F., Miyazaki, H., Sakamoto, N., Becquet, C., Machida, Y., Kaneko, K., . . . Nukina, N. (2006). Sodium channel b4 subunit: down-regulation and possible involvement in neuritic degeneration in Huntington's disease transgenic mice. *Journal of Neurochemistry (98)*, 518-529.

Pan, Z., Kao, T., Hovath, Z., Lemos, J., Sul, J.-Y., Cranstoun, S., . . . Cooper, E. (2006). A Common Ankyrin-G-Based Mechanism Retains KCNQ and NaV Channels at Electrically Active Domains of the Axon. *The Journal of Neuroscience 26(10)*, 2599-2613.

Patino, G., & Isom, L. (2010). Electrophysiology and Beyond: Multiple Roles of Na+ Channel Beta Subunits in Development and Disease. *Neuroscience Letters, Vol.486*, 53-59.

Patino, G., Claes, L., Lopez-Santiago, L., E.A., S., Dondeti, R., Chen, C., . . . Isom, L. (2009). A Functional Null Mutation of SCN1B in a Patient with Dravet Syndrome. *Journal of Neuroscience*, 10764-10778.

Payandeh, J., Scheuer, T., Zheng, N., & Catterall, W. (2011). The Crystal Structure of a Voltage-Gated Sodium Channel. *Nature (475)*, 353-358.

Pedraza, L., Huang, J., & Colman, D. (2001). Organizing Principles of the Axoglial Apparatus. *Neuron (30)*, 335 - 344.

Ranganathan, R., & Ross, E. (1997). PDZ Domain Proteins: Scaffolds for Signaling Complexes. *Current Biology 7(12)*, 770-773.

Sadamoto, H., Takahashi, H., Okada, T., Kenmoku, H., Toyota, M., & Asakawa, Y. (2012). De Novo Sequencing and Transcriptome Analysis of the Central Nervous System of Mollusc Lymnaea stagnalis by Deep RNA Sequencing. *PloS One (7)*, 1-13.

Scheuer, T. (2011). Regulation of Sodium Channel Activity by Phosphorylation. *Seminars in cell & developmental biology*, 160-165.

Senatore, A., Guan, W., Boone, A., & Spafford, J. (2014). T-type Channels Become Highly Permeable to Sodium Ions Using an Alternate Extracellular Turret Region (S5-P) Outside the Selectivity Filter . *The journal of Biological Chemistry /9289)*, 11970. doi:10.1074/jbc.P114.551473 .

Sheng, M. (1996). PDZs and Receptor/Channel Clustering: Rounding Up the Latest Suspects. *Neuron (17)*, 575–578.

Sheng, M., & Sala, C. (2001). PDZ Domains and the Organization of Supramolecular Complexes. *Annual Reveiw of Neurosciece 24 (1)*, 1-29.

Shimoda, Y., & Watanabe, K. (2009). Contactins: Emerging Key Roles in the Development and Function of the Nervous System. *Cell Adhesion & Migration 3(1)*, 64-70.

Soong, T., & Venkatesh, B. (2006). Adaptive Evolution of Tetrodotoxin Resistance in Animals. *Trends in genetics 22(11)*, 621-526.

Spafford, J., Grigoriev, N., & Spencer, A. (1996). Pharmacological properties of voltage gated Na+ currents in motor neurones from a hydrozoan jellyfish Polyorchis penicillatus. *The Journal of Experimental Biology (199)*, 941-948.

Stohr, H., Berger, C., Frohlich, & Weber, B. (2002). A Novel Gene Encoding a Putative Transmembrane Protein With Two Extracellular CUB Domains and a Low-Density Lipoprotein Class A Module: Isolation of Alternatively Spliced Isoforms in Retina and Brain. *Gene: an international journal on genes and genoms*, 223-231.

Syed, N., Ridgway, R., Lukowiak, K., & Bulloch, A. (1992). Transplantation and functional integration of an identified respiratory interneuron in lymnaea stagnalis. *Neuron*, 767-774.

Tan, J., Liu, Z., Nomura, Y., Goldin, A., & Dong, K. (2002). Alternative Splicing of an Insect Sodium Channel Gene Generates Pharmacologically Distinct Sodium Channels. *The Journal of Neuroscience, Vol.22*, 5300-5309.

Tonikian, R., Zhang, Y., Sazinsky, S., Currell, B., Yeh, J.-H., Reva, B., . . . Sidhu, S. (2008). A Specificity Map for the PDZ Domain Family. *PLoS Biol 6(9)*, e239. doi: 10.1371/journal.pbio.0060239.

Twarog, B., Hidaka, T., & Yamaguchi, H. (1972). Resistanse to Tetrodotoxin and Saxitoxin in ivalve Molluscs. *Toxicon*, 273-278.

Tyrrell, L., Renganathan, M., Dib-Hajj, S., & Waxman, S. (2001). Glycosylation Alters Steady-State Inactivation of Sodium Channel Nav1.9/NaN in Dorsal Root Ganglion Neurons and Is Developmentally Regulated. *The Journal of Neuroscience (21)*, 9629–9637.

Van Petegem, F., Lobo, P., & Ahern, C. (2012). Seeing the Forest through the Trees: towards a Unified View on Physiological Calcium Regulation of Voltage-Gated Sodium Channels. *Biophysical Journal 103*, 2243–2251.

Wang, R., Mellem, J. E., Jensen, M., Brockie, P. J., Walker, C. S., Hoerndli, F., . . . Maricq, A. V. (2012). The SOL-2/Neto auxiliary protein modulates the function of AMPA-subtype ionotropic glutamate receptors. *Neuron*, 1-48.

Warmke, J., Reenan, R., Wang, P., Qian, S., Arena, J., Wang, J., . . . Cohen, C. (1997). Functional Expression of Drosophila para Sodium Channels: Modulation by the Membrane Protein TipE and Toxin Pharmacology. *The Journal of General Phisiology, Vol.101*, 119-133.

Widmark, J., Sundstrom, G., Daza, D., & Larhammar, D. (2010). Differential Evolution of Voltage-Gated Sodium Channels in Tetrapods and Teleost Fishes. *Molecular Biology and Evolution*, 859-871.

Wollner, D., Messner, D., & Catterall, W. (1987). Beta2 Subunits of Sodium Channels from Vertebrate Brain. *The journal of Biological Chemistry 262(30)*, 14709-14715.

Woodall, A. J., Naruo, H., Prince, D., Z.P., F., Winlow, W., Takasaki, M., & Syed, N. (2003). Anesthetic Treatment Blocks Synaptogenesis but not Neuronal Regeneration of Cultured Lymnaea Neurons. *Journal of Neurophysiology (90)*, 2232-2239.

Yoshida, S. (1994). Tetrodotoxin-Resistant Sodium Channels. *Cellular and Molecular Neurobiology*, 227-245.

Yu, F. H., & Catterall, W. A. (2003). Overview of the Voltage-Gated Sodium Channel Family. *Genome Biology, Vol.207*, 1-7.

Yu, F., Westenbroek, R., Silos-Santiago, I., McCormick, K., Lawson, D., Ge, P., . . . Curtis, R. (2003). Sodium Channel B4, a New Disulfide-Linked Auxiliary Subunit with Similarity to B2. *The Journal of Neuroscience, (20)*, 7577–7585.

Zakon, H. (2012). Adaptive Evolution of Voltage-Gated Sodium Channels:. *PNAS*, 10619–10625.

Zhang, T., Wang, Z., Wang, L., Luo, N., Jiang, L., Liu, Z., . . . Dong, K. (2013). Role of the DSC1 Channel in Regulating Neuronal Excitability in Drosophila melanogaster: Extending Nervous System Stability under Stress. *PLOS*, 1-10.

Zhang, X., Ren, W., DeCaen, P., Yan, C., Tao, X., Tang, L., . . . Yan, N. (2012). Crystal Structure of an Orthologue of the NaChBac Voltage-Gated Sodium Channel. *Nature (486)*, 130-134.

Zheng, Y., Mellem, J. E., Brockie, P. J., D., M., & Maricq, A. (2003). SOL-1 is a CUB-domain Protein Required for GLR-1 Glutamate Receptor Function in C. elegans. *Nature (427)*, 451-457.

Zonta, B., Desmazieres, A., Rinaldi, A., Tait, S., Sherman, D., & Nolan, M. P. (2011). A Critical Role for Neurofascin in Regulating Action Potential Initiation through Maintenance of the Axon Initial Segment. *Neuron (69)*, 945–956.